



**THESIS APPROVAL**  
**GRADUATE SCHOOL, KASETSART UNIVERSITY**

Master of Science (Chemistry)

DEGREE

Chemistry

FIELD

Chemistry

DEPARTMENT

**TITLE:** Quantum Chemical Calculations on Particular Interaction Energy of HIV-1 RT Inhibitors (68nv, T4 and T5) Bound in Various Types of HIV-1 RT Enzymes

**NAME:** Miss Amphawan Maitarad

**THIS THESIS HAS BEEN ACCEPTED BY**

THESIS ADVISOR

( Miss Patchreenart Suparparkorn, Ph.D. )

THESIS CO-ADVISOR

( Associate Professor Supa Hannongbua, Dr.rer.nat. )

THESIS CO-ADVISOR

( Associate Professor Supanna Techasakul, Ph.D. )

DEPARTMENT HEAD

( Assistant Professor Noojaree Prasitpan, Ph.D. )

**APPROVED BY THE GRADUATE SCHOOL ON** \_\_\_\_\_

DEAN

( Associate Professor Gunjana Theeragool, D.Agr. )

THESIS

QUANTUM CHEMICAL CALCULATIONS ON PARTICULAR  
INTERACTION ENERGY OF HIV-1 RT INHIBITORS  
(68NV, T4 AND T5) BOUND IN VARIOUS TYPES  
OF HIV-1RT ENZYMES

AMPHAWAN MAITARAD

A Thesis Submitted in Partial Fulfillment of  
the Requirements for the Degree of  
Master of Science (Chemistry)  
Graduate School, Kasetsart University  
2009

Amphawan Maitarad 2009: Quantum Chemical Calculations on Particular Interaction Energy of HIV-1 RT Inhibitors (68nv, T4 and T5) Bound in Various Types of HIV-1 RT Enzymes. Master of Science (Chemistry), Major Field: Chemistry, Department of Chemistry. Thesis Advisor: Miss Patchreenart Suparpakorn, Ph.D. 79 pages.

Mutations of the HIV-1 Reverse Transcriptase protein (HIV-1 RT) are an increasing problem in the treatment of HIV and considerable effort has been expended in both industry and academic to tackle this problem. In effort to minimize the loss in potency of nevirapine derivatives to HIV-1 RT mutants has led to the synthesis of 2-chloro-8-arylthiomethyl dipyridodiazepinone derivatives which show very interesting biological activities at known mutants.

Therefore, the aim of this computationally based study is to investigate the role of the key residues in the HIV-1 RT allosteric binding pocket and to understand their roles in inhibitor binding. Theoretical protein-ligand complexes for HIV-1 RT proteins (wild-type (WT), K103N and Y181C) and three NNRTIs were generated using: GOLD docking (model A) and GOLD docking with AMBER minimization (model B). The pairwise interaction energies between the inhibitors and individual residues within 4 Å were calculated at B3LYP/6-31G(d,p) and MP2/6-31G(d,p) levels of theory and energies were also corrected with basis set super position error.

In addition, the principal components analysis (PCA) was used to study the relationship between the theoretical parameters obtained from the 3 different inhibitors at 3 distinct protein variants, because of the large number of variables generated and the significant cross correlation in the dataset. An analysis of the loading and score plots derived PCA model were discussed. The obtained results can be summarized as following: (a) the impact of the different starting models. The results found that the AMBER force field minimizations (model B) can decrease more repulsive interaction energy in binding site of Gold docking (model A) and it can remain important attractive interaction in binding site. Moreover, (b) analysis of structural and energetic parameters of model B and (c) the relationship between the quantum energies and IC<sub>50</sub> differences found that the results from calculations agreed well with their experimental activities.

---

Student's signature

---

Thesis Advisor's signature

/ /

## **ACKNOWLEDGMENTS**

I would like to express my appreciation to my advisor, Dr. Patchreenart Saparpakorn, for her excellent supervision, inspiring guidance and helpful criticism throughout the course of this study. I am also thankful to my co-advisor, Associate Professor Dr. Supa Hannongbua, for her valuable guidance, supporting scholarship, kindness, inspiration, and encouragement. Moreover, I would like to thank Dr. Phornphimon Maitarad, Dr. Witcha Treesuwan and Dr. Paul Matthew Gleeson for their kind comments and criticism to make thesis completed.

Furthermore, I would like to thank my advisory committee Associate Professor Dr. Supanna Techasakul, Dr. Mayuso Kuno and Dr. Songwut Suramitr for their helpful criticism and suggestion.

Fully financial support by The National Center of Excellent on Petroleum, Petrochemical Technology and Advanced Materials (NCE-PPAM) and The Center of Nanotechnology, Kasetsart University, were gratefully acknowledged.

Special thanks are also due to the High Performance Computing Center of the National Electric and Computer Technology (NECTEC), for providing SYBYL program. The Laboratory for Computational and Applied Chemistry (LCAC) at Kasetsart University are also gratefully acknowledged for computational resource and software facilities.

I appreciate all of my colleagues at LCAC at Kasetsart University for their helpful and friendship during the past three years.

Finally, I would like to thank my family for their love, sincere care and great encouragement during this work.

Amphawan Maitarad

September, 2009



## TABLE OF CONTENTS

	<b>Page</b>
TABLE OF CONTENTS	i
LIST OF TABLES	ii
LIST OF FIGURES	iv
LIST OF ABBREVIATIONS	x
INTRODUCTION	1
OBJECTIVES	7
LITERATURE REVIEW	8
METHODS OF CALCULATIONS	13
RESULTS AND DISCUSSION	18
CONCLUSIONS	60
LITERATURE CITED	62
APPENDICES	66
Appendix A Supporting information	67
Appendix B Presentations	69
CURRICULUM VITAE	78

## LIST OF TABLES

Table		Page
1	Structures and inhibitory activity of 2-chloro-8-arylthiomethyl dipyrindodiazepinone derivatives against HIV-1 RT	4
2	Interaction energy between inhibitors (68nv, T4 and T5) with individual residues (in kcal/mol), calculated at B3LYP/6-31G(d,p) and MP2/6-31G(d,p) levels of theory for WT in model A	20
3	Interaction energy between inhibitors (68nv, T4 and T5) with individual residues (in kcal/mol), calculated at B3LYP/6-31G(d,p) and MP2/6-31G(d,p) levels of theory for K103N HIV-1 RT in model A	21
4	Interaction energy between inhibitors (68nv, T4 and T5) with individual residues (in kcal/mol), calculated at B3LYP/6-31G(d,p) and MP2/6-31G(d,p) levels of theory for Y181C HIV-1 RT in model A	22
5	Interaction energy between inhibitors (68nv, T4 and T5) with individual residues (in kcal/mol), calculated at B3LYP/6-31G(d,p) and MP2/6-31G(d,p) levels of theory for WT HIV-1 RT in model B	29
6	Interaction energy between inhibitors (68nv, T4 and T5) with individual residues (in kcal/mol), calculated at B3LYP/6-31G(d,p) and MP2/6-31G(d,p) levels of theory for K103N HIV-1 RT in model B	30
7	Interaction energy between inhibitors (68nv, T4 and T5) with individual residues (in kcal/mol), calculated at B3LYP/6-31G(d,p) and MP2/6-31G(d,p) levels of theory for Y181C HIV-1 RT in model B	31
8	$r^2$ and $q^2$ of PCA plot in model A, calculated at MP2/6-31G(d,p) levels of theory	34

**LIST OF TABLES (Continued)**

<b>Table</b>		<b>Page</b>
9	$r^2$ and $q^2$ of PCA plot in model B, calculated at MP2/6-31G(d,p) levels of theory	35
10	$r^2$ and $q^2$ of PCA plot of inhibitor-residue distances and energy of model B, calculateddd at MP2/6-31G(d,p) levels of theory	47
11	The interaction and key distances between the residue and ligand	51

## LIST OF FIGURES

Figure		Page
1	Structures of anti-HIV nucleoside analogues (NRTIs)	2
2	Structures of non-nucleoside reverse transcriptase inhibitor (NNRTIs)	3
3	The structure of HIV-1 RT, PDB coded 1KLM	5
4	The binding site of HIV-1 RT complex with delavirdine inhibitor	6
5	Orientations of 68nv (A), T4 (B) and T5 (C) in binding site of WT HIV-1 RT	18
6	Orientations of 68nv (A), T4 (B) and T5 (C) in binding site of K103N HIV-1RT	19
7	Orientations of 68nv (A), T4 (B) and T5 (C) in binding site of Y181C HIV-1RT	19
8	Superimposition between Model A (pink) and Model B (yellow) of 68nv in WT HIV-1 RT	24
9	Superimposition between Model A (pink) and Model B (yellow) of T4 in WT HIV-1 RT	24
10	Superimposition between Model A (pink) and Model B (yellow) of T5 in WT HIV-1 RT	25
11	Superimposition between Model A (pink) and Model B (yellow) of 68nv in K103N HIV-1 RT	25
12	Superimposition between Model A (pink) and Model B (yellow) of T4 in K103N HIV-1 RT	26
13	Superimposition between Model A (pink) and Model B (yellow) of T5 in K103N HIV-1 RT	26
14	Superimposition between Model A (pink) and Model B (yellow) of 68nv in Y181C HIV-1 RT	27

## LIST OF FIGURES (Continued)

Figure		Page
15	Superimposition between Model A (pink) and Model B (yellow) of T4 in Y181C HIV-1 RT	27
16	Superimposition between Model A (pink) and Model B (yellow) of T5 in Y181C HIV-1 RT	28
17	PCA scores (left) and loading (right) plots: plot of component one (x axis) against component two (y axis) of model A, calculated at MP2/6-31G(d,p) levels of theory	34
18	PCA scores plot (left) and loading plot (right): plot of component one (x axis) against component two (y axis) of model B, calculated at MP2/6-31G(d,p) levels of theory	36
19	Superimposition between model A (atom-type color) and model B (orange) of 68nv with residues (Tyr181, Pro236, Val106 and Lys103) in WT HIV-1 RT	38
20	Superimposition between model A (atom-type color) and model B (pink) of T4 with residues (Tyr181, Pro236, Val106 and Lys103) in WT HIV-1 RT	38
21	Superimposition between model A (atom-type color) and model B (green) of T5 with residues (Tyr181, Pro236, Val106 and Lys103) in WT HIV-1 RT	39
22	Superimposition between model A (atom-type color) and model B (orange) of 68nv with residues (Tyr181, Pro236, Val106 and Lys103) in K103N HIV-1 RT	39
23	Superimposition between model A (atom-type color) and model B (pink) of T4 with residues (Tyr181, Pro236, Val106 and Lys103) in K103N HIV-1 RT	40

## LIST OF FIGURES (Continued)

Figure		Page
24	Superimposition between model A (atom-type color) and model B (green) of T5 with residues (Tyr181, Pro236, Val106 and Lys103) in K103N HIV-1 RT	40
25	Superimposition between model A (atom-type color) and model B (orange) of 68nv with residues (Cys181, Pro236, Val106 and Lys103) in Y181C HIV-1 RT	41
26	Superimposition between model A (atom-type color) and model B (pink) of T4 with residues (Cys181, Pro236, Val106 and Lys103) in Y181C HIV-1 RT	41
27	Superimposition between model A (atom-type color) and model B (green) of T5 with residues (Cys181, Pro236, Val106 and Lys103) in Y181C HIV-1 RT	42
28	Superimposition between model A (atom-type color) and model B (orange) of 68nv with residues (Lys101, Leu100, Trp229 and Glu138) in WT HIV-1 RT	42
29	Superimposition between model A (atom-type color) and model B (pink) of T4 with residues (Lys101, Leu100, Trp229 and Glu138) in WT HIV-1 RT	43
30	Superimposition between model A (atom-type color) and model B (green) of T5 with residues (Lys101, Leu100, Trp229 and Glu138) in WT HIV-1 RT	43
31	Superimposition between model A (atom-type color) and model B (orange) of 68nv with residues (Lys101, Leu100, Trp229 and Glu138) in K103N HIV-1 RT	44
32	Superimposition between model A (atom-type color) and model B (pink) of T4 with residues (Lys101, Leu100, Trp229 and Glu138) in K103N HIV-1 RT	44

## LIST OF FIGURES (Continued)

Figure		Page
33	Superimposition between model A (atom-type color) and model B (green) of T5 with residues (Lys101, Leu100, Trp229 and Glu138) in K103N HIV-1 RT	45
34	Superimposition between model A (atom-type color) and model B (orange) of 68nv with residues (Lys101, Leu100, Trp229 and Glu138) in Y181C HIV-1 RT	45
35	Superimposition between model A (atom-type color) and model B (pink) of T4 with residues (Lys101, Leu100, Trp229 and Glu138) in Y181C HIV-1 RT	46
36	Superimposition between model A (atom-type color) and model B (green) of T5 with residues (Lys101, Leu100, Trp229 and Glu138) in Y181C HIV-1 RT	46
37	PCA scores plot (left) and loading plot (right): plot of component one (x axis) against component two (y axis) of inhibitor-residue distances of model B, calculated at MP2/6-31G(d,p) levels of theory	48
38	Interaction between inhibitors (68nv (left), T4 (middle) and T5 (right)) and Glu138 residue in WT (atom-type color), K103N (blue) and Y181C (pink) HIV-1 RT	52
39	Interaction between inhibitors (68nv (left), T4 (middle) and T5 (right)) and Lys101 residue in WT (atom-type color), K103N (blue) and Y181C (pink) HIV-1 RT	52
40	Interaction between inhibitors (68nv (left), T4 (middle) and T5 (right)) and Lys102 residue in WT (atom-type color), K103N (blue) and Y181C (pink) HIV-1 RT	52

## LIST OF FIGURES (Continued)

Figure		Page
41	Interaction between inhibitors (68nv (left), T4 (middle) and T5 (right)) and Lys103 residue in WT (atom-type color), K103N (blue) and Y181C (pink) HIV-1 RT	53
42	Interaction between inhibitors (68nv (left), T4 (middle) and T5 (right)) and Asn103 residue in K103N HIV-1 RT	53
43	Interaction between inhibitors (68nv (left), T4 (middle) and T5 (right)) and Trp229 residue in WT (atom-type color), K103N (blue) and Y181C (pink) HIV-1 RT	53
44	Interaction between inhibitors (68nv (left), T4 (middle) and T5 (right)) and Tyr181 residue in WT (atom-type color), K103N (blue) and Y181C (pink) HIV-1 RT	54
45	Interaction between inhibitors (68nv (left), T4 (middle) and T5 (right)) and Cys181 residue in Y181C HIV-1 RT	54
46	Interaction between inhibitors (68nv (left), T4 (middle) and T5 (right)) and Tyr188 residue in WT (atom-type color), K103N (blue) and Y181C (pink) HIV-1 RT	54
47	Overlapping factor between chloride atom in three inhibitors and hydrogen atom in side chain of Cys181	55
48	Steric interaction of inhibitors (68NV (left), T4 (middle) and T5 (right)) and Asn103	55
49	Relative of pIC <sub>50</sub> from experiment (left) on PCA score plot and PCA loading plot (right)	56
50	Relationship of three inhibitor (68nv, T4 and T5) in WT calculated at MP2/6-31G(d,p) level of theory	58
51	Relationship of three inhibitor (68nv, T4 and T5) in K103N calculated at MP2/6-31G(d,p) level of theory	58



**LIST OF FIGURES (Continued)**

<b>Figure</b>		<b>Page</b>
52	Relationship of three inhibitor (68nv, T4 and T5) in Y181C calculated at MP2/6-31G(d,p) level of theory	59

## LIST OF ABBREVIATIONS

3TC	=	Lamivudine
8-Cl <i>TIBO</i>	=	Tivirapine
AIDs	=	Acquired immunodeficiency syndrome
Asn	=	Asparagine
Asp	=	Aspartic acid
AZT	=	Zidovudine
B3LYP	=	Beck's three parameter hybrid functional using the LYP correlation functional
BSSE-CP	=	Basis set superposition error based on the counterpoise scheme
CG	=	Conjugated Gradient
Comp	=	Compounds
Cys	=	Cysteine
d4T	=	Stavudine
ddC	=	Zalcitabine
ddI	=	Didanosine
DFT	=	Density functional theory
DNA	=	Deoxyribonucleic acid
Glu	=	Glutamic
Gly	=	Glycine
His	=	Histidine
HIV	=	Human immunodeficiency virus
HF	=	Hartree-fock theory
IC <sub>50</sub>	=	The half maximal inhibitory concentration
kDa	=	kiloDalton
kcal	=	kilocalorie
Leu	=	Leucine
Lys	=	Lysine
MFCC	=	Molecular fractionation with conjugate caps
MP2	=	Second order Möller-plesset

**LIST OF ABBREVIATIONS (Continued)**

NNRTIs	=	Non-nucleoside reverse transcriptase inhibitors
NRTIs	=	Nucleoside reverse transcriptase inhibitors
PCA	=	Principal Components analysis
PDB	=	Protein Data Bank
PETT-2	=	phenylethylthiazolylthiourea
Phe	=	Phenylalanine
Pro	=	Proline
RNA	=	Ribonucleic acid
RMS	=	Root mean square
rmse	=	Root-mean-square error
RT	=	Reverse transcriptase
SD	=	Steepest Descent
Ser	=	Serine
TNK-651	=	6-benzyl-1-benzyloxymethyl-5-isopropyl
Tyr	=	Tyrosine
UC-781	=	A thaiocarboxanilide pentenylaxy ether
Val	=	Valine
WT	=	Wild-type

# QUANTUM CHEMICAL CALCULATIONS ON PARTICULAR INTERACTION ENERGY OF HIV-1 RT INHIBITORS (68NV, T4 AND T5) BOUND IN VARIOUS TYPES OF HIV-1RT ENZYMES

## INTRODUCTION

Acquired immunodeficiency syndrome (AIDs) is a disease caused by the human immunodeficiency virus (HIV). The human immunodeficiency virus type 1 (HIV-1) is a major worldwide infection (San Juan, 2008). The important enzyme of HIV-1 is reverse transcriptase (RT), which is a special enzyme converting the single-standed RNA viral genome into a double-standed proviral DNA before integrating into the host chromosome (De Clercq, 1995). Moreover, HIV-1 RT is an asymmetric heterodimer consisting of a p66 and p51 subunits that is responsible for the replication of single-standed viral RNA into double-standed DNA prior to integration into the genome of the human host (Jacobo-Molina *et al.*, 1993). Therefore, HIV-1 RT is widely studied because it is an important target in treatment of AIDs.

RT inhibitors can be divided into two main types; Nucleoside reverse transcriptase inhibitors (NRTIs) such as azidothymidine (AZT), didanosine (ddI), zalcitabine (ddC), stavudine (d4T), lamivudine (3TC), acyclovir (De Clercq, 1995; Sarafianos *et al.*, 2004) (Figure 1) and Non-nucleoside reverse transcriptase inhibitors (NNRTIs) such as nevirapine, delavirdine, efavirenz, DAPY NNRTIs (Campiani *et al.*, 2002; Das *et al.*, 2008; De Clercq, 1995; De Clercq, 2001; De Clercq, 2002; , 2004) (Figure 2). NRTIs are competitive inhibitors. As the structures of NRTIs are similar to nucleoside, thus, they compete with the viral DNA to bind in the active site. While NNRTIs are non competitive inhibitors, these inhibitors bind near active site of reverse transcriptase enzyme. NNRTIs have an effect on conformational changes relative to activity of enzyme (De Clercq, 1999). The NNRTIs are much less toxic than NRTIs. Therefore, the new potent drugs have been widely developed for clinical utility of the non-nucleoside inhibitors (Chan *et al.*, 2004; De Clercq, 2002). However,

the efficiency of non-nucleoside inhibitors is limited by relative rapid emergence of drug-resistant HIV-1 strain.

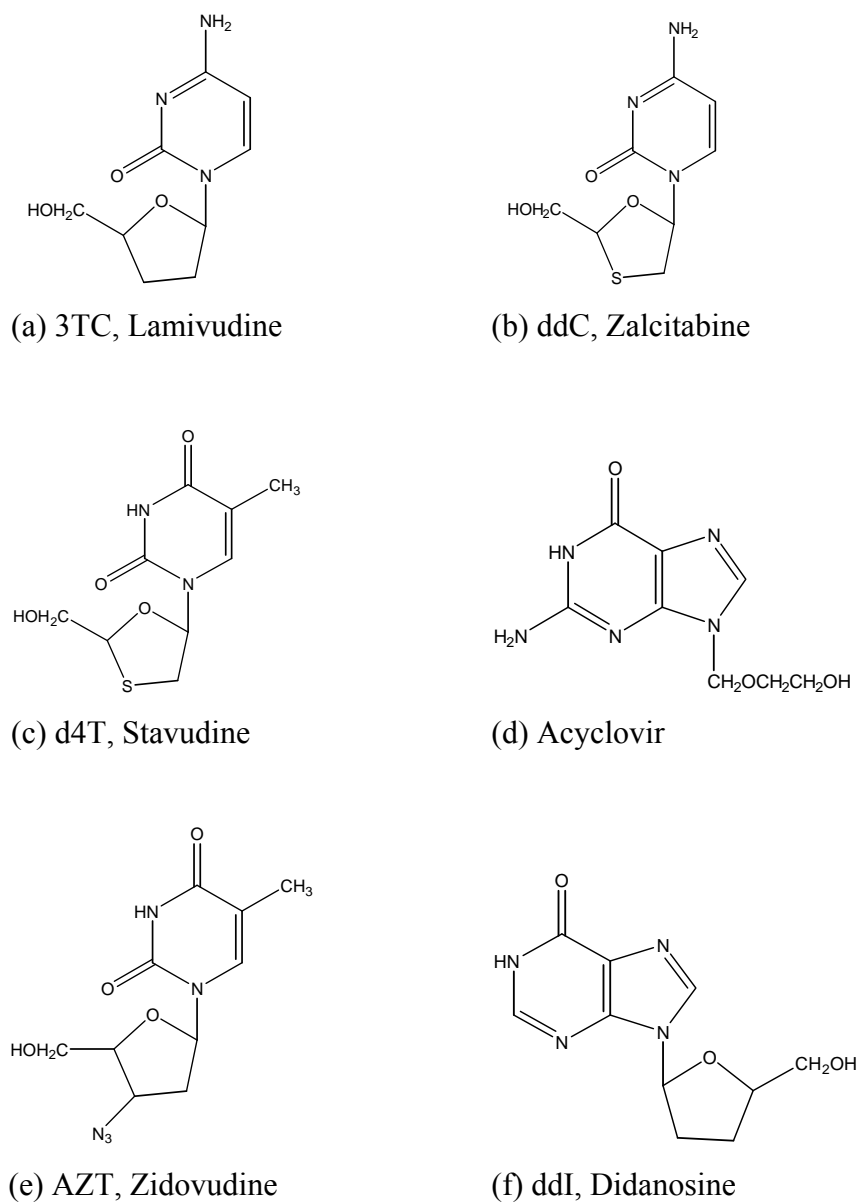
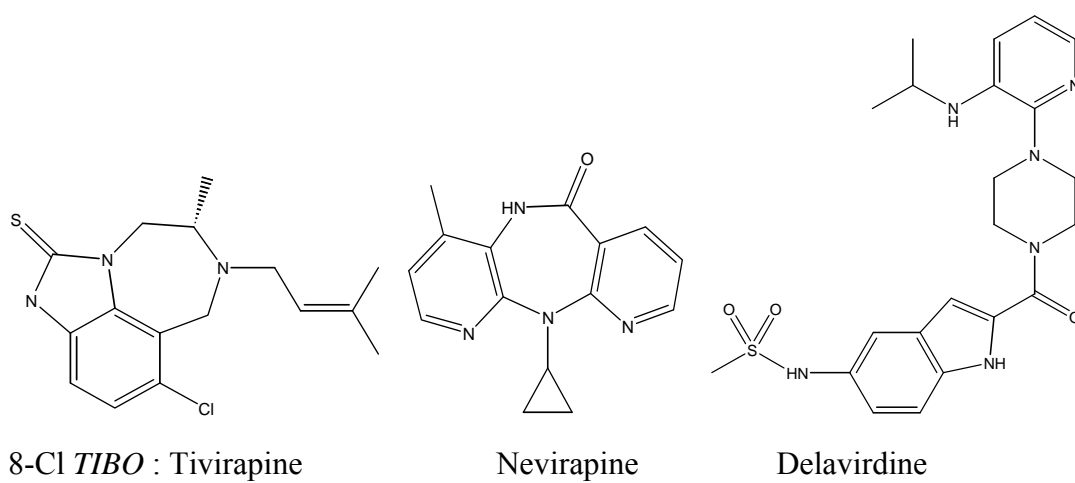
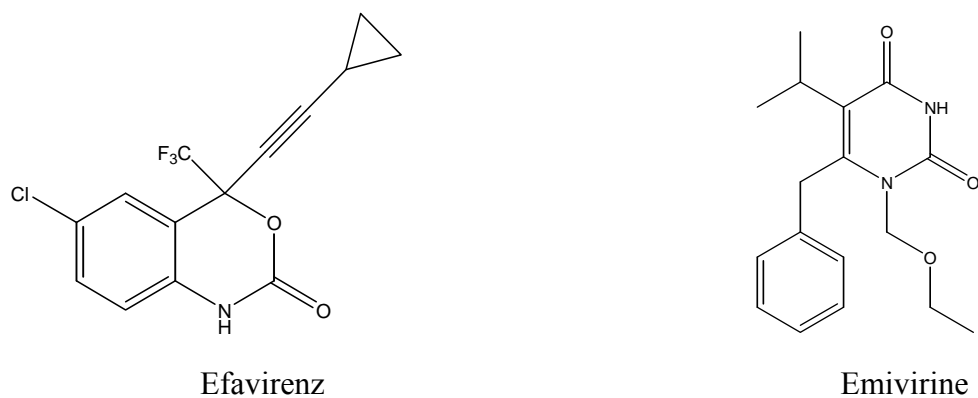


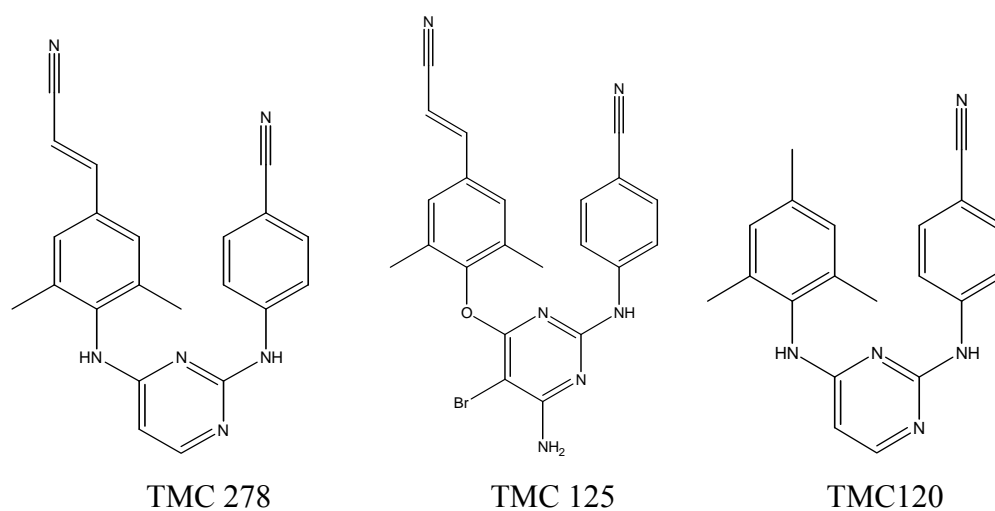
**Figure 1** Structures of anti-HIV nucleoside analogues (NRTIs).



### First generation NNRTIs



### Second generation NNRTIs

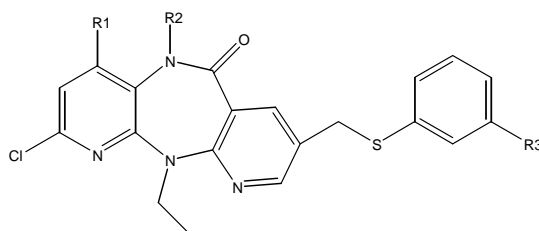


### Third generation NNRTIs

**Figure 2** Structures of non-nucleoside reverse transcriptase inhibitor (NNRTIs).

Nevirapine is the first generation of non-nucleoside inhibitors of HIV-1 RT. The efficiency of nevirapine is satisfied for WT HIV-1 RT but it loss efficiency for mutant type (Bardsley-Elliot and Perry, 2000). In particular, the K103N and Y181C HIV-1 RT mutant types are mostly reported in the resistance of nevirapine inhibitors (Saparpakorn *et al.*, 2006). In an attempt to improve the activity of nevirapine against mutant RT enzyme, the 2-chloro-8-arylthiomethyl dipyridodiazepinone derivatives (Khunnawutmanotham *et al.*, 2007; Klunder *et al.*, 1998), which containing unsubstituted lactam nitrogen and 2-chloro-8-arylthiomethyl (T4 and T5) moiety, have been focused. As compared with 68NV, T4 and T5 are also effective for the K103N and Y181C HIV-1 RT, as shown in Table 1.

**Table 1** Structures and inhibitory activity of 2-chloro-8-arylthiomethyl dipyridodiazepinone derivatives against HIV-1 RT.



Comp	R1	R2	R3	IC <sub>50</sub> (μM)		
				WT	K103N	Y181C
68NV	H	CH <sub>3</sub>	H	0.0858	0.3900	0.0046
T4	CH <sub>3</sub>	H	H	0.0186	0.2240	0.2690
T5	CH <sub>3</sub>	H	OCH <sub>3</sub>	0.0229	0.4280	0.0593

( Khunnawutmanotham *et al.*, 2009)

The Protein Data Bank (PDB) (RCSB PDB, <http://www.rcsb.org>) is the depository for crystal structures of biological macromolecules from experimental. Currently, the Protein Data Bank has provided x-ray crystallography more than 53,000 crystal structures from 1971 - 2008. In addition, the crystal structure of HIV-1 RT are available in the Protein Data Bank more than 100 crystal structures (Dutta *et al.*, 2009). The crystallization structure of the wild-type of HIV-1 RT complex with delavirdine inhibitor at 2.65 Å resolutions (PDB code 1KLM) (Esnouf *et al.*, 1997), displayed in Figure 3, has been used in this study. The binding site of HIV-1 RT complex with delavirdine inhibitor is shown in Figure 4.

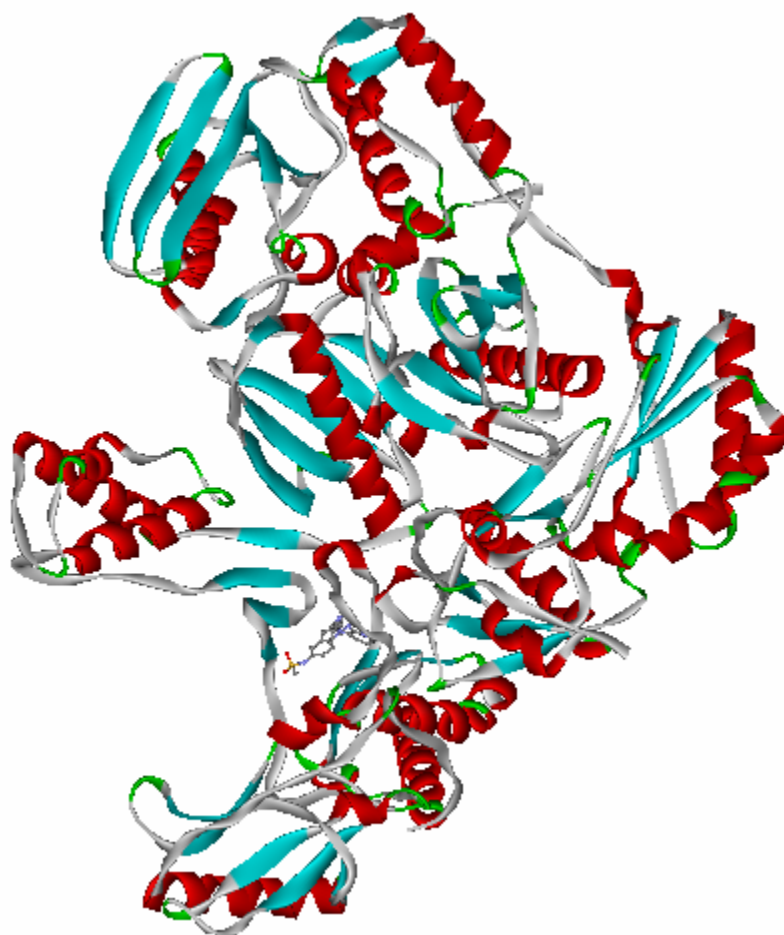


**Figure 3** The structure of HIV-1 RT, PDB coded 1KLM.



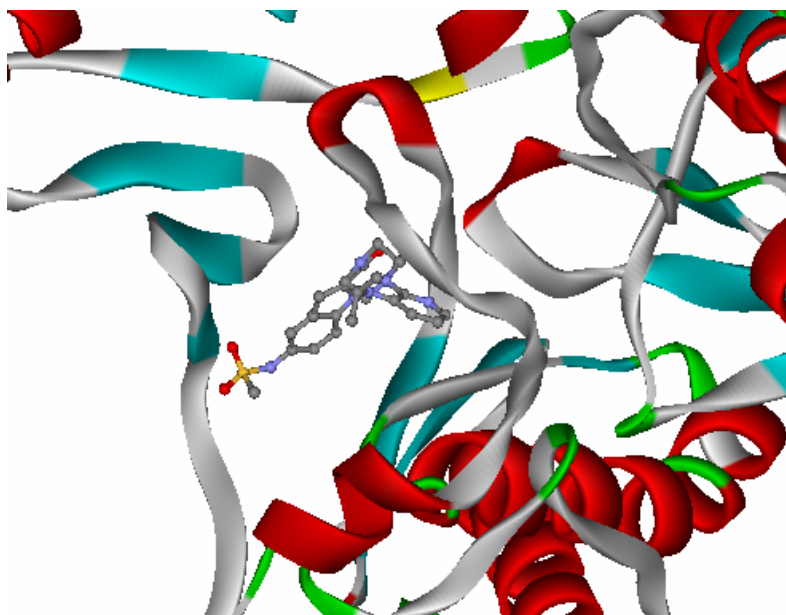


**Figure 4** The binding site of HIV-1 RT complex with delavirdine inhibitor.

In order to understand more deeper in molecular interaction between inhibitor and residues in binding pocket which is not observed by experimental, therefore, theoretical investigation has been an alternative method to investigate the enzyme and inhibitor interaction in details for large molecular system. Recently, quantum chemical calculations were used to study the effect of mutation related to inhibitor resistant. It was found that the calculations are important for guiding the cause of resistant (He *et al.*, 2005; Kuno *et al.*, 2003a; Kuno *et al.*, 2006; Kuno *et al.*, 2003b; Mei *et al.*, 2005; Nunrium *et al.*, 2005).

In the present study, the particular interaction energy of inhibitors (68NV, T4 and T5) with individual residue in binding site of various type of HIV-1RT (WT, K103N and Y181C HIV-1RT) have been focused on the molecular interaction investigations.

## OBJECTIVES

1. To calculate interaction energies between inhibitors (68NV, T4 and T5) and residues surrounding the binding pocket in WT and both mutant types HIV-1 RT (K103N and Y181C) HIV-1 RT, based on the quantum chemical calculations at B3LYP/6-31G(d,p) and MP2/6-31G(d,p) levels.
2. To observe the main contributed interaction of residues in the binding site.
3. To compare the particular interaction energy on the WT and both mutant types (K103N and Y181C) HIV-1 RT complexed with 68NV, T4 and T5 inhibitors.
4. To compare the efficiency from quantum chemical calculations with their experimental activities.

## LITERATURE REVIEW

The viral infection caused by HIV type 1 (HIV-1) is a major worldwide pandemic (San Juan, 2008). In 1993, Jacobo-Molina *et al.* studied crystal structure of HIV-1 RT complex with double-stranded DNA at 3.0 resolution showed bent DNA. It was found that HIV-1 RT is a multifunctional heterodimer of a 66-kDa molecular mass p66 subunit and a 51-kDa molecular mass p51 subunit (as a proteolytic product of the p66 subunit). P51 unit has the same sequence but adopts a different conformation. DNA polymerase and RNase H catalytic activities are both conferred on the enzyme by larger p66 subunit of the enzyme. Crystal structure of a ternary complex of HIV-1 RT heterodimer and a monoclonal antibody Fab fragment was determined at 3.0 Å resolutions. The four individual subdomains of RT that make up the polymerase domains of p66 and p51 were named Fingers palm, thumb, and connection. The overall folding of the subdomains was similar in p66 and p51 but the spatial arrangements of the subdomains were dramatically different. The template-primer has A-form and B-form regions separated by a significant bend (40-45°). The most numerous nucleic acid interactions with protein occurred primarily along the sugar-phosphate backbone of DNA and involved amino acid residues of the palm, thumb, and Fingers of p66. Highly conserved regions were located in the p66 palm near the polymerase active site. These structural elements, together with two  $\alpha$ -helix of the thumb of p66, act as a clamp to position the template-primer relative to the polymerase active site. The 3'-hydroxyl of the primer terminus was closed to the catalytically essential Asp110, Asp185 and Asp186 residues at the active site and was in a position for nucleophilic attack on the  $\alpha$ -phosphate of an incoming nucleoside triphosphate.

RT enzyme is responsible for copying the single-stranded viral RNA into double-stranded DNA, which is subsequently integrated into host cell chromosomes by the viral enzyme integrase. RT is an important target for drug therapy, it not only is essential for viral replication but also contains multiple sites where drug can bind. The two types of RT inhibitors are;

- (i) NRTIs: *i.e.* Azidothymidine (AZT), didanosine (ddI), zalcitabine (ddC), stavudine (d4T), lamivudine (3TC), abacavir (ABC), emtricitabine (De Clercq, 1995; Sarafianos *et al.*, 2004)
- (ii) NNRTIs: *i.e.* nevirapine, delavirdine, efavirenz, DAPY NNRTIs (Campiani *et al.*, 2002; Das *et al.*, 2008; De Clercq, 1995; De Clercq, 2001; De Clercq, 2002; , 2004)

The NRTIs compete with the viral DNA to bind in the same site, while NNRTIs bind in an allosteric site, which interferes with viral RNA binding to HIV-1 RT by inducing a conformational change of the enzyme. NNRTIs were notorious for rapidly eliciting resistance due to the mutations of the amino acids surrounding the NNRTIs binding site (De Clercq, 1999). The NNRTIs are much less toxic than NRTIs. However, the efficiency of highly potent inhibitors is limited by relatively rapid emergence of drug-resistant HIV-1 strains. Therefore, new potent drugs have been widely developed. Clinical utility of the non-nucleoside inhibitors was adversely affected by the emergence of drug-resistant HIV-1 RT variants (Chan *et al.*, 2004; De Clercq, 2002).

Nevirapine is the first generation of NNRTIs to be approved for use in HIV-1 RT infected individuals, including children. It was highly efficiency inhibitor of HIV-1 RT but has limited by the emergence of drug-resistant such as K103N, V106A, Y181C, Y188H, G190A and P236L (Bardsley-Elliot and Perry, 2000). Therefore, nevirapine have been widely developed activity against resistance of RT enzyme. Particularly, the K103N and Y181C mutant types are important resistance RT enzyme of nevirapine inhibitor (Saparpakorn *et al.*, 2006).

Hsiou *et al.* (2001) reported a novel mechanism of K103N mutation which is substitution lysine at position 103 by asparagine of HIV-1 RT. Mechanism for drug resistance could explain the reduced susceptibility of K103N HIV-1 RT to NNRTIs. Amino acid 103 in the p66 subunit of HIV-1 RT is located near a putative entrance to a hydrophobic pocket that binds NNRTIs. The structures of wild-type and K103N HIV-1 RT in complexes with NNRTIs are quite similar overall as well as in the vicinity of the bound NNRTIs. Comparision of unligand wild-type and K103N HIV-1

RT structures reveals a network of H-bond interactions in the K103N that is not present in the wild-type enzyme. These results are consistent with kinetic data indicating that NNRTIs bind more slowly to K103N than wild-type HIV-1 RT. This novel drug-resistance mechanism explains the broad cross-resistance of K103N HIV-1 RT to different classes of NNRTIs. Design of NNRTIs that make favorable interactions with the Asn103 side-chain should be relatively effective against the K103N drug-resistant mutant.

Structure mechanisms of drug resistance for Y181C mutation in HIV-1 RT were investigated by (Ren *et al.*, 2001). For Y181C mutation, HIV-1 RT containing cysteine in place of tyrosine at position 181 is frequently in the presence of NNRTIs and gives high level resistance to many first generation non-nucleoside inhibitors such as nevirapine. A series of seven crystal structures of mutant RTs in complexes with first and second generation NNRTIs as well as one example of an unliganded mutant RT were determined. These are Y181C RT(TNK-651) with 2.4 Å resolution, Y181C RT(efavirenz) with 2.6 Å resolution, Y181C RT (nevirapine) with 3.0 Å resolution, Y181C RT(PETT-2) with 3.0 Å resolution, Y188C RT (nevirapine) with 2.6 Å resolution, Y188C RT (UC-781) with 2.6 Å resolution and Y188C RT (unliganded) with 2.8 Å resolution. In case of the second generation compounds efavirenz with Y181C RT and UC-781 with Y188C HIV-1 RT revealed small rearrangements of either inhibitor within the binding site compared to wild-type RT. This also showed for the first generation compounds, TNK-651, PETT-2 and nevirapine with Y181C RT. They concluded that protein conformational changes and rearrangements of drug molecules within the mutated sites were not general features of these particular inhibitor/mutant combinations. The main contribution to drug resistance for Y181C and Y188C RT mutations was the loss of aromatic ring stacking interaction for first generation compounds, providing a simple explanation for the resilience of second generation NNRTIs, such as interaction make much less significant contribution to their binding.

To develop a second generation of nevirapine inhibitor with improved activity against mutant RT enzyme. The dipyrindodiazepinone nevirapine was selected for drug

resistant variants of HIV-1 RT, both in cell culture and patients. Klunder *et al.* (1998) attempted to improve dipyrindodiazepinone nevirapine, which containing arylethyl substituent at the 8-position of the tricyclic dipyrindodiazepinone skeleton. It confers enhanced potency against Y181C RT and several analogues of this series display good broad spectrum potency against a panel of mutant enzymes. Inspection of the crystal structure of HIV-1 RT reveals the presence of a number of aromatic amino acid residues in the non-nucleoside binding pocket that appear to be within reach of the 8-aryethyl substituent including Phe227, Trp229 and Tyr232. Favorable interaction between the side chain aryl substituent of the inhibitor with these aromatic residues may contribute to binding affinity and diminish the importance of interactions with residues such as Tyr 181. Then Khunnawutmanotham *et al.* (2007) presented chloro-8-arylthiomethyl dipyrindodiazepinone nevirapine derivatives on the basis of molecular modeling analysis against wild-type and Y181C HIV-1 RT, it was shown that the dipyrindodiazepinone nevirapine derivatives containing unsubstituted lactam nitrogen and 2-chloro-8-arylthiomethyl moiety were effective inhibitors for this mutant enzyme and some of them with N-methyl of lactam nitrogen also exhibited good potency against wild-type enzyme. In addition, 8-amino derivative of nevirapine and its hydrochloride salt also provide interesting potency.

Current quantum chemical calculations study of mutation effect could provide us the following insight, which could be useful in designing more mutation resistant inhibitors. For example, it is important for the potential inhibitors to have relatively strong attractive interaction (such as H-bond interaction) to those residues that are conserved upon mutations. He *et al.* (2005) used quantum chemical calculations to analyze binding interactions of nevirapine to HIV-1 reverse transcriptase (RT) and single point mutants K103N and Y181C. In this study, the entire system of HIV-1 RT/nevirapine complex with over 15,000 atoms is explicitly treated by using a recently developed MFCC (molecular fractionation with conjugate caps) approach. Quantum calculations of protein-drug interaction energy are performed at Hartree-Fock and DFT levels. The present calculation provides a quantum mechanical interaction spectrum that explicitly shows interaction energies between nevirapine and individual amino-acid fragments of RT. Detailed interactions that are responsible for

drug resistance of two major RT mutations are elucidated based on computational analysis in relation to the crystal structures of binding complexes. The present result provides a qualitative molecular understanding of HIV-1 RT drug resistance to nevirapine and gives useful guidance in designing improved inhibitors with better resistance to RT mutation. Mei *et al.* (2005) used quantum chemical calculations to study binding of efavirenz, which is a second generation NNRTIs, to HIV-1 RT and its K103N and Y181C mutants. The binding interaction energies between efavirenz and each protein fragment were calculated using a combination of HF/3-21G, B3LYP/6-31G(d) and MP2/6-31G(d) *abinitio* levels. Nunrium *et al.* (2005) investigated the particular interaction between efavirenz and the HIV-1 RT binding site, based on the B3LYP/6-31G(d,p). Kuno *et al.* (2003b) studied the orientation and interaction energy of water molecule in the HIV-1 RT active site by quantum chemical calculations. To obtain basic information such as interaction between the water molecule and amino acids in the active site of HIV-1 RT, *ab initio* molecular orbital calculations were performed. In addition, in the same year they study the isolated complex of pyridine (part of nevirapine) and methyl phenol (part of Tyr181) was found at the MP2/6-31+G(d) level, show a off-centered parallel stacking structure indicating the importance of the  $\pi$ - $\pi$  interaction. Moreover, in 2006 they used quantum chemical calculations in the intermolecular interactions between ethanol and ethylene by forming  $H\cdots\pi$  complex systems and investigated using B3LYP, MP2 level of theories with a 6-31G(d,p) basis set. Additionally, all binding energies were corrected using the counterpoise method of Boys-Bernardi approach.

## METHODS OF CALCULATIONS

### 1. Starting Complex Structures

#### 1.1 Molecular docking by GOLD Docking program (Model A)

Molecular Docking is computer-based method for predicting the structure of ligand-protein complex. The aim of docking is to search for the best orientation of ligand in binding site. It is very useful in drug design due to it can be constructed and identified novel protein inhibitors lead to novel inhibitors with high affinity. The procedure of docking is consisted three important steps: binding site identification and characterization, orientation of the ligand within the binding site and evaluation of the orientation for appropriateness of fit. Early approaches of docking such as original DOCK algorithm have limited about computational cost and rigid docking since this problem lead to new process such as AutoDock, FlexX, GOLD and Surflex. In this work, GOLD docking program were constructed starting complex structures.

#### Protein structure preparation

The X-ray structure of HIV-1 RT in wild-type with delavirdine was retrieved from the Protein Data Bank (PDB entry code:1KLM). Then delavirdine was removed from protein structure. All hydrogen atoms were added to the protein structure by using SYBYL 7.0 program. K103N and Y181C HIV-1 RT was prepared by mutating the residue using biopolymer module in sybyl 7.0 program.

#### Inhibitors preparation

In this work 68NV, T4 and T5 NNRTIs were studied for various types of HIV-1 RT. Starting geometry of inhibitors were constructed and optimized at HF/3-21G level of theory using Gaussian 03 program.



## Complex structure preparation

The complex structures were obtained from molecular docking by GOLD docking program. The binding site was defined by using the center of mass of ligand and the radius of the binding site was set to 12 Å. For setting the GA parameter, the default parameters of library screening settings were used. The number of chromosome in each population and the number of operation were set to 50 and 1000, respectively. The GOLDScore fitness function was used to determine the fitness score.

### 1.2 Minimization by AMBER force fields (Model B)

Molecular mechanics force field is constructed and parameterized by comparison with a number of molecules. This force field then can be used for other molecules similar to those for which it was parameterized. To perform a molecular mechanics calculation, a force field is chosen and suitable molecular structure values (natural bond lengths, angles, etc.) are set. The structure then is optimized by changing the structure incrementally to minimize the strain energy and spread it over the entire molecule. This minimization is orders of magnitude faster than a quantum mechanical calculation on an equivalent molecule so that it is reasonable to use molecular mechanics force field instead of quantum mechanical calculation for molecular dynamics simulations. For this study, Cornell et al. force field was used, because it is the force field that was developed specifically for the simulations of organic molecules, DNA, and proteins.

#### Force field set up for ligand

Starting geometry of ligands were obtained from GAUSSIAN 03 program at B3LYP/6-31G(d,p). Single point calculation at HF/6-31G\*(d) level was performed to calculate force and Merz-Kollman Singh charge method (MK) was used for charge calculation of ligands. Antechamber module in AMBER9 was used to generate inhibitor topology from the output of single point calculation. Finally, force field for inhibitor molecule was generated by parmchk subprogram.

### Complex structure preparation

The starting complex structure of WT and both mutant type HIV-1RT (K103N and Y181C) were obtained from GOLD docking program. For the set up complex structure studied. Hydrogen atoms were removed due to no parameter available. Then hydrogen atoms were added into enzymes and ligands were added into the system after force field of ligand was generated.

### Minimization

Minimization were performed on AMBER9 program (Case *et al.*, 2006) with the Duan *et al.* (2003) force field as represented a latest improvement force field for protein. Start from Minimization inhibitors by Steepest Descent (SD) 1000 steps followed by Conjugated Gradient (CG) 500 steps. Then the complex structure was minimized with SD 5000 steps followed by CG 2500 steps.

## 2. Quantum chemical calculations

Quantum chemical calculations were used to calculate particular interactions energy of all complex structure. These results from calculations can be related to activity from experimental. Therefore, the quantum chemical calculations are important for investigating molecular interactions in various types of HIV-1 RT to 68NV, T4 and T5 inhibitors.

### 2.1 System studies

The complex structure from GOLD docking program (model A) and minimization by AMBER force fields (model B) were performed by selecting amino acid surrounding inhibitors within the inter atomic distance of 4 Å. The twenty residues used in this study were Pro095, Leu100, Lys101, Lys102, Lys103/Asn103, Lys104, Ser105, Val106, Glu138, Val179, Tyr181/Cys181, Tyr188, Val189, Gly190, Phe227, Trp229, Leu234, His235, Pro236 and Tyr318.

## 2.2 Particular interaction energy

The particular interaction energy was focused on the couple of inhibitor and each amino acid. Then, hydrogen atoms were added into the cutting regions using SYBYL 7.0 program and was investigated using B3LYP/6-31G(d,p) and MP2/6-31G(d,p) level of calculations by GAUSSIAN 03 program. Moreover, the basis set superposition error (BSSE) based on counterpoise scheme of Boys-Bernardi were also computed in the interaction energy.

The particular interaction energy can be defined as shown in equation (1):

$$E_{\text{int}} = E_{\text{complex}}^{AB} - E_{\text{inhibitor}}^A - E_{\text{residue}}^B \quad (1)$$

Moreover, the basis set superposition error (BSSE) based on counterpoise scheme of Boys-Bernardi were also computed to correct the particular interaction energy as shown in equation (2):

$$E_{\text{int}} = E_{\text{complex}}^{AB} - E_{\text{inhibitor}}^{AB} - E_{\text{residue}}^{AB} \quad (2)$$

Where  $E_{\text{complex}}$  is the energy of inhibitor-residue,  $E_{\text{inhibitor}}$  is the energy of inhibitor and  $E_{\text{residue}}$  is the energy of individual residue.  $AB$  is molecular orbital of inhibitor-residue.

## 3. Principal Components Analysis

Principal Components analysis (PCA), a standard tool in multivariate analysis, was used to extract as much information as possible from the large number of quantum chemical calculations, on 3 different inhibitors in 3 different HIV-1 RT proteins (wild-type and 2 mutants). The PCA a widely use statistical techniques in quantitative structure-activity relationships (QSARs) and comparative molecular-field analysis was employed. PCA is a statistical method for reducing the amount of data to

be analyzed by exploiting the correlated nature of the variables within a dataset. Linear combinations of the correlated variables are chosen such that the majority of the variance of the original data can be described by a few orthogonal components.

#### Data set for Principal Components Analysis

PCA models were generated from the 20 interaction energies obtained from the GOLD and AMBER models. Additionally, PCA was also used to analyse the AMBER model in more detail. In this case both the interaction energies and key distances between the residue and ligand were extracted and analyzed.

All PCA models were built in SIMCA-P10. All descriptors were mean centered and scaled to unit variance because the numerical values of the descriptors vary significantly. This gives each variable the same opportunity of influencing the PCA models. Components were added to a model if they passed SIMCA's internal cross-validation procedures. Data analysis was undertaken in OopenOffice.org.

## RESULTS AND DISCUSSION

### 1. Quantum Chemical Calculation Details

#### 1.1 Molecular docking by GOLD Docking program (Model A)

Based on the available of the complex structure of nevirapine derivative inhibitors and the HIV-1RT, PDB code: 1KLM, the 68NV, T4 and T5 inhibitors can be docked into the binding pocket of all target enzymes, using the GOLD Docking program. Hence, the orientations of three inhibitors in binding site which bound into three types of HIV-1 RT; WT, K103N mutant type and Y181C mutant type, as shown in Figures 5-7. All nine complex systems were used as the starting geometries for further particular interaction energy using the B3LYP/6-31G(d,p) and MP2/6-31G(d,p) of quantum chemical calculations. The obtained results of B3LYP and MP2 particular interaction energy between inhibitor and amino acids surrounding the binding pocket within the interatomic interaction with inhibitor about 4 Å are shown in Tables 2-4 for wild-type , K103N and Y181C HIV-1 RT, respectively.

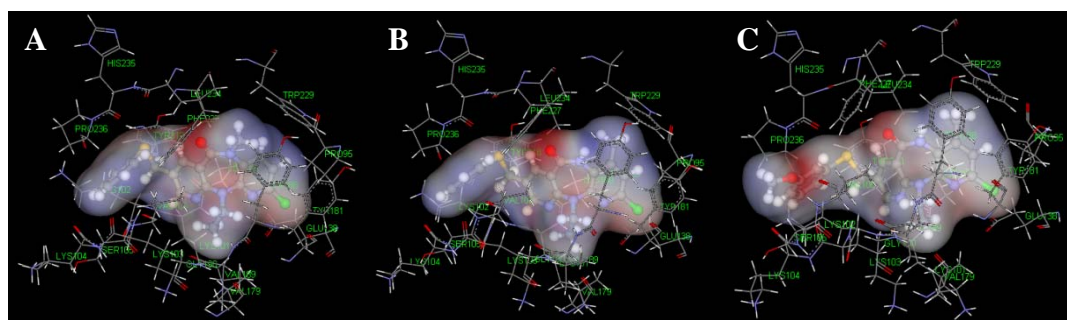


**Figure 5** Orientations of 68NV (A), T4 (B) and T5 (C) in binding site of WT HIV-1 RT.

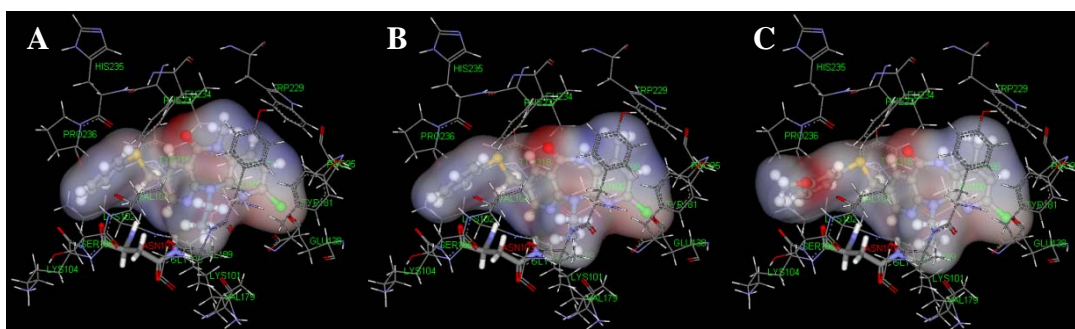


**Figure 6** Orientations of 68NV (A), T4 (B) and T5 (C) in binding site of K103N HIV-1 RT.

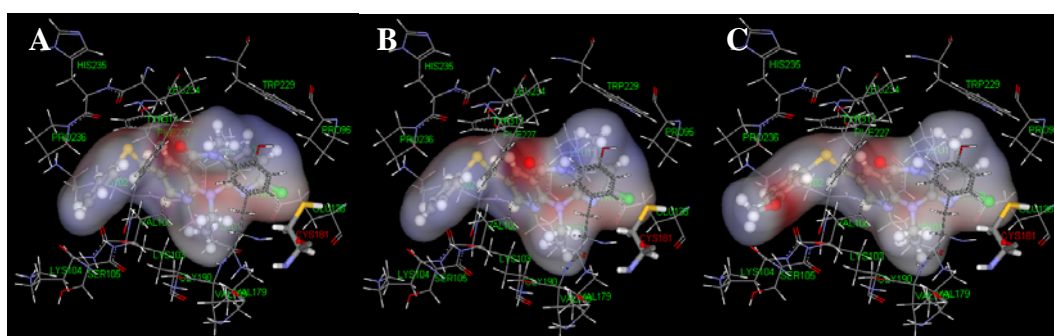


**Figure 7** Orientations of 68NV (A), T4 (B) and T5 (C) in binding site of Y181C HIV-1RT.

**Table 2** Interaction energy between inhibitors (68NV, T4 and T5) with individual residues (in kcal/mol), calculated at B3LYP/6-31G(d,p) and MP2/6-31G(d,p) levels of theory for WT HIV-1 RT in model A.

residues	Interaction Energies (kcal/mol) in WT HIV-1 RT					
	B3LYP/6-31G(d,p)			MP2/6-31G(d,p)		
	68NV	T4	T5	68NV	T4	T5
GLU138B	4.21	6.82	8.79	3.06	5.46	7.16
GLY190A	2.10	0.79	0.61	1.34	-0.51	-0.85
HIS235A	3.42	0.47	0.58	2.30	-0.70	-0.78
LEU100A	3.37	1.89	2.43	-1.99	-2.82	-3.13
LEU234A	5.81	1.19	1.08	0.46	-2.37	-2.16
LYS101A	-1.63	-2.07	-2.00	-2.32	-2.78	-2.87
LYS102A	0.92	1.24	2.19	-0.81	-0.36	-0.62
LYS103A	6.16	7.67	6.61	2.35	3.39	1.10
LYS104A	0.41	0.81	1.64	-0.84	-0.58	0.03
PHE227A	4.99	5.01	1.61	1.24	1.94	-0.53
PRO236A	2.25	1.40	9.68	-1.09	-1.67	4.14
PRO95A	0.49	0.54	0.22	-0.56	-0.52	-0.84
SER105A	0.79	0.90	0.57	-0.41	-0.49	-0.86
TRP229A	-1.05	6.19	1.75	-4.81	0.89	-2.31
TYR181A	7.53	9.84	8.94	1.96	2.42	2.17
TYR188A	7.74	6.41	2.17	1.33	-0.05	-3.02
TYR318A	7.12	2.28	4.99	2.53	-0.82	0.45
VAL106A	12.22	13.56	5.17	3.52	3.98	-1.85
VAL179A	0.05	0.46	1.03	-0.72	-0.89	-0.61
VAL189A	0.20	0.45	0.52	-1.05	-0.79	-0.61

**Table 3** Interaction energy between inhibitors (68NV, T4 and T5) with individual residues (in kcal/mol), calculated at B3LYP/6-31G(d,p) and MP2/6-31G(d,p) levels of theory for K103N HIV-1 RT in model A.

residues	Interaction Energies (kcal/mol) in K103N HIV-1 RT					
	B3LYP/6-31G(d,p)			MP2/6-31G(d,p)		
	68NV	T4	T5	68NV	T4	T5
GLU138B	4.21	6.82	8.79	3.06	5.46	7.16
GLY190A	2.10	0.79	0.61	1.34	-0.51	-0.85
HIS235A	3.42	0.47	0.58	2.30	-0.70	-0.78
LEU100A	3.37	1.89	2.43	-1.99	-2.82	-3.13
LEU234A	5.81	1.19	1.08	0.46	-2.37	-2.16
LYS101A	-1.63	-2.07	-2.00	-2.32	-2.78	-2.87
LYS102A	0.92	1.24	2.19	-0.81	-0.36	-0.62
ASN103A	6.30	9.66	13.28	1.96	4.95	7.45
LYS104A	0.41	0.81	1.64	-0.85	-0.58	0.03
PHE227A	4.99	5.01	1.61	1.24	1.94	-0.53
PRO236A	2.25	1.40	9.68	-1.09	-1.67	4.14
PRO95A	0.49	0.54	0.22	-0.56	-0.52	-0.84
SER105A	0.79	0.90	0.57	-0.41	-0.49	-0.86
TRP229A	-1.05	6.19	1.75	-4.81	0.89	-2.31
TYR181A	7.53	9.84	8.94	1.96	2.42	2.17
TYR188A	7.74	6.41	2.17	1.33	-0.05	-3.02
TYR318A	7.12	2.28	4.99	2.56	-0.82	0.45
VAL106A	12.22	13.56	5.17	3.52	3.98	-1.85
VAL179A	0.05	0.46	1.03	-0.73	-0.89	-0.61
VAL189A	0.20	0.45	0.52	-1.05	-0.79	-0.61



**Table 4** Interaction energy between inhibitors (68NV, T4 and T5) with individual residues (in kcal/mol), calculated at B3LYP/6-31G(d,p) and MP2/6-31G(d,p) levels of theory for Y181C HIV-1 RT in model A.

residues	Interaction Energies (kcal/mol) in Y181C HIV-1 RT					
	B3LYP/6-31G(d,p)			MP2/6-31G(d,p)		
	68NV	T4	T5	68NV	T4	T5
GLU138B	4.21	6.82	8.79	3.06	5.46	7.16
GLY190A	2.10	0.79	0.61	1.34	-0.51	-0.85
HIS235A	3.42	0.47	0.58	2.30	-0.71	-0.78
LEU100A	3.37	1.89	2.43	-1.99	-2.82	-3.13
LEU234A	5.81	1.19	1.08	0.46	-2.37	-2.16
LYS101A	-1.63	-2.07	-2.00	-2.32	-2.78	-2.87
LYS102A	0.92	1.24	2.19	-0.81	-0.36	-0.62
LYS103A	6.16	7.67	6.61	2.35	3.39	1.10
LYS104A	0.41	0.81	1.64	-0.84	-0.58	0.03
PHE227A	4.99	5.01	1.61	1.24	1.94	-0.53
PRO236A	2.25	1.40	9.68	-1.09	-1.67	4.14
PRO95A	0.49	0.54	0.22	-0.56	-0.52	-0.84
SER105A	0.79	0.90	0.57	-0.41	-0.49	-0.86
TRP229A	-1.05	6.19	1.75	-4.81	0.89	-2.31
CYS181A	10.39	10.39	8.45	8.70	7.21	5.56
TYR188A	7.42	6.41	2.17	1.33	-0.05	-3.02
TYR318A	7.12	2.28	4.99	2.53	-0.82	0.45
VAL106A	12.22	13.56	5.17	3.52	3.98	-1.85
VAL179A	0.05	0.46	1.03	-0.72	-0.89	-0.61
VAL189A	0.20	0.45	0.52	-0.87	-0.79	-0.61

The interaction energies obtained from B3LYP/6-31G(d,p) showed more repulsive interactions of three inhibitors in binding site than MP2/6-31G(d,p). Both methods of calculations found attractive interaction between three inhibitor and Lys101 in all complex structures because they can take the electrostatic, steric, polarization and charge transfer interaction (Nunrium *et al.*, 2005). Furthermore, the interaction energies between inhibitors and Trp229 exhibited repulsive interaction in B3LYP calculations and attractive interaction in MP2 calculations because the MP2 calculations include the dispersion interactions. B3LYP calculations can not take of this interaction, thus, MP2 calculations give more accurate interaction energies than B3LYP calculations.

Although particular interaction energy of three inhibitors in three binding pocket had more attractive at MP2 calculations, the attractive interaction remained low values in binding pocket. In addition, the key mutation residues (Asn103 and Cys181) are more repulsive with three inhibitors whereas the inhibitory activity of three inhibitors is satisfied in experimental. Therefore, the obtained complex geometries of GOLD Docking are required to minimize the whole complex structure using the AMBER force fields.

## 1.2 Minimization by AMBER force fields

The obtained AMBER force fields of the nine complex structures, consisting 68NV-WT, 68NV-K103N, 68NV-Y181C, T4-WT, T4-K103N, T4-Y181C, T5-WT, T5-K103N and T5-Y181C which were superimposed with its GOLD Docking starting geometries, are displayed in Figure 8-16, respectively. The superimposition of the backbone atom between model A (pink) and Model B (yellow) gives RMS 0.83 Å of all complex structures. This implied that the conformational change of complex structures might be influenced to the particular interaction energies. Consequently, the particular interaction energy was again performed on all systems using both B3LYP/6-31G(d,p) and MP2/6-31G(d,p) level of calculations. The obtained energy results are listed in Tables 5-7 of 68NV, T4 and T5, respectively.

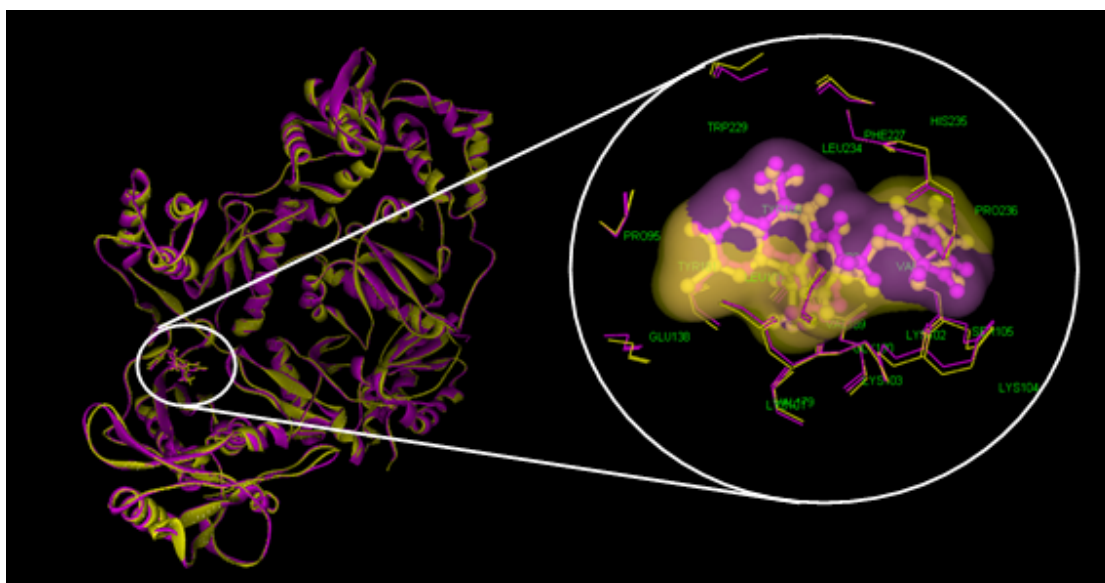


**Figure 8** Superimposition between Model A (pink) and Model B (yellow) of 68NV in WT HIV-1 RT.

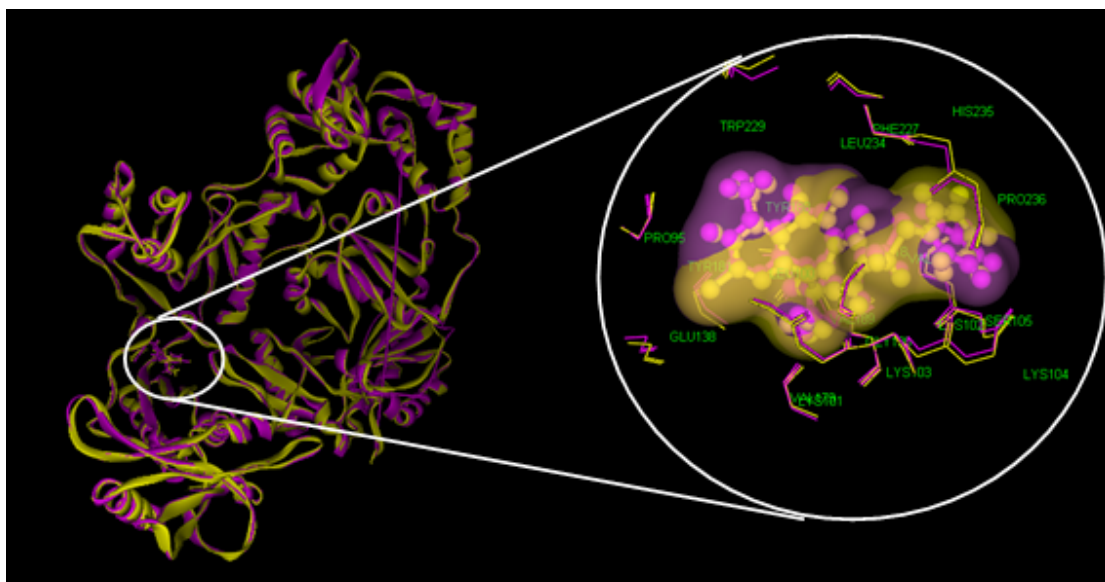


**Figure 9** Superimposition between Model A (pink) and Model B (yellow) of T4 in WT HIV-1 RT.

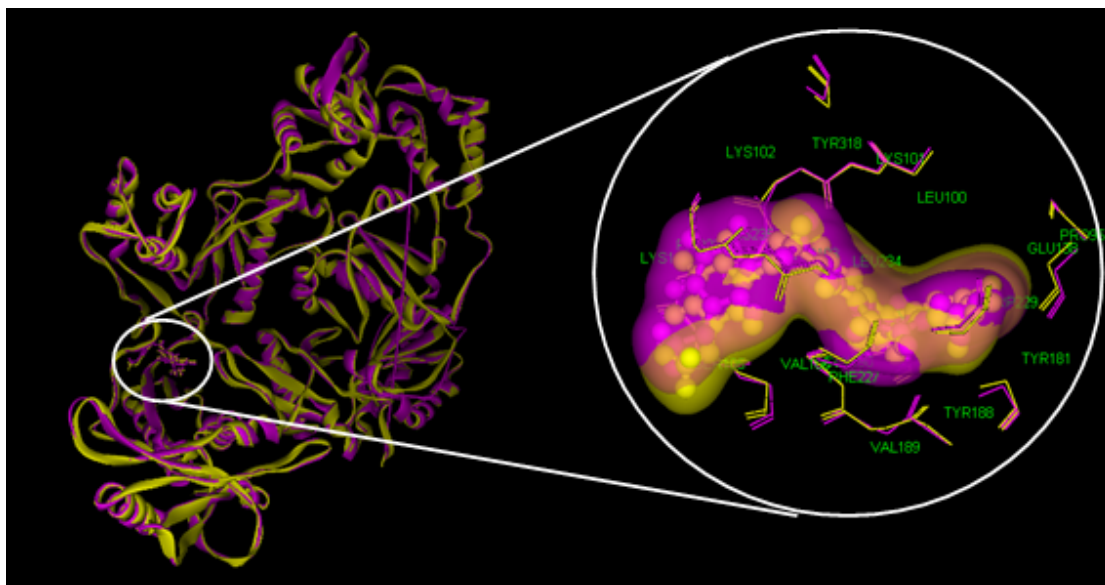


**Figure 10** Superimposition between Model A (pink) and Model B (yellow) of T5 in WT HIV-1 RT.

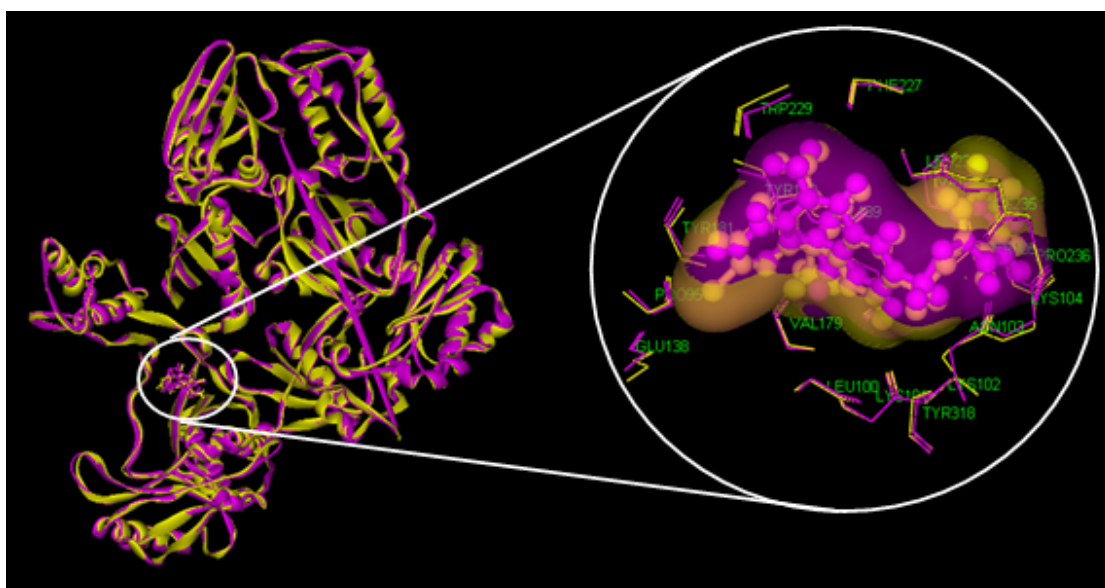


**Figure 11** Superimposition between Model A (pink) and Model B (yellow) of 68NV in K103N HIV-1 RT.

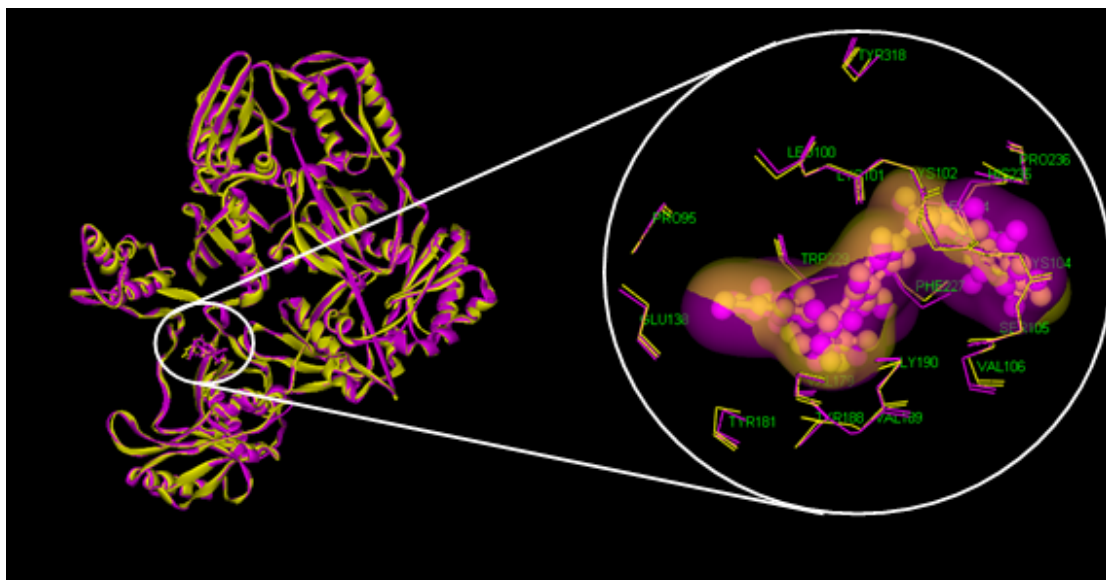


**Figure 12** Superimposition between Model A (pink) and Model B (yellow) of T4 in K103N HIV-1 RT.

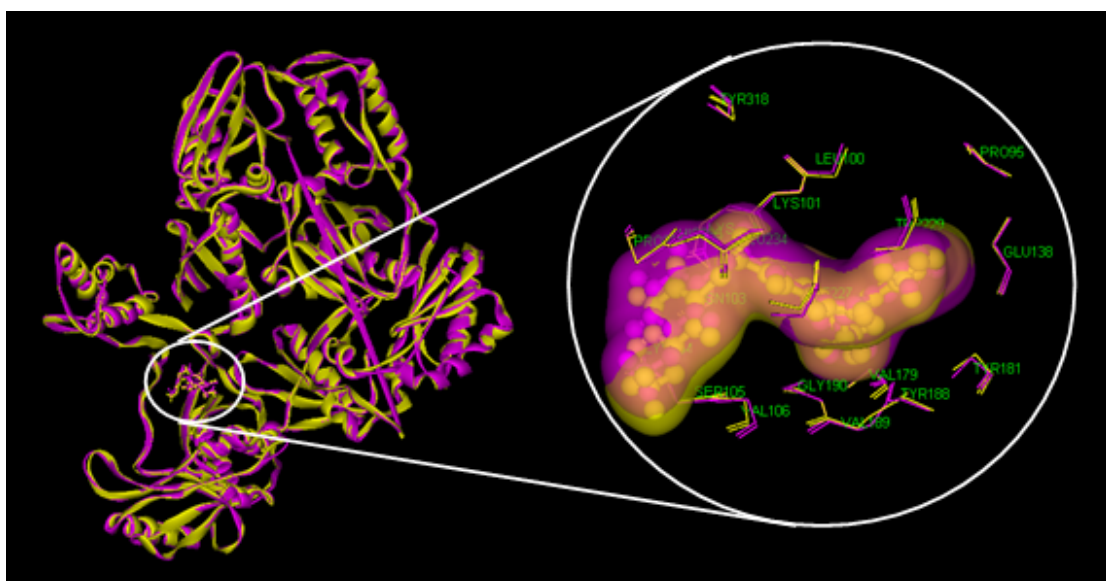


**Figure 13** Superimposition between Model A (pink) and Model B (yellow) of T5 in K103N HIV-1 RT.

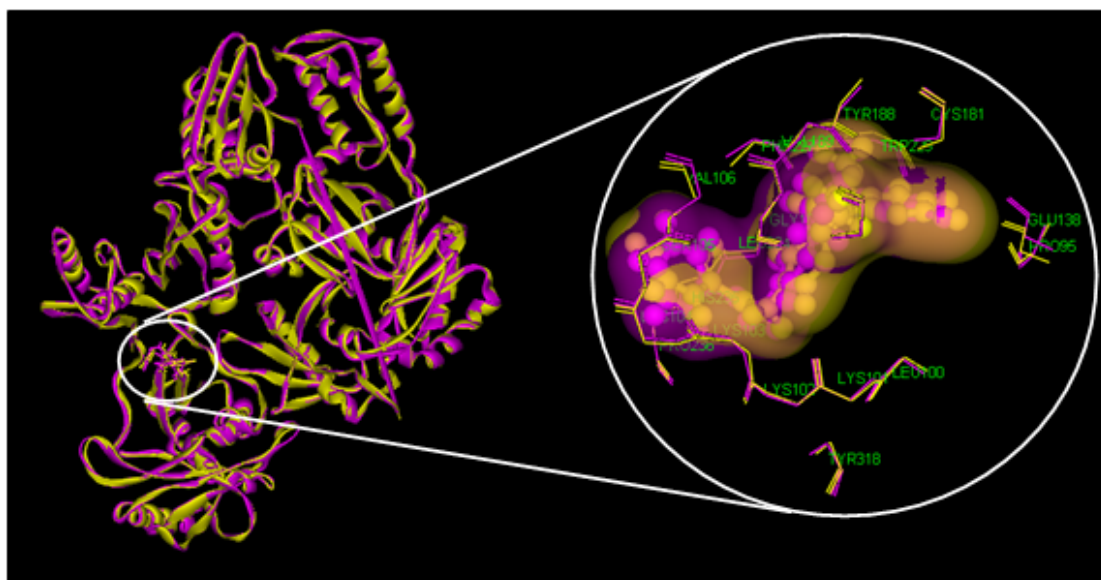


**Figure 14** Superimposition between Model A (pink) and Model B (yellow) of 68NV in Y181C HIV-1 RT.

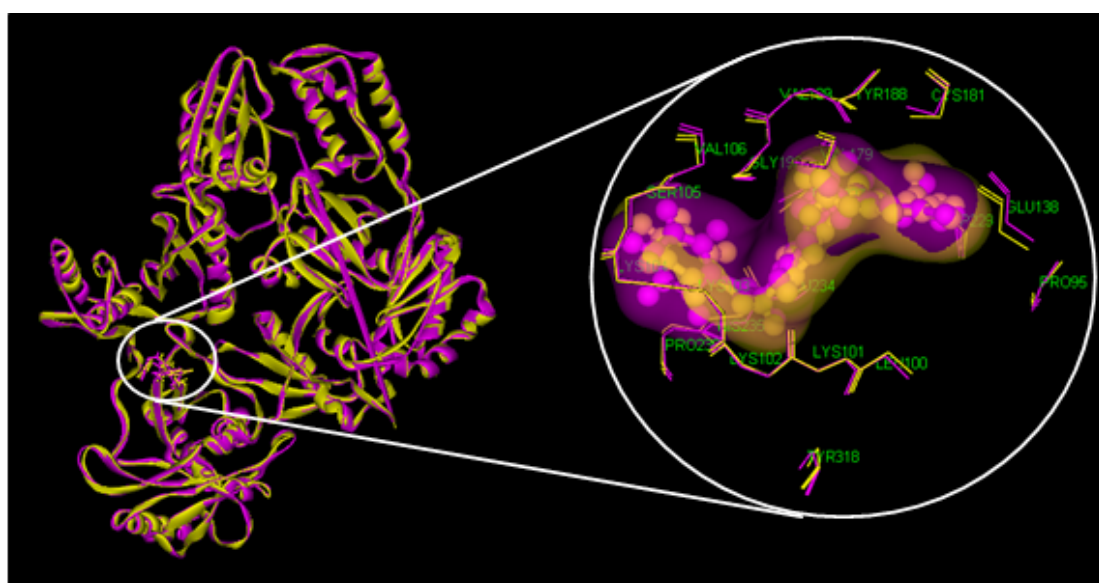


**Figure 15** Superimposition between Model A (pink) and Model B (yellow) of T4 in Y181C HIV-1 RT.

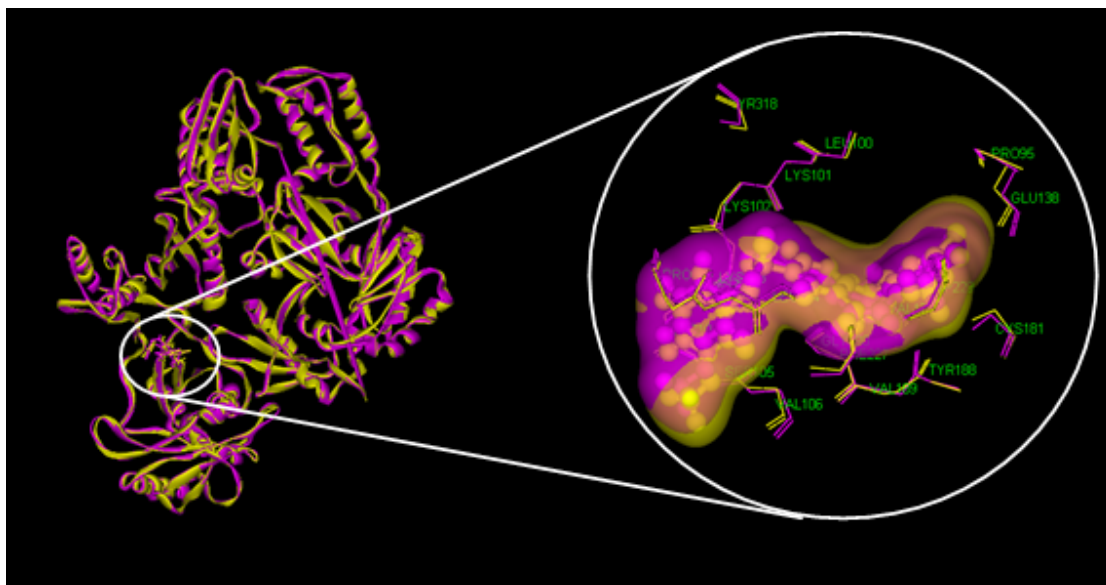


**Figure 16** Superimposition between Model A (pink) and Model B (yellow) of T5 in Y181C HIV-1 RT.



**Table 5** Interaction energy between inhibitors (68NV, T4 and T5) with individual residues (in kcal/mol), calculated at B3LYP/6-31G(d,p) and MP2/6-31G(d,p) levels of theory for WT HIV-1 RT in model B.

residues	Interaction Energies (kcal/mol) in WT HIV-1 RT					
	B3LYP/6-31G(d,p)			MP2/6-31G(d,p)		
	68NV	T4	T5	68NV	T4	T5
GLU138B	4.24	6.89	5.14	3.51	3.38	4.44
GLY190A	1.42	2.26	1.31	0.51	0.95	0.01
HIS235A	-0.98	-0.76	-0.62	-2.25	-2.05	-1.47
LEU100A	3.19	2.42	2.54	-2.48	-2.62	-2.90
LEU234A	1.49	0.96	1.79	-2.81	-2.99	-1.53
LYS101A	-2.98	-3.14	-3.65	-3.85	-3.97	-4.56
LYS102A	-2.10	-0.83	1.06	-4.00	-2.97	-0.89
LYS103A	-0.87	-1.47	-0.70	-3.74	-4.72	-4.01
LYS104A	0.02	0.09	0.57	-0.65	-0.62	-0.85
PHE227A	1.13	0.88	0.53	-2.45	-2.00	-1.69
PRO236A	1.23	1.10	1.79	-2.55	-2.82	-2.32
PRO95A	1.49	0.72	0.85	0.24	-0.33	-0.28
SER105A	-0.20	-0.24	-0.46	-1.02	-1.12	-2.29
TRP229A	-0.71	-0.39	-0.39	-4.67	-3.22	-3.32
TYR181A	1.30	1.09	0.64	-0.32	-0.11	-0.51
TYR188A	4.40	4.78	4.31	-0.95	-4.85	-5.06
TYR318A	4.90	1.81	1.03	-0.77	-2.31	-3.09
VAL106A	3.85	4.72	4.79	-3.35	-3.08	-3.18
VAL179A	0.17	0.47	0.42	-1.20	-1.12	-1.08
VAL189A	-0.10	-0.11	-0.02	-1.36	-1.32	-1.02



**Table 6** Interaction energy between inhibitors (68NV, T4 and T5) with individual residues (in kcal/mol), calculated at B3LYP/6-31G(d,p) and MP2/6-31G(d,p) levels of theory for K103N HIV-1 RT in model B.

residues	Interaction Energies (kcal/mol) in K103N HIV-1 RT					
	B3LYP/6-31G(d,p)			MP2/6-31G(d,p)		
	68NV	T4	T5	68NV	T4	T5
GLU138B	633.86	4.51	656.41	3.00	3.73	4.16
GLY190A	1.52	2.29	1.69	0.52	1.17	0.53
HIS235A	-0.92	-0.75	-1.14	-2.29	-2.09	-2.02
LEU100A	3.17	2.69	2.47	-2.04	-2.12	-2.39
LEU234A	1.78	0.77	1.62	-2.81	-3.26	-1.89
LYS101A	-3.12	-3.75	-4.40	-4.08	-4.64	-5.31
LYS102A	-2.48	-0.72	1.04	-4.42	-2.42	-0.65
ASN103A	-0.52	-3.16	0.27	-4.19	-6.72	-3.67
LYS104A	-0.02	0.03	0.24	-0.66	-0.66	-1.09
PHE227A	1.63	1.20	1.30	-2.14	-1.93	-1.27
PRO236A	1.62	0.92	2.01	-2.32	-2.97	-2.12
PRO95A	0.44	0.61	0.79	-0.49	-0.42	-0.30
SER105A	-0.14	-0.24	-0.47	-0.87	-1.04	-2.31
TRP229A	-1.25	-0.35	-0.40	-4.36	-3.13	-3.26
TYR181A	4.14	4.39	4.28	-0.23	-0.37	-0.71
TYR188A	5.10	2.60	2.21	-0.49	-4.51	-4.69
TYR318A	1.39	1.17	0.64	-2.35	-2.26	-2.41
VAL106A	3.87	4.70	5.11	-3.34	-3.16	-2.89
VAL179A	0.27	0.56	0.65	-1.25	-1.14	-0.99
VAL189A	-0.02	-0.14	-0.03	-1.48	-1.60	-1.29

**Table 7** Interaction energy between inhibitors (68NV, T4 and T5) with individual residues (in kcal/mol), calculated at B3LYP/6-31G(d,p) and MP2/6-31G(d,p) levels of theory for Y181C HIV-1 RT in model B.

residues	Interaction Energies (kcal/mol) in Y181C HIV-1 RT					
	B3LYP/6-31G(d,p)			MP2/6-31G(d,p)		
	68NV	T4	T5	68NV	T4	T5
GLU138B	4.58	633.00	620.82	3.82	3.94	4.65
GLY190A	1.65	1.70	1.17	0.67	0.51	-0.09
HIS235A	-0.97	-0.82	-0.79	-2.18	-2.15	-1.54
LEU100A	2.64	2.09	1.74	-3.13	-3.27	-3.58
LEU234A	1.21	0.77	1.74	-2.93	-3.25	-1.47
LYS101A	-3.05	-3.29	-3.80	-3.95	-4.13	-4.69
LYS102A	-1.62	-0.72	1.10	-3.50	-2.56	-0.77
LYS103A	-0.68	-1.44	-0.09	-3.57	-4.45	-3.49
LYS104A	0.05	0.14	0.52	-0.61	-0.54	-0.86
PHE227A	0.87	1.06	0.81	-2.57	-2.02	-1.46
PRO236A	1.10	1.00	2.17	-2.57	-2.89	-1.96
PRO95A	1.34	1.14	1.22	0.06	0.07	0.07
SER105A	-0.23	-0.26	-0.53	-1.05	-1.09	-2.28
TRP229A	-0.30	-0.19	-0.22	-4.79	-2.74	-3.19
CYS181A	2.78	3.83	3.42	-0.01	2.10	1.31
TYR188A	5.32	2.38	1.34	-0.80	-5.25	-5.45
TYR318A	1.26	1.01	0.69	-2.07	-2.30	-2.78
VAL106A	4.06	4.20	4.31	-3.24	-3.21	-3.26
VAL179A	0.22	0.40	0.41	-1.16	-1.12	-1.09
VAL189A	0.00	-0.08	0.04	-1.43	-1.20	-0.99

The obtained results of particular interaction energies from model B, the B3LYP/6-31G(d,p) shows more repulsive interaction between inhibitor and residues in binding site whereas MP/6-31G(d,p) reveals more attractive interaction between inhibitor and residues in binding site. Moreover, both methods can take the electrostatic, steric, polarization and charge transfer interaction as seen in Lys101. Furthermore, MP2 calculations can take of the dispersion interactions whereas B3LYP calculations can not take of this interaction, as seen in Glu138, Trp229 and Tyr188. These results are similar to model A. Therefore, the obtained MP2/6-31G(d,p) will be used to analyze the deeply molecular details of the interaction types between inhibitor and residues.

## **2. Principal Components Analysis**

We required the use of PCA to effectively interpret the large number of theoretical interaction energies and distances derived from simulations of 3 different inhibitors at 3 distinct protein variants, which are modeled using 20 active site amino acids. This allowed us to transform the large number of inherently correlated variables into a smaller number of uncorrelated, so called latent variables or components. The PCA method was applied to interaction energies of both model A (GOLD docking derived protein-ligand complex) and B (GOLD docking derived protein-ligand complex, which is followed by AMBER force fields and minimization protocols). Three separate models were generated; Model A interaction energies, Model B interaction energies and Model B interaction energies and key distances between the protein and ligand. The statistics obtained from these analyses are shown in Tables 8-10 and the corresponding scores and loading plots obtained in Figures 17-19.

In order to interpret the PCA data it is necessary to understand the relationship between scores and loading plots. The loading plot is a multi-dimensional representation of the correlation between the descriptors used in the model. The dimensionality is determined by the numbers of components fitted, the scores plot shows the corresponding relationship between the observations based on the correlation between their descriptors and both plots can be interpreted together. On

the loading plot, descriptors found at the extreme ends of either the  $x$  or  $y$  axes have the most significant impact on the component that defines that axis. Descriptors found close to each other in PCA space are highly correlated while those that are similar on just one component are still correlated, but to a lesser extent. In contrast, those descriptors found at opposite ends of the component(s) are inversely correlated. Descriptors that are found close to zero have a negligible effect on that component. The scores plot is interpreted in an identical manner, those observations found clustered together on say the first component are correlated with each other, and these depend positively on the descriptors with a positive value on the corresponding loading plot, and negatively with descriptors with a negative loading on that same component.

Using this information, and by a systematic examination of the loadings and scores plot, we can extract a significant amount of information not easily obtained from more traditional analysis. This allows us to easily chart the changes in the different types of HIV-1 RT, whether their variation is positively or negatively correlated, or whether the particular changes are negligible. In our case all models led to the data being projected onto just two, easily interpretable lower dimensions as a result of the high degree of correlation between the descriptors.

## 2.1 Molecular docking by GOLD Docking program (Model A)

The  $r^2$  value describes the extent to which the descriptors used in the model are described by the  $N$  components. The PCA results for the interaction energies derived from model A show that 94% of the total variance in the descriptors are described by just 3 components. This corresponds to 66%, 18% and 10% for component 1, 2 and 3, respectively, as shown in Table 8. We use only the first two components for the purpose of interpretation given that the  $q^2$  increases dramatically for components 1 and 2. While the  $q^2$  associated with the 2 chosen components may seem relatively small, we are not using the model in a predictive sense, rather using it to help evaluate the results in combination with a visual analysis of the 3D results and additional knowledge of active site derived from other SDM studies.

**Table 8**  $r^2$  and  $q^2$  of PCA plot in model A, calculated at MP2/6-31G(d,p) level of theory.

Number of component	$r^2$	$q^2$
1	0.66	0.47
2	0.84	0.63
3	0.94	0.75

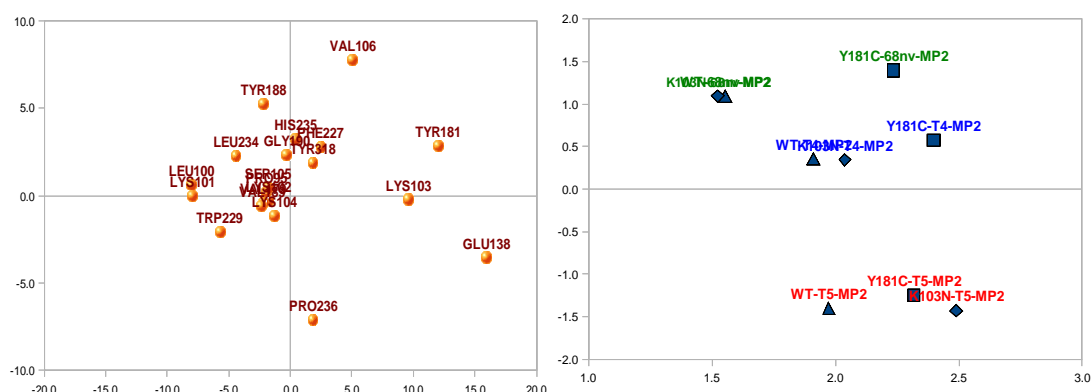


**Figure 17** PCA scores (left) and loading (right) plots: plot of component one (x axis) against component two (y axis) of model A, calculate at MP2/6-31G(d,p) level of theory.

Figure 17, the loading plot (right), component one cannot separate variables because they are very similarity. The component two can separate type of inhibitor. The score plot (left), component one, descriptors such as Tyr181, Lys103 and Glu138 have important in positive significant. Therefore, they are correlative in positive sense with all inhibitors in all enzymes in loading plot. On the other hand, Leu100, Lys101 and Trp229 have negative significant on this component. So, they are inversely correlated with positive sense. These results indicate that interaction energy decrease from positive to negative. Consideration component two, descriptors have small effect on this component, which separate T5 from each other in loading plot, Tyr188 and Val106 have positive significant. Thus they are correlative with 68NV

and T4 in positive sense and they are correlative with T5 in negative sense, indicating that interaction energy decrease in T5 than other. Only Pro236 has negative significant. Thus it has inverse correlation with positive score plot.

## 2.2 Minimization by AMBER force fields (Model B)

The results from the PCA model building shows that we can explain 99% of the total information contained in the interaction energies of model B using just 3 components. These correspond to approximately 93%, 4% and 2% for component 1, 2 and 3, respectively, as shown in Table 9. Again, we restrict ourselves to just two components due to reasons of cross-validation and also because the 3<sup>rd</sup> component do not add significantly to the amount of data being explained.

**Table 9**  $r^2$  and  $q^2$  of PCA plot in model B, calculated at MP2/6-31G(d,p) level of theory.

Number of Component	$r^2$	$q^2$
1	0.93	0.90
2	0.97	0.94
3	0.99	0.94

The PCA analysis of model B, based on interaction energy obtaining from MP2/6-31G(d,p) describes approximately 97% of total variance in the 20 descriptors by using 2 component. The first component extracted describes 93% of total variance in the descriptors, whereas the second describes just 4%.

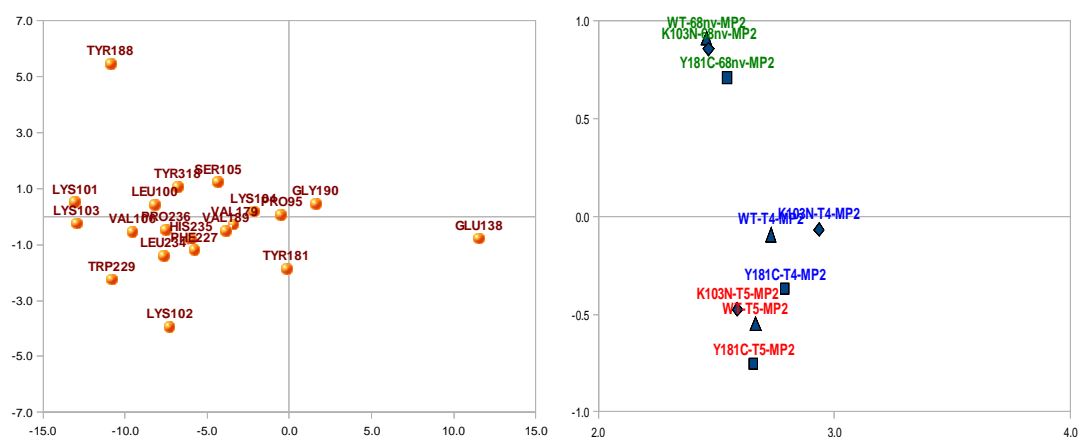


**Figure 18** PCA scores plot (left) and loading plot (right): plot of component one (x axis) against component two (y axis) of model B, calculated at MP2/6-31G(d,p) level of theory.

In Figure 18, the loading plot (right), component one cannot separate variables because they are very similar. Component two type separates of inhibitor. The score plot (right), component one, descriptors such as Glu138 has important positive significant on this component. Therefore, it is correlative in positive sense with all inhibitors in all enzymes. On the other hand, Lys101, Lys103, Tyr188 and Trp229 have important negative significant which inversely correlated with positive sense. These results indicate that interaction energy decrease from positive to negative. Consideration component two, descriptors have small effect on this component, which separate 68NV from each other in loading plot. Only Tyr188 has positive significant. Thus they are correlative with 68NV in positive sense and they are correlative with T4 and T5 in negative sense, indicating that interaction energy increase in 68nv than other. Lys102, Tyr181 and Trp229 have negative significant. Thus it has inverse correlation with positive score plot.

### 2.3 Starting Complex Structure Comparison

When considering the PCA score plot of model A compare with model B in Figure 17 and Figure 18, respectively. Component one negative significant Leu100, Trp229 and Lys101 showed less significant difference, these implied that the interaction have small change between two models. Component one positive significant Glu138 showed less significant difference whereas Tyr181 and Lys103 show high significant difference by inverse to negative loading in model B. These implied that the interaction have small change in Glu138 and large change in Tyr181 and Lys103 between two models. Component two positive significant Val106 showed high significant difference by inverse to negative loading in model B these implied that the interaction has large change between two models. Component two negative significant Pro236 showed high significant difference by inverse to positive significant in model B. These implied that the interaction showed large change between two models.

This means that the AMBER force field minimizations of model B can dominantly decrease the interaction energy of Tyr181, Lys103, Val106 and Pro236, comparing with the GOLD docking of model A as shown in Figure 19-27. Consideration of all superimposing figures, they seem to be closer between the inhibitor and residues around the binding sites when compare with Model A. On the other hand it can be remainder interaction energy of Leu100, Lys101, Trp229 and Glu138 as shown in Figure 28-36. Therefore, the obtained particular interaction energies of AMBER force fields of model B at MP2/6-31G(d,p) will be used to analyze the deeply molecular details of inhibitor-residues distance interactions.



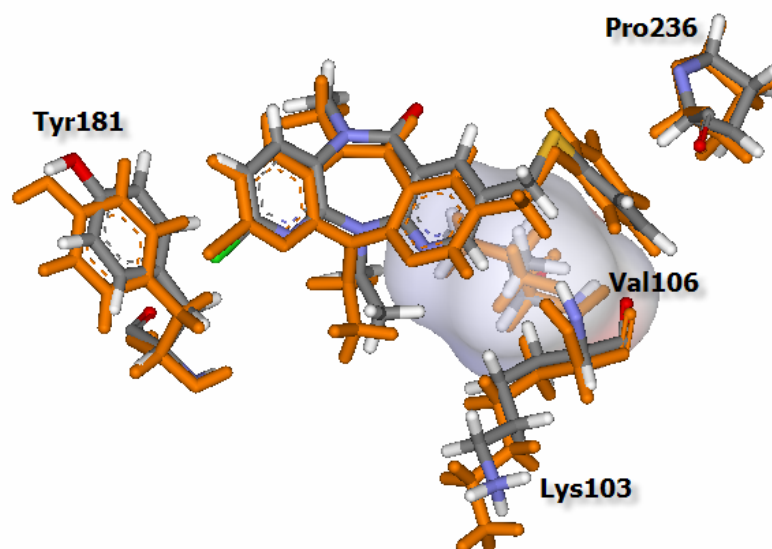


**Figure 19** Superimposition between model A (atom-type color) and model B (orange) of 68NV with residues (Tyr181, Pro236, Val106 and Lys103) in WT HIV-1 RT.

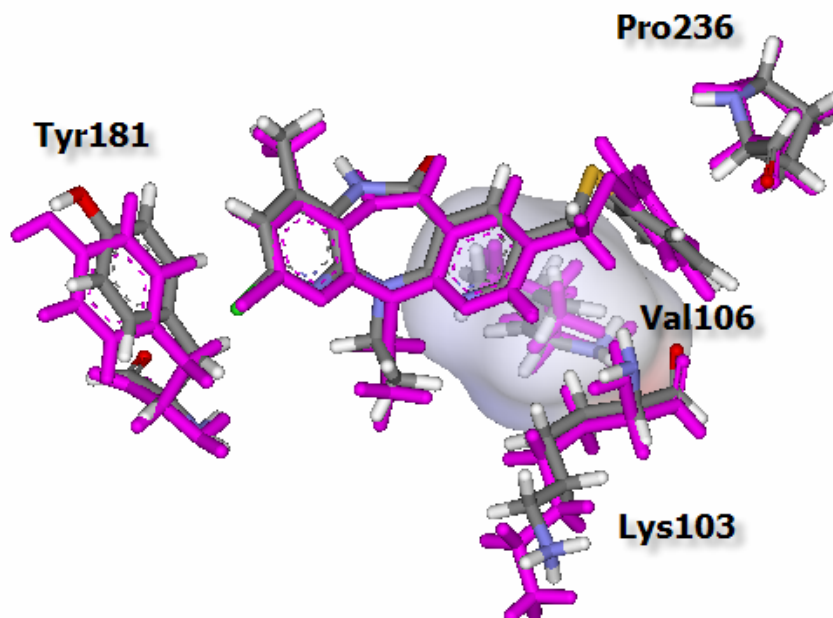


**Figure 20** Superimposition between model A (atom-type color) and model B (pink) of T4 with residues (Tyr181, Pro236, Val106 and Lys103) in WT HIV-1 RT.

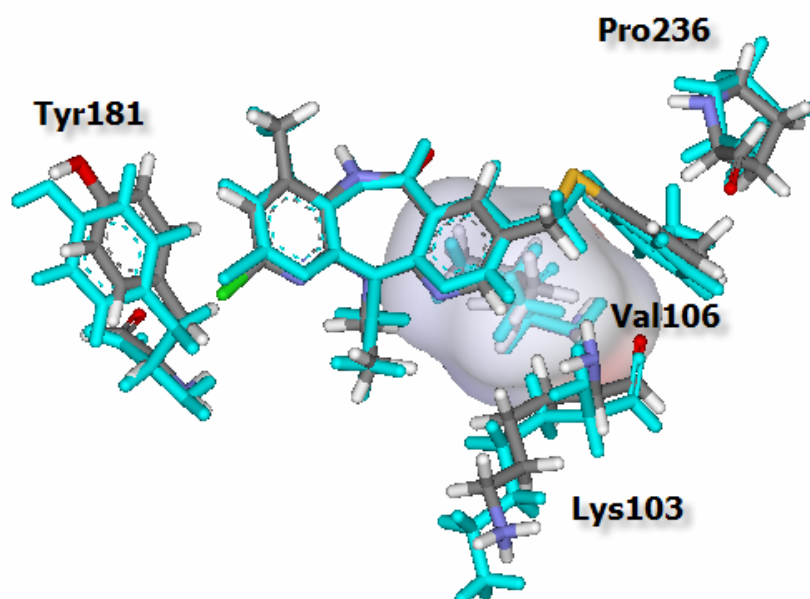


**Figure 21** Superimposition between model A (atom-type color) and model B (green) of T5 with residues (Tyr181, Pro236, Val106 and Lys103) in WT HIV-1 RT.

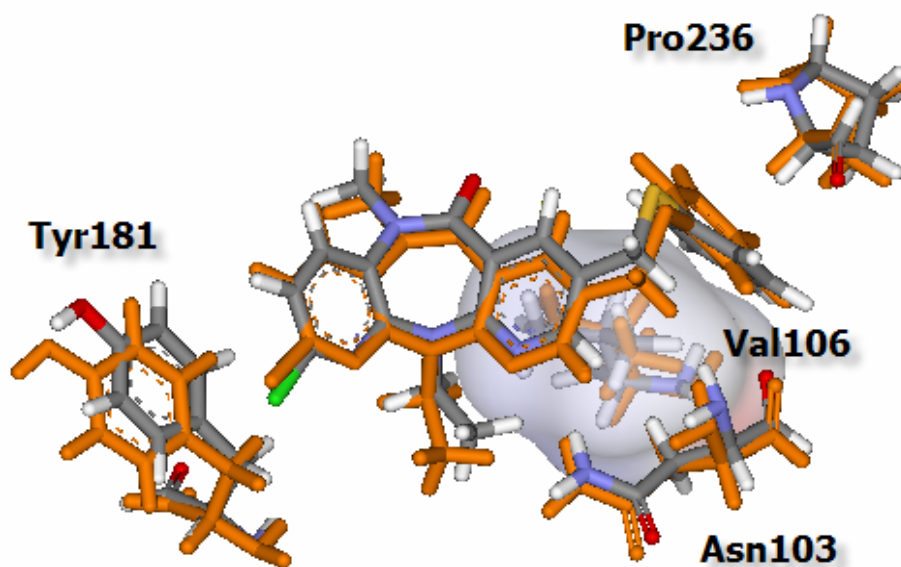


**Figure 22** Superimposition between model A (atom-type color) and model B (orange) of 68NV with residues (Tyr181, Pro236, Val106 and Asn103) in K103N HIV-1 RT.

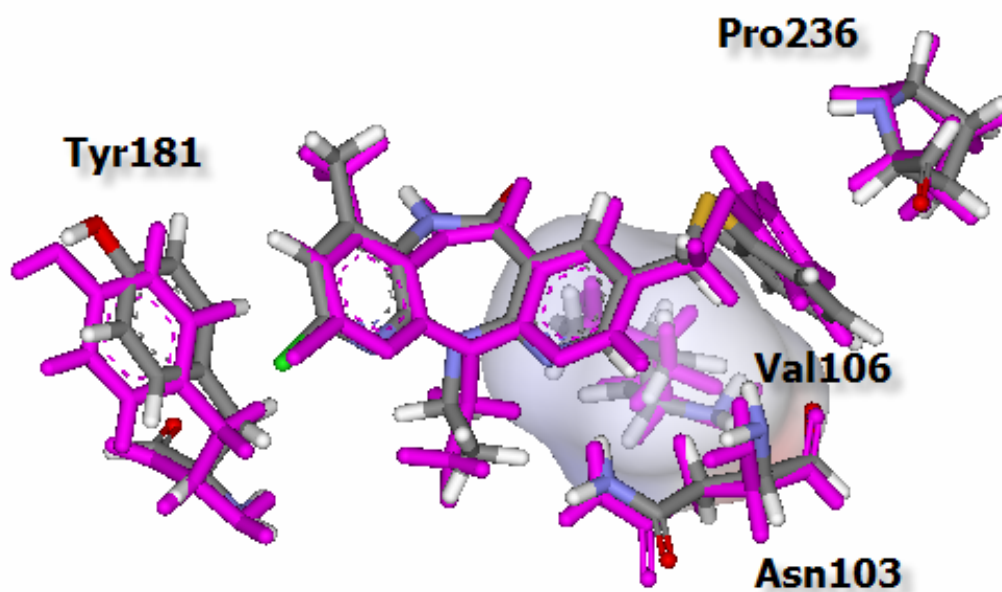


**Figure 23** Superimposition between model A (atom-type color) and model B (pink) of T4 with residues (Tyr181, Pro236, Val106 and Asn103) in K103N HIV-1 RT.

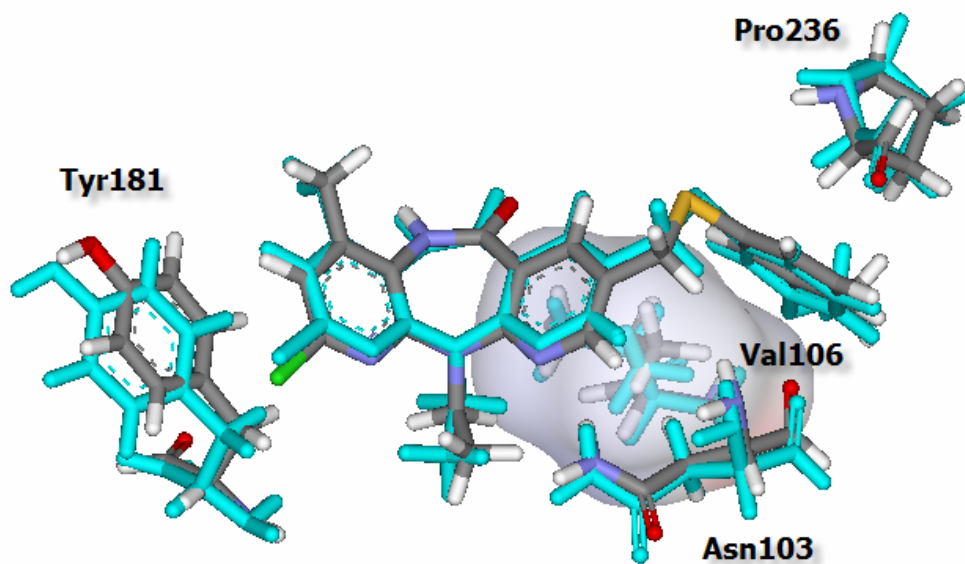


**Figure 24** Superimposition between model A (atom-type color) and model B (green) of T5 with residues (Tyr181, Pro236, Val106 and Asn103) in K103N HIV-1 RT

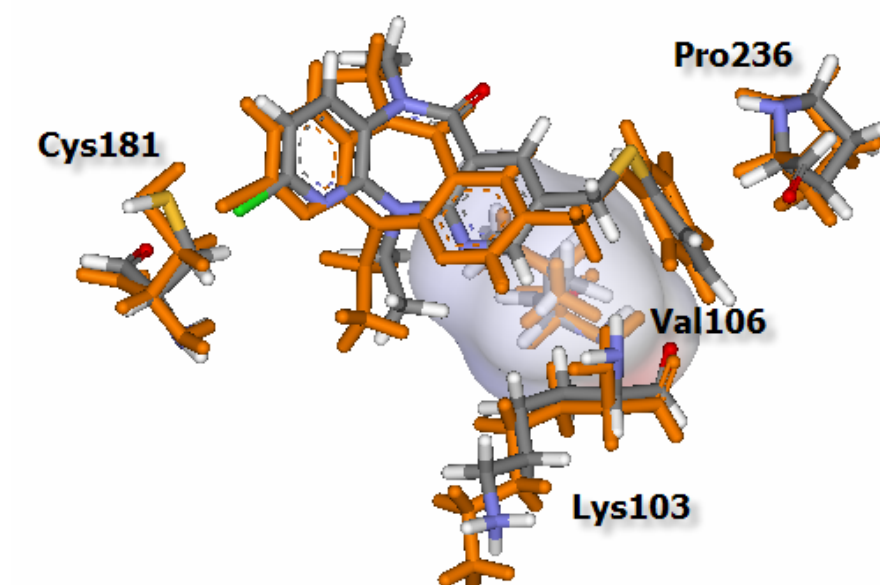


**Figure 25** Superimposition between model A (atom-type color) and model B (orange) of 68NV with residues (Cys181, Pro236, Val106 and Lys103) in Y181C.

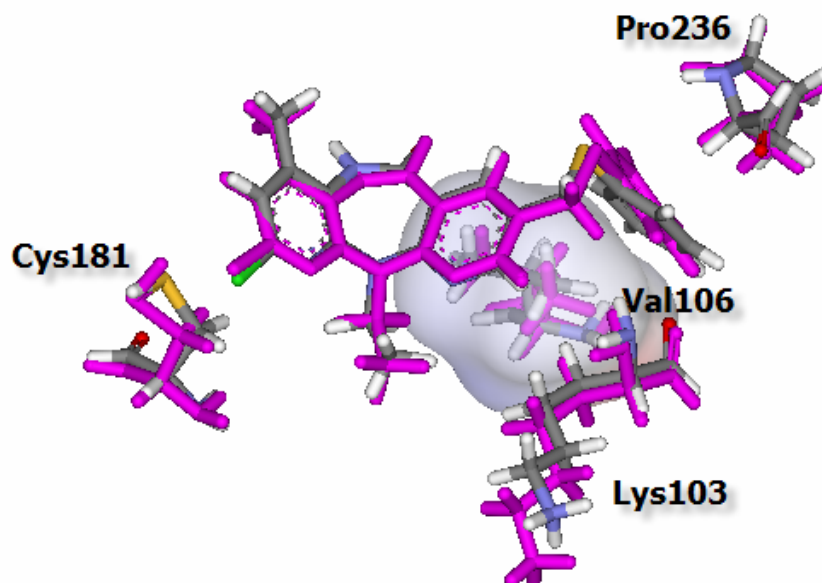


**Figure 26** Superimposition between model A (atom-type color) and model B (pink) of T4 with residues (Cys181, Pro236, Val106 and Lys103) in Y181C HIV-1 RT.

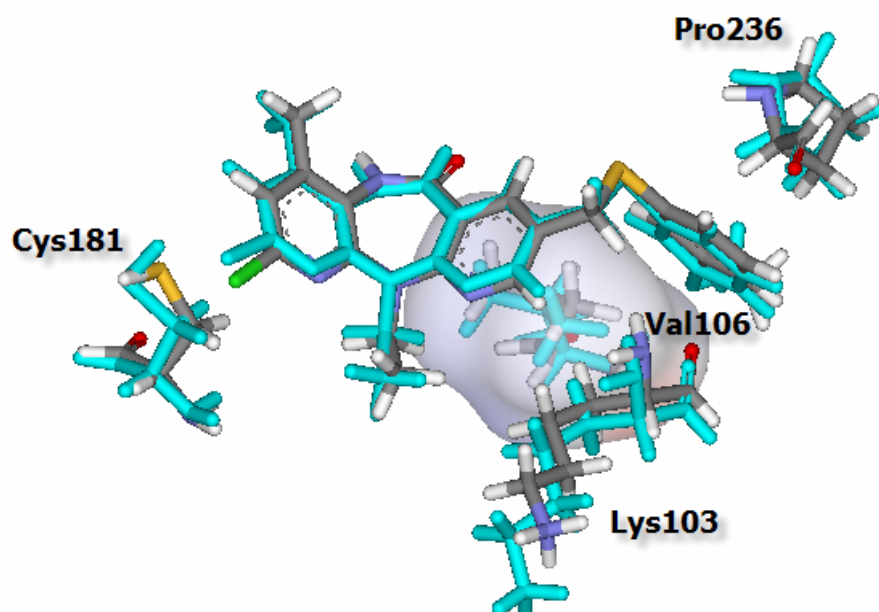


**Figure 27** Superimposition between model A (atom-type color) and model B (green) of T5 with residues (Cys181, Pro236, Val106 and Lys103) in Y181C HIV-1 RT.

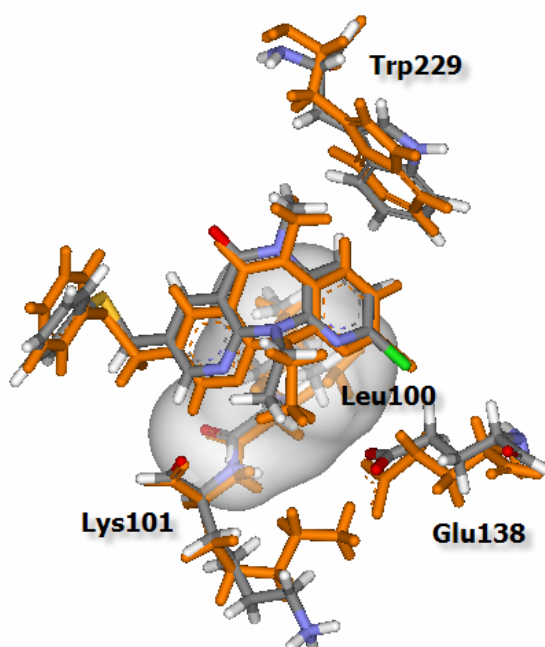


**Figure 28** Superimposition between model A (atom-type color) and model B (orange) of 68NV with residues (Lys101, Leu100, Trp229 and Glu138) in WT HIV-1 RT.

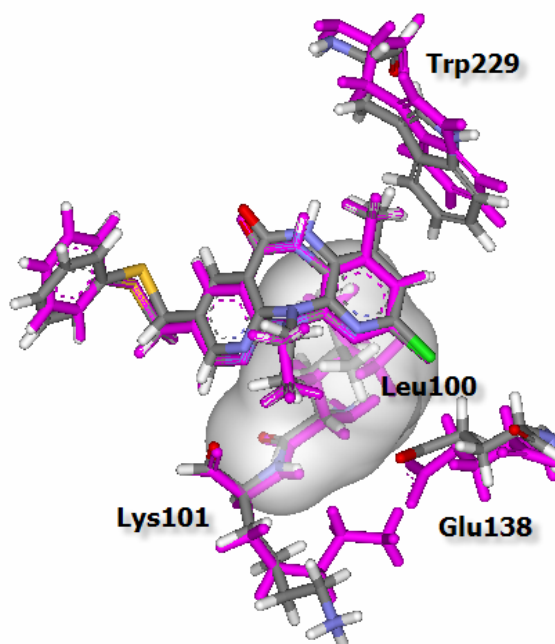


**Figure 29** Superimposition between model A (atom-type color) and model B (pink) of T4 with residues (Lys101, Leu100, Trp229 and Glu138) in WT HIV-1 RT.

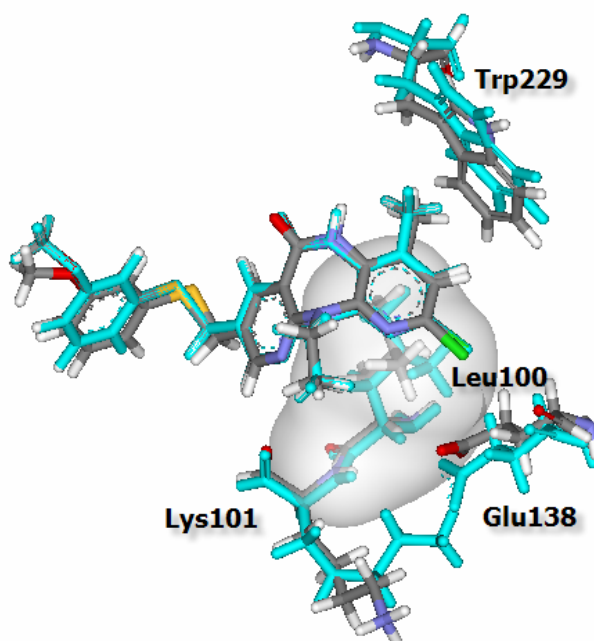


**Figure 30** Superimposition between model A (atom-type color) and model B (green) of T5 with residues (Lys101, Leu100, Trp229 and Glu138) in WT HIV-1 RT.

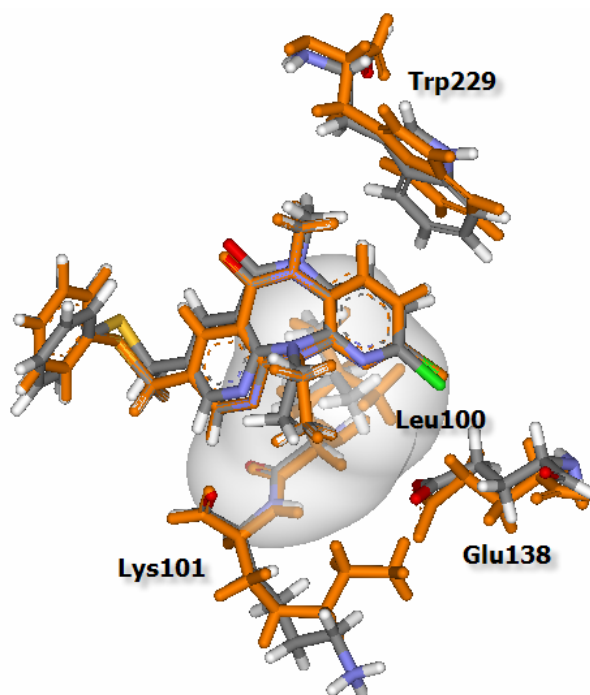


**Figure 31** Superimposition between model A (atom-type color) and model B (orange) of 68NV with residues (Lys101, Leu100, Trp229 and Glu138) in K103N HIV-1 RT.

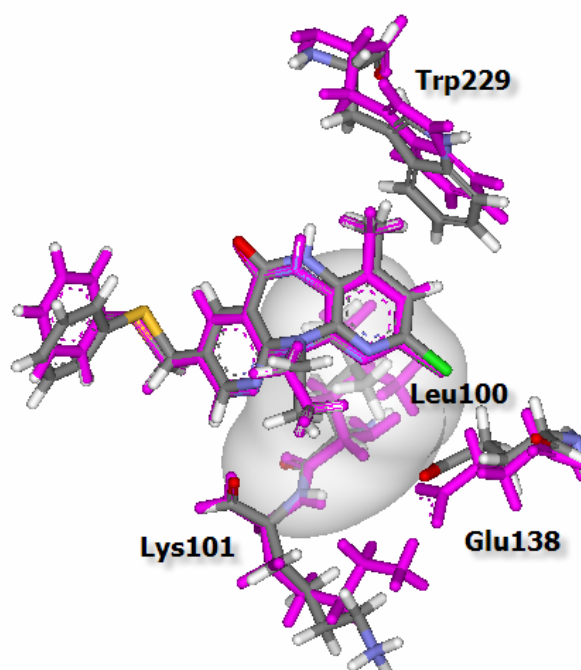


**Figure 32** Superimposition between model A (atom-type color) and model B (pink) of T4 with residues (Lys101, Leu100, Trp229 and Glu138) in K103N HIV-1 RT.



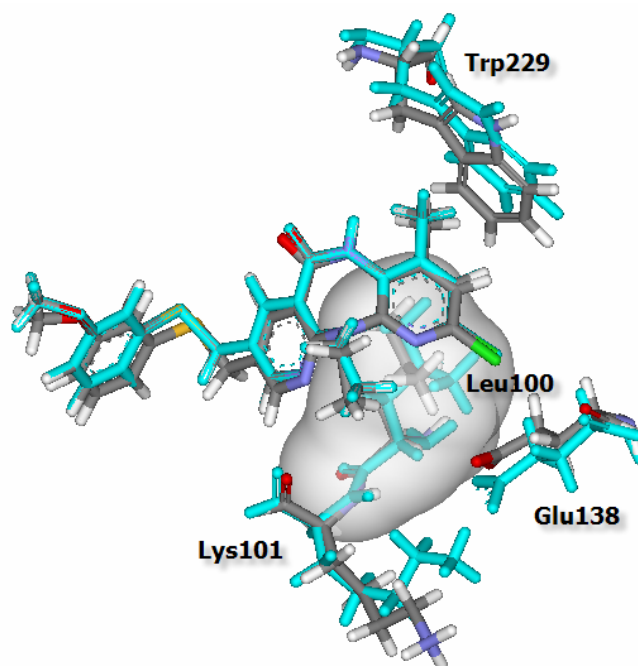


**Figure 33** Superimposition between model A (atom-type color) and model B (green) of T5 with residues (Lys101, Leu100, Trp229 and Glu138) in K103N HIV-1 RT.

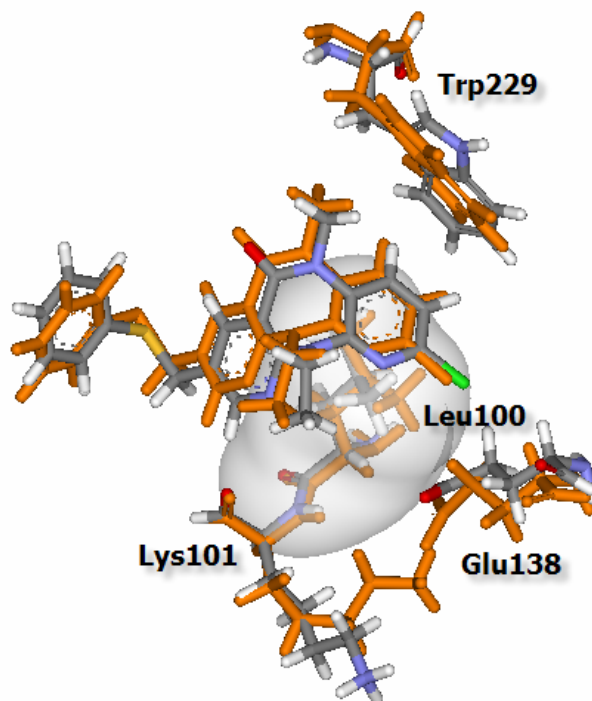


**Figure 34** Superimposition between model A (atom-type color) and model B (orange) of 68NV with residues (Lys101, Leu100, Trp229 and Glu138) in Y181C HIV-1 RT.



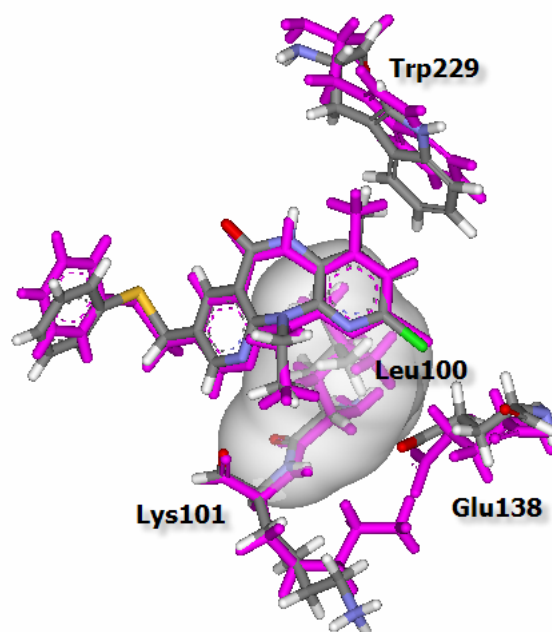


**Figure 35** Superimposition between model A (atom-type color) and model B (pink) of T4 with residues (Lys101, Leu100, Trp229 and Glu138) in Y181C HIV-1 RT.

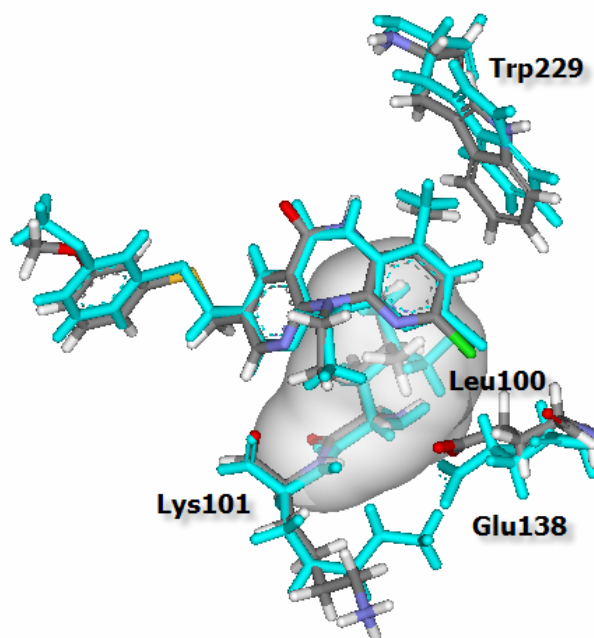


**Figure 36** Superimposition between model A (atom-type color) and model B (green) of T5 with residues (Lys101, Leu100, Trp229 and Glu138) in Y181C HIV-1 RT.

## 2.4 Model B Result: Analysis of Structural and Energetic Parameters

In addition to the interaction energies, distances associated with each of the key residues were extracted and these were used to build the PCA model. The residues chosen for the analysis are: Lys101, Lys102, Lys103, Tyr188, Tyr181, Trp229 and Glu138 as these all form important H- $\pi$  stacking or H-bond interaction interactions with the NNRT inhibitors and have significant loadings on the PCA loading plot of model B. The interaction energies and key distances between the residues and ligand were showed in Table 11 and Figures 38-46.

PCA was again used to analyze the quantum chemical calculation results and the details are shown in Table 10 and Figure 37. The  $r^2$  value indicates that the PCA model can describe 84% of the total variance using just 3 components; approximately 49%, 19% and 16% for component 1, 2 and 3, respectively. As before, we focus on the first two components as the final two have suboptimal cross-validation statistics and do not add particularly to the total explained variance above the first two components.

**Table 10**  $r^2$  and  $q^2$  of PCA plot of inhibitor-residue distances and energy of model B, calculated at MP2/6-31G(d,p) level of theory.

Number of Component	$r^2$	$q^2$
1	0.49	0.25
2	0.68	0.30
3	0.84	0.34

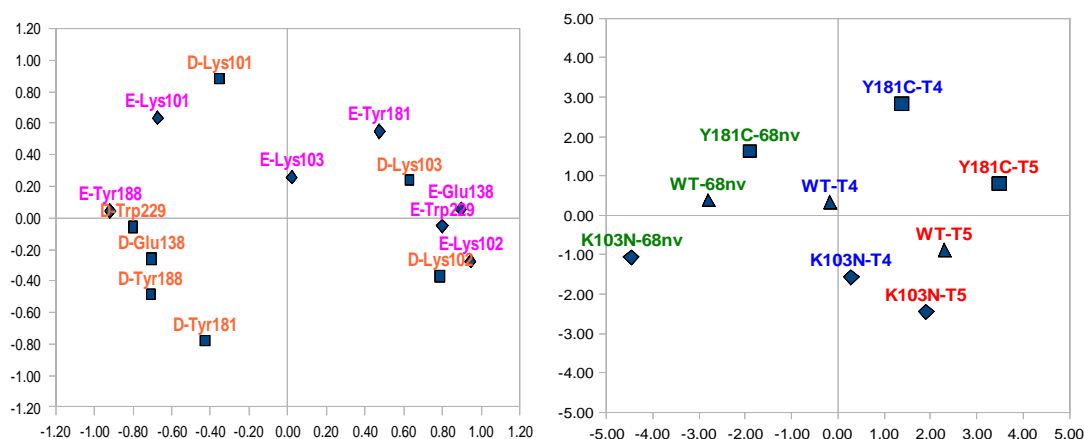


**Figure 37** PCA scores plot (left) and loading plot (right): plot of component one (x axis) against component two (y axis) of inhibitor-residue distances of model B, calculated at MP2/6-31G(d,p) level of theory.

Figure 37, the score plot (right), firstly considering correlation between interaction energy and distance found that interaction energy and distance are consistent in all cases except Glu138, Trp229 and Tyr181.

Then considering relationship between inhibitors and residues in score and loading plots, component one which can separate type of inhibitor in score plot found that Glu138, Trp229 and Lys102 have important positive significant. They are high correlation with T5, T4 and 68NV, respectively, in each enzyme, Glu138 revealed repulsive electrostatic interaction between chloride atom in pyridine ring of inhibitors and hydrogen atom in side chain of residue due to effect of anion charge in side chain of residue (Figure 38). Lys102 revealed attractive electrostatic interaction with 68NV and T4 occurred between sulfur atom of two inhibitors and cation charge in side chain of residue, while T5 is not found this interaction (Figure 40), Trp229 revealed H- $\pi$  interaction with three inhibitors occurred between hydrogen atom in pyridine ring of inhibitor and  $\pi$ -center of aromatic in side chain of residue in 68NV, while T4 and T5 found H- $\pi$  interaction between hydrogen atom of methyl group of two inhibitors and  $\pi$ -center of aromatic in side chain of residue (Figure 43). From this

results indicating that interaction energy between inhibitor and these residues decrease from T5 to T4 and 68NV, respectively in each enzyme.

On the other hand Tyr188 and Lys101 have important negative significant. It is high correlation with 68NV, T4 and T5, respectively, in each enzyme, Tyr188 revealed H- $\pi$  interaction with three inhibitors, 68NV occurred between hydrogen atom of methyl group of inhibitor and  $\pi$ -center of aromatic in side chain of residue, T4 and T5 found two H- $\pi$  interactions. Firstly, hydrogen atom of methyl group of two inhibitors and  $\pi$ -center of aromatic in side chain of residue. Secondly, hydrogen atom in pyridine ring and  $\pi$ -center of aromatic in side chain of residue, respectively (Figure 46), Lys101 revealed H-bond interaction with three inhibitors occurred between hydrogen atom in pyridine ring of three inhibitors and carbonyl group in backbone of residue (Figure 39). The results indicate that interaction energy between inhibitor and these residues decrease from 68NV to T4 and T5, respectively in each enzyme.

Moreover, Tyr181 has high correlation with T4 in Y181C, Tyr181 change to Cys181 in this enzyme, indicating that interaction energy increase on T4 than other because Cys181 revealed steric interaction between chloride atom in pyridine ring of inhibitor and hydrogen atom in side chain of residue (Figure 45) overlapping factor about 0.94, 0.81 and 0.83 in 68NV, T4 and T5, respectively (Figure 47). So, it has high repulsive with T4 than other. For other enzyme this residue show weak H-bond interaction with three inhibitors occurred between center of pyridine ring of three inhibitors and hydrogen atom of aromatic in backbone of residue (Figure 44).

Lys103 has high inverse correlation with T4 in K103N, which Lys103 change to Asn103 in this enzyme, indicating that interaction energy decrease on T4 than other because Asn103 revealed two H-bond interaction interactions with 68NV and T4 (Figure 42). Firstly, H-bond interaction between hydrogen atom in pyridine ring of inhibitors and carbonyl group in backbone of residue is shown but 68NV found steric interaction between hydrogen atom in pyridine ring of inhibitor and hydrogen atom in amino group in side chain of residue (Figure 48). So, T4 has stronger this H-bond interaction than 68NV. Secondly, it is found the H-bond

interaction between nitrogen atom in pyridine ring of inhibitors and hydrogen atom of amino group in side chain of residue, while T5 found just one H-bond interaction between nitrogen atom in pyridine ring of inhibitors and hydrogen atom of amino group in side chain of residue (Figure 42). So, it has high attractive with T4 than other. For other enzymes this residue revealed two H-bond interaction with 68NV and T4. Firstly, it is H-bond interaction between hydrogen atom in pyridine ring of inhibitors and carbonyl group in backbone of residue. Secondly, it shows H-bond interaction between hydrogen atom in pyridine ring of inhibitors and nitrogen atom in backbone of residue, while T5 found just one H-bond interaction between hydrogen atom in pyridine ring of inhibitors and nitrogen atom in backbone of residue (Figure 41).

**Table 11** The interaction and key distances between the residue and ligand.

Residues	Interaction (Inh-res)	Distance (Å)									Figure
		68nv			T4			T5			
		WT	K103N	Y181C	WT	K103N	Y181C	WT	K103N	Y181C	
Glu138	Cl-H	2.66	2.78	2.71	2.62	2.68	2.65	2.64	2.68	2.64	38
Lys101	(Pr-H)-O	2.50	2.43	2.51	2.45	2.38	2.51	2.42	2.38	2.43	39
Lys102	S-NH <sub>3</sub> <sup>+</sup>	5.32	5.17	5.64	5.42	5.73	5.68	-	-	-	40
Lys103	(Ar-H)-O	2.56	-	2.57	2.61	-	2.66	-	-	-	41
	(Ar-H)-N	3.44	-	3.53	2.98	-	3.34	3.33	-	3.48	
Asn103	N-HN	-	2.32	-	-	2.20	-	-	2.38	-	42
	(Ar-H)-O	-	2.48	-	-	2.58	-	-	-	-	
Trp229	(Pr-H)-π	2.87	3.38	2.81	2.72	2.75	2.84	2.66	2.71	2.67	43
Tyr181	π - (H-Ar)	3.32	3.53	-	3.38	3.35	-	3.39	3.29	-	44
Cys181	Cl-HS	-	-	2.67	-	-	2.31	-	-	2.37	45
Tyr188	CH-π	2.89	2.99	2.83	2.80	2.76	2.64	2.81	2.83	2.77	46
	NH-π	-	-	-	3.63	3.57	3.37	3.62	3.36	3.40	

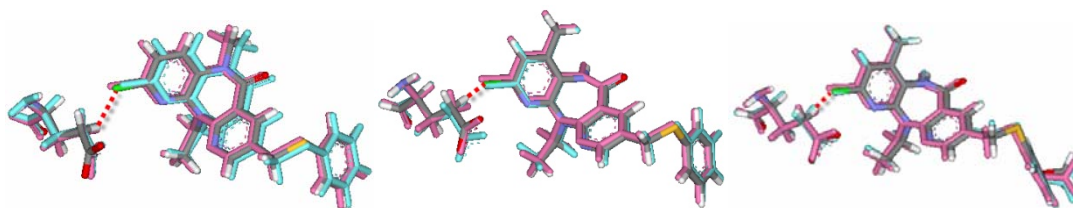


**Figure 38** Interaction between inhibitors (68NV (left), T4 (middle) and T5 (right)) and Glu138 residue in WT (atom-type color), K103N (blue) and Y181C (pink) HIV-1 RT.

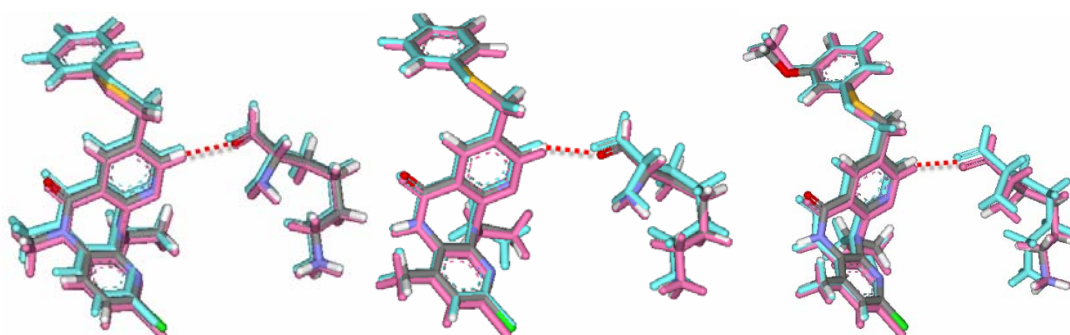


**Figure 39** Interaction between inhibitors (68NV (left), T4 (middle) and T5 (right)) and Lys101 residue in WT (atom-type color), K103N (blue) and Y181C (pink) HIV-1 RT.

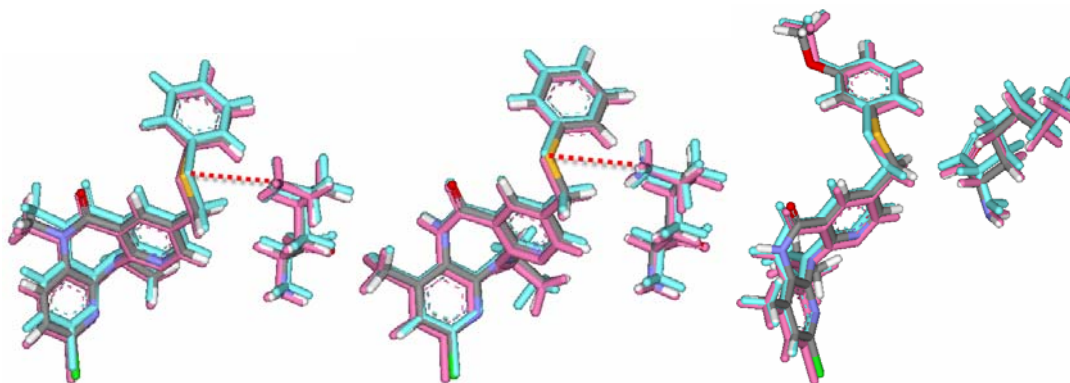


**Figure 40** Interaction between inhibitors (68NV (left), T4 (middle) and T5 (right)) and Lys102 residue in WT (atom-type color), K103N (blue) and Y181C (pink) HIV-1 RT.

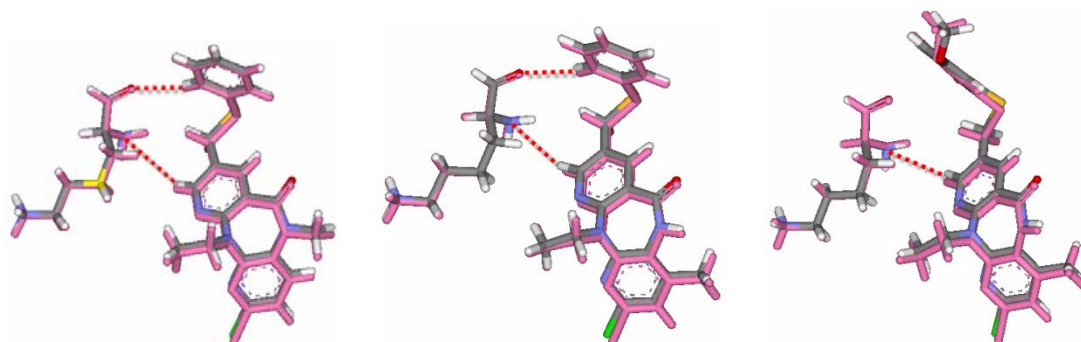


**Figure 41** Interaction between inhibitors (68NV (left), T4 (middle) and T5 (right)) and Lys103 residue in WT (atom-type color) and Y181C (pink) HIV-1 RT.

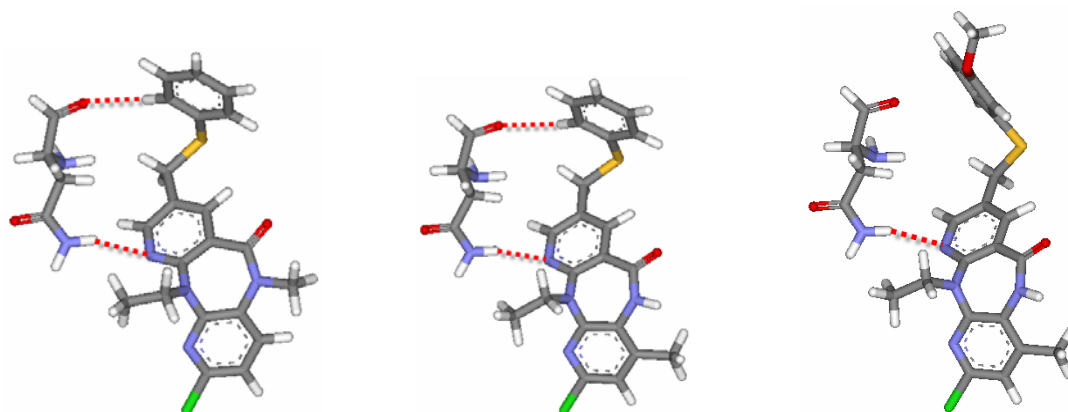


**Figure 42** Interaction between inhibitors (68NV (left), T4 (middle) and T5 (right)) and Asn103 residue in K103N HIV-1 RT.

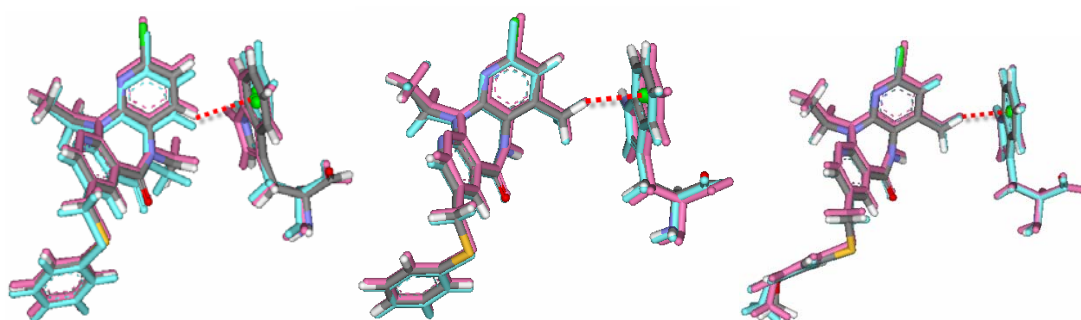


**Figure 43** Interaction between inhibitors (68NV (left), T4 (middle) and T5 (right)) and Trp229 residue in WT (atom-type color), K103N (blue) and Y181C (pink) HIV-1 RT.



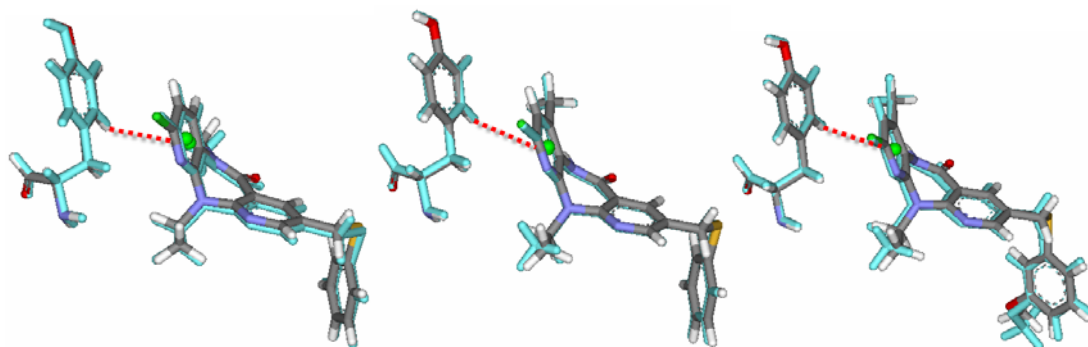


**Figure 44** Interaction between inhibitors (68NV (left), T4 (middle) and T5 (right)) and Tyr181 residue in WT (atom-type color) and K103N (blue) HIV-1 RT.

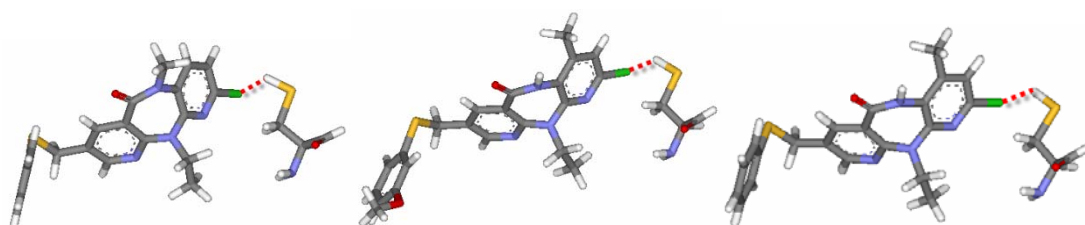


**Figure 45** Interaction between inhibitors (68NV (left), T4 (middle) and T5 (right)) and Cys181 residue in Y181C HIV-1 RT.

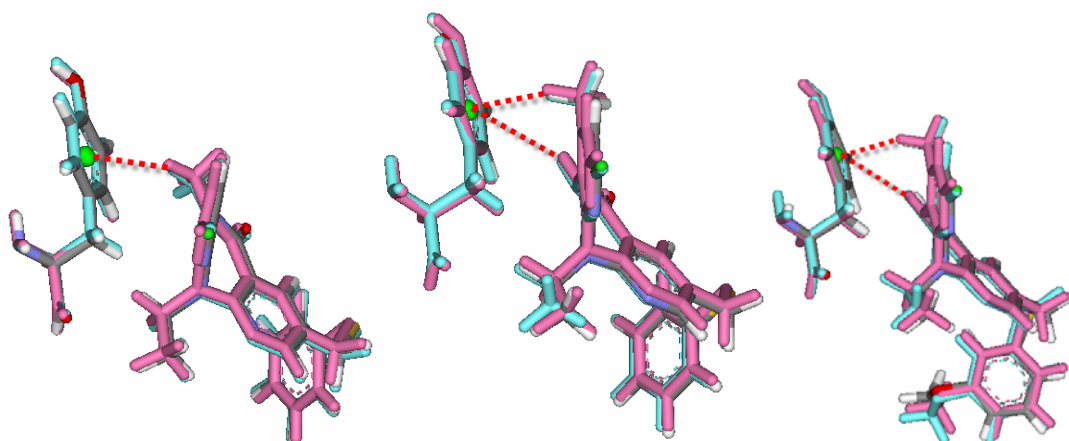


**Figure 46** Interaction between inhibitors (68NV (left), T4 (middle) and T5 (right)) and Tyr188 residue in WT (atom-type color), K103N (blue) and Y181C (pink) HIV-1 RT.

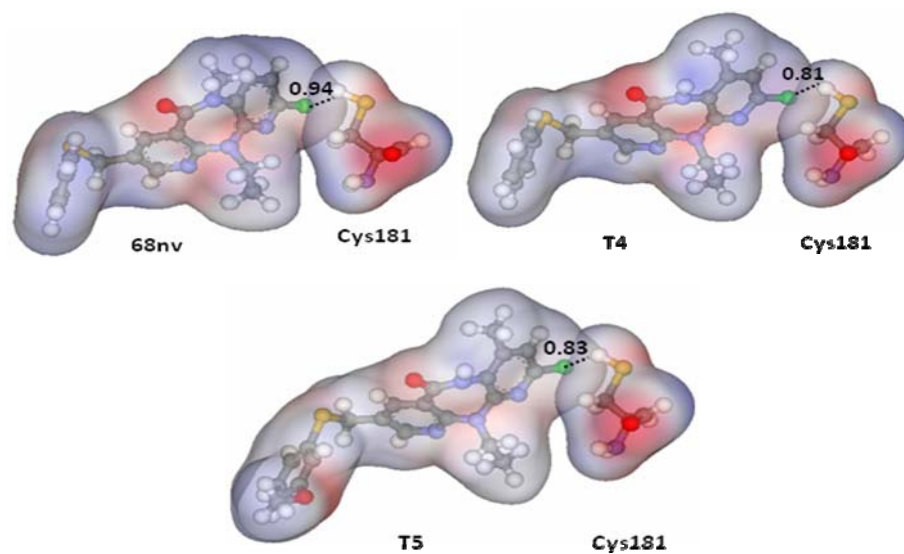


**Figure 47** Overlapping factor between chloride atom in three inhibitors and hydrogen atom in side chain of Cys181.

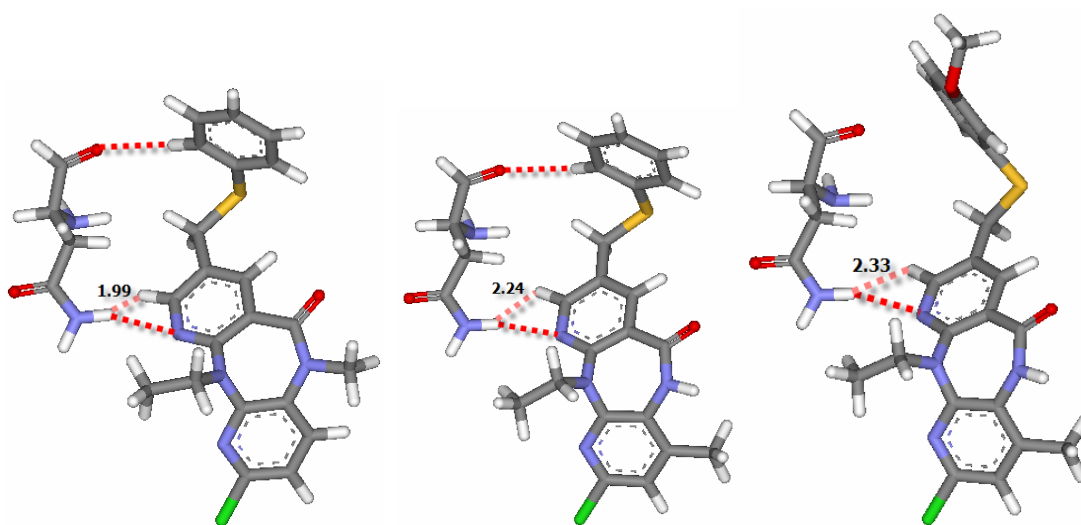


**Figure 48** Steric interaction of inhibitors (68NV (left), T4 (middle) and T5 (right)) and Asn103.

## 2.5 Relationship between the quantum energies and pIC<sub>50</sub> differences

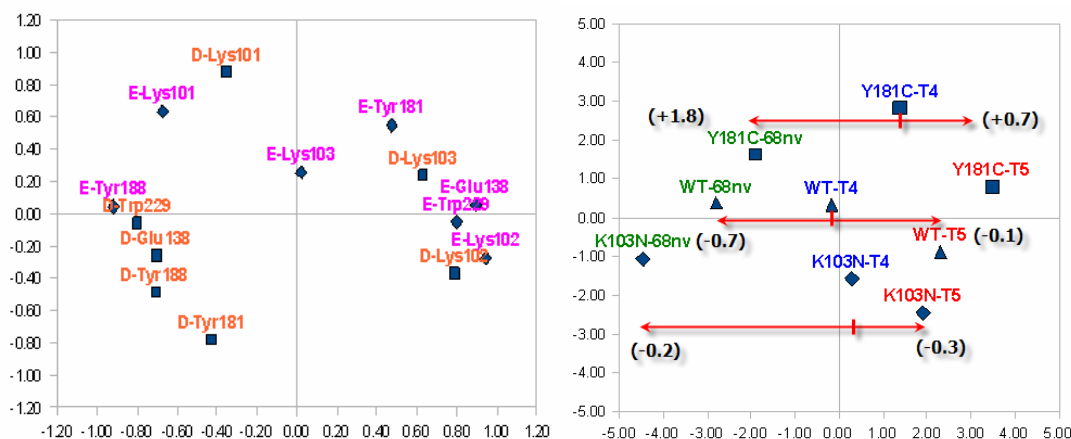


**Figure 49** PCA loading plot (left) and relative of pIC<sub>50</sub> from experiment on PCA loading plot (right).

Component two which can separate type of enzyme in loading plot found that in WT, Tyr188, Lys102, Trp229 and Glu138 have effect on this enzyme, which Tyr188 have converse correlation with Lys102, Trp229 and Glu138 between 68NV and T5. Glu138 shows repulsive interaction with three inhibitors, whereas Trp229 gives attractive interaction with three inhibitors. The difference of interactions of three inhibitors are clearly seen in Tyr188 and Lys102 as seen in Figure 50, T4 and T5 gave high contributions to Tyr188 about -4.85 kcal/mol and -5.06 kcal/mol, respectively. 68NV gave the highest contribution to Lys102, T4 and T5 gave lower contribution about -4.00 kcal/mol, -2.97 kcal/mol and -0.89 kcal/mol, respectively, indicating that T4 has high potent than T5 and 68NV, respectively. Then the experimental activity found that the activity decrease from T4 to 68NV and T4 to T5 about 0.7 and 0.1, respectively, indicating that T4 has high potent than T5 and 68NV, respectively. Therefore the calculated results from quantum chemical calculations are consistent with their experimental activities in this enzyme.

For mutation enzyme investigations, the K103N enzyme found that Lys101, Lys103 and Tyr181 have high correlation in negative sense, Lys101 revealed

H-bond interaction with three inhibitors. The difference of interactions of three inhibitors are clearly seen in Lys103 or Asn103, which as shown in Figure 52. It give attractive interactions about -4.19, -6.72 and -3.67 kcal/mol in 68NV, T4 and T5, respectively, indicating that T4 has high potent than 68NV and T5, respectively. Then the experimental activity found that the experimental activity decrease from T4 to 68NV and T4 to T5 about 0.2 and 0.3, respectively, indicating that T4 has high potent than 68NV and T5, respectively. Therefore the calculated results from quantum chemical calculations are consistent with their experimental activities in this enzyme.

In Y181C HIV-1 RT found that Lys101, Lys103 and Tyr181 have high correlation with Y181C enzyme in positive sense. Lys101 and Lys103 revealed H-bond interaction with three inhibitors. The difference of interactions of three inhibitors are clearly seen in Tyr181 or Cys181 as shown in Figure 51. It is found that attractive energy with 68NV about -0.01 kcal/mol and repulsive energy with T4 and T5 about 2.10 and 1.31 kcal/mol, respectively. Then, the experimental activity found that the activity increase from T4 to 68NV and T4 to T5 about 1.8 and 0.7, respectively, indicating that 68NV has high potent than T5 and T4, respectively. Therefore the calculated results from quantum chemical calculations are consistent with their experimental activities in this enzyme.

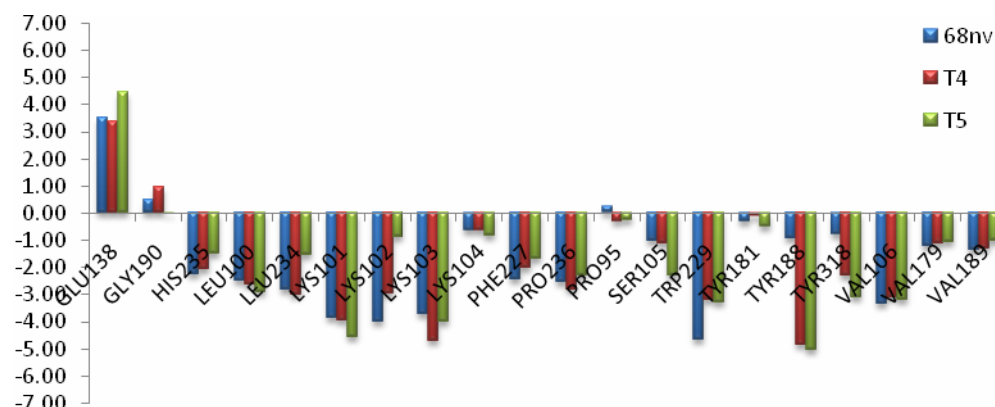


**Figure 50** Relationship of three inhibitor (68NV, T4 and T5) in WT HIV-1 RT calculated at MP2/6-31G(d,p) level of theory.

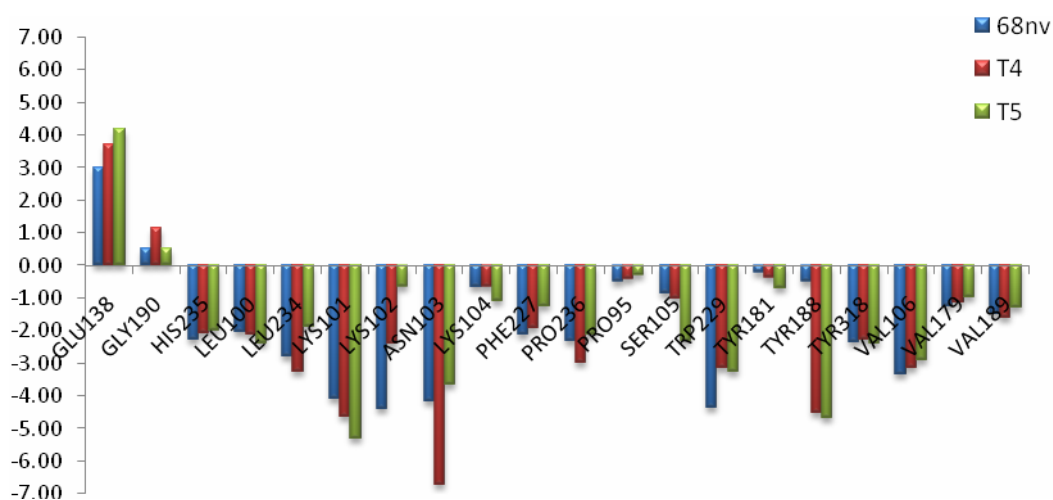


**Figure 51** Relationship of three inhibitor (68NV, T4 and T5) in K103N HIV-1 RT calculated at MP2/6-31G(d,p) level of theory.

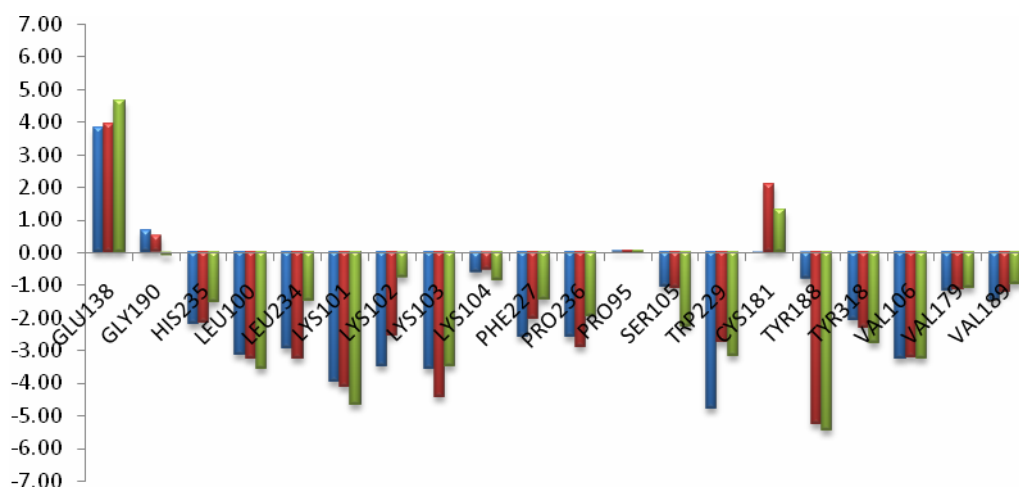


**Figure 52** Relationship of three inhibitor (68NV, T4 and T5) in Y181C HIV-1 RT calculated at MP2/6-31G(d,p) level of theory.

## CONCLUSIONS

This work was focused on the particular interaction energy between an inhibitor, which is nevirapine derivatives (68NV, T4 and T5), and an amino acid in active site of various types of HIV-1 RT to understand the relationship of these amino acids with these inhibitors for explaining the experimental activity. Therefore, in this study, we used theoretical investigation for understanding molecular deeper of interaction between inhibitor and residues in binding pocket applied by using quantum chemical calculations. The PCA method was applied to analyze the results obtained from quantum chemical calculations.

The particular interaction of two models calculated at B3LYP and MP2 methods with 6-31G(d,p) basis set. The B3LYP calculations revealed more attractive interaction than MP2 calculations in the same basis set of two models. Moreover, the Glu138 residue which is anion amino acid, shows influence on the particular interaction by over repulsive interaction from B3LYP calculations but it is not found from MP2 calculations. Therefore, MP2/6-31G(d,p) level is reasonable for considering the deeply molecular detail.

The particular interaction obtained from MP2/6-31G(d,p) level in two models were analyzed by using PCA because of the large number of theoretical interaction energies. Firstly, considering starting complex structure comparison of two model, it is found that the AMBER force field minimizations (model B) can decrease more repulsive interaction energy of in binding site of GOLD docking (model A) and can show important attractive interaction in binding site. The results can be infer that AMBER force field minimizations are essential in the starting geometry of enzyme complex. Then, the particular interaction obtained from model B at MP2/6-31G(d,p) used to analysis the structural and energetic parameters. The last, considering the correlation between experimental activity and interaction from calculate results, It is found that the results from calculations agree well with their experimental activities.

Taken into account, the quantum chemical calculations are useful to investigate the role of amino acid surrounding the binding pocket. The obtained results can be use to explain the experimental activity of their inhibitors. Therefore, the quantum chemical calculations are important for proposed binding pattern of various types of HIV-1 RT to 68NV, T4 and T5.



## LITERATURE CITED

- Bardsley-Elliot, A. and C.M. Perry. 2000. Nevirapine: A Review of its Use in the Prevention and Treatment of Paediatric HIV Infection. **Paediatric Drugs** 2373-407.
- Campiani, G., A. Ramunno, G. Maga, V. Nacci, C. Fattorusso, B. Catalanotti, E. Morelli and E. Novellino. 2002. Non-Nucleoside HIV-1 Reverse Transcriptase (RT) Inhibitors: Past, Present, and Future Perspectives. **Current Pharmaceutical Design** 8615-657.
- Chan, J.H., G.A. Freeman, J.H. Tidwell, K.R. Romines, L.T. Schaller, J.R. Cowan, S.S. Gonzales, G.S. Lowell, C.W. Andrews, D.J. Reynolds, M. St Clair, R.J. Hazen, R.G. Ferris, K.L. Creech, G.B. Roberts, S.A. Short, K. Weaver, G.W. Koszalka and L.R. Boone. 2004. Novel Benzophenones as Non-nucleoside Reverse Transcriptase Inhibitors of HIV-1. **Journal of Medicinal Chemistry** 47(5):1175-1182.
- Das, K., J.D. Bauman, A.D. Clark, Y.V. Frenkel, P.J. Lewi, A.J. Shatkin, S.H. Hughes and E. Arnold. 2008. High-resolution structures of HIV-1 reverse transcriptase/TMC278 complexes: Strategic flexibility explains potency against resistance mutations. **Proceedings of the National Academy of Sciences** 105(5):1466-1471.
- De Clercq, E. 1995. Toward Improved Anti-HIV Chemotherapy: Therapeutic Strategies for Intervention with HIV Infections. **Journal of Medicinal Chemistry** 38(14):2491-2517.
- \_\_\_\_\_. 1999. Perspectives of non-nucleoside reverse transcriptase inhibitors (NNRTIs) in the therapy of HIV-1 infection. **Il Farmaco** 54(1-2):26-45.

De Clercq, E. 2001. Antiviral drugs: current state of the art. **Journal of Clinical Virology** 2273-89.

\_\_\_\_\_. 2002. New developments in anti-HIV chemotherapy. **Biochimica et Biophysica Acta (BBA) - Molecular Basis of Disease** 1587(2-3):258-275.

\_\_\_\_\_. 2004. Antiviral drugs in current clinical use. **Journal of Clinical Virology** 30(2):115-133.

Dutta, S., K. Burkhardt, J. Young, G. Swaminathan, T. Matsuura, K. Henrick, H. Nakamura and H. Berman. 2009. Data Deposition and Annotation at the Worldwide Protein Data Bank. **Molecular Biotechnology** 42(1):1-13.

Esnouf, R.M., J. Ren, A.L. Hopkins, C.K. Ross, E.Y. Jones, D.K. Stammers and D.I. Stuart. 1997. Unique features in the structure of the complex between HIV-1 reverse transcriptase and the bis(heteroaryl)piperazine (BHAP) U-90152 explain resistance mutations for this nonnucleoside reverse transcriptase inhibitor. **Proceedings of the National Academy of Sciences of the United States of America** 94(8):3984-3989.

He, X., Y. Mei, Y. Xiang, D.W. Zhang and J.Z.H. Zhang. 2005. Quantum computational analysis for drug resistance of HIV-1 reverse transcriptase to nevirapine through point mutations. **Proteins-Structure Function and Bioinformatics** 61(2):423-432.

Jacobo-Molina, A., J. Ding, R.G. Nanni, A.D. Clark, X. Lu, C. Tantillo, R.L. Williams, G. Kamer, A.L. Ferris and P. Clark. 1993. Crystal structure of human immunodeficiency virus type 1 reverse transcriptase complexed with double-stranded DNA at 3.0 Å resolution shows bent DNA. **Proceedings of the National Academy of Sciences of the United States of America** 90(13):6320-6324.

Khunnawutmanotham, N., N. Chimnoi, P. Saparpakorn, P. Pungpo, S. Louisirirochanakul, S. Hannongbua and S. Techasakul. 2007. Novel 2-Chloro-8-arylthiomethyldipyridodiazepinone Derivatives with Activity against HIV-1 Reverse Transcriptase. **Molecules** 12(2):218-230.

\_\_\_\_\_, \_\_\_\_\_, A. Thitiyahanont, \_\_\_\_\_ and \_\_\_\_\_. 2009. Dipyridodiazepinone Derivatives; Synthesis and Anti HIV-1 Activity. **Beilstein Journal of Organic Chemistry** accepted (2009).

Klunder, J.M., M. Hoermann, C.L. Cywin, E. David, J.R. Brickwood, R. Schwartz, K.J. Barringer, D. Pauletti, C.-K. Shih, D.A. Erickson, C.L. Sorge, D.P. Joseph, S.E. Hattox, J. Adams and P.M. Grob. 1998. Novel Nucleoside Inhibitors of HIV-1 Reverse Transcriptase. 7. 8-Arylethyldipyridodiazepinones as Potent Broad-Spectrum Inhibitors of Wild-Type and Mutant Enzymes. **Journal of Medicinal Chemistry** 41(16):2960-2971.

Kuno, M., \_\_\_\_\_ and K. Morokuma. 2003a. Theoretical investigation on nevirapine and HIV-1 reverse transcriptase binding site interaction, based on ONIOM method. **Chemical Physics Letters** 380(3-4):456-463.

\_\_\_\_\_, R. Palangsantikul and \_\_\_\_\_. 2003b. Investigation on an Orientation and Interaction Energy of the Water Molecule in the HIV-1 Reverse Transcriptase Active Site by Quantum Chemical Calculations. **Journal of Chemical Information and Computer Sciences** 43(5):1584-1590.

\_\_\_\_\_, \_\_\_\_\_, \_\_\_\_\_, \_\_\_\_\_ and \_\_\_\_\_. 2005. Quantum study of mutational effect in binding of efavirenz to HIV-1 RT. **Proteins-Structure Function and Bioinformatics** 59(3):489-495.

- Nunrium, P., \_\_\_\_\_, S. Saen-oon and \_\_\_\_\_. 2005. Particular interaction between efavirenz and the HIV-1 reverse transcriptase binding site as explained by the ONIOM2 method. **Chemical Physics Letters** 405(1-3):198-202.
- Ren, J., C. Nichols, L. Bird, P. Chamberlain, K. Weaver, S. Short, D.I. Stuart and D.K. Stammers. 2001. Structural mechanisms of drug resistance for mutations at codons 181 and 188 in HIV-1 reverse transcriptase and the improved resilience of second generation non-nucleoside inhibitors. **Journal of Molecular Biology** 312(4):795-805.
- San Juan, A.A. 2008. 3D-QSAR models on clinically relevant K103N mutant HIV-1 reverse transcriptase obtained from two strategic considerations. **Bioorganic & Medicinal Chemistry Letters** 18(3):1181-1194.
- \_\_\_\_\_, \_\_\_\_\_ and D. Rognan. 2006. Design of nevirapine derivatives insensitive to the K103N and Y181C HIV-1 reverse transcriptase mutants. **SAR and QSAR in Environmental Research** 17:183-194.
- Sarafianos, S.G., S.H. Hughes and E. Arnold. 2004. Designing anti-AIDS drugs targeting the major mechanism of HIV-1 RT resistance to nucleoside analog drugs. **The International Journal of Biochemistry & Cell Biology** 36(9):1706-1715.
- Tantanak, D., J. Limtrakul and M.P. Gleeson. 2005. Probing the Structural and Electronic Factors Affecting the Adsorption and Reactivity of Alkenes in Acidic Zeolites Using DFT Calculations and Multivariate Statistical Methods. **Journal of Chemical Information and Modeling** 45(5):1303-1312.

## **APPENDICES**

**Appendix A**  
Supporting information

## Overlap Factor Calculations

Steric effects arise from the fact that each atom within a molecule occupies a certain amount of space. If atoms are brought too close together, there is an associated cost in energy due to overlapping electron clouds, and this may affect the molecule's preferred shape, conformation, and reactivity.

The definition we use for a clear of steric clash is the "overlap factor", which is defined as the ratio of the distance between two atom centers to the sum of their van der Waals radii.

$$\text{Overlap factor} = \frac{R^{A-B}}{R^A + R^B}$$

Where the term of  $R^{A-B}$  is a distance between atom A and B,  $R^A$  and  $R^B$  are the van der Waals radii of atom A and B, respectively.

This definition has the advantage that it is independent of the atom types. This number will be less than 1 if the two atom spheres interpenetrate at all. Anyways, some interpenetration is atom-type color, for example in a hydrogen bonding arrangement, and does not lead to a huge Lennard-Jones energy. Overlap factors of 0.8 or even 0.75 are common for hydrogen in high resolution x-ray crystal structures. This factor is also useful for screening out conformations of the protein.

## **Appendix B**

### **Presentations**



## 1. Proceeding

Amphawan Maitarad, Withcha Treesuwan, Phornphimon Maitarad, Patchreenart Saparpakorn, Supanna Techasakul, and Supa Hannongbua. Quantum Chemical Calculations on Particular Interaction Energy of HIV-1 reverse transcriptase Inhibitors (68NV, T4 and T5) Bound in K103N HIV-1 RT. Pure and Applied Chemistry International Conference (PACCON), 2009, Naresuan University, Phisanulok, Thailand.

## Quantum Chemical Calculations on Particular Interaction Energy of HIV-1 Reverse Transcriptase Inhibitors (68nv, T4 and T5) Bound in K103N HIV-1 RT

Amphawan Maitarad<sup>1,2</sup>, Witcha Treesuwan<sup>1,2</sup>, Phornphimon Maitarad<sup>1,2</sup>, Patchreenart Saparpakorn<sup>1,2</sup>, Supanna Techasakul<sup>1</sup>, and Supa Hannongbua<sup>1,2\*</sup>

<sup>1</sup>Department of Chemistry, Faculty of Science, Kasetsart University, Bangkok 10900, Thailand,

<sup>2</sup>Center of Nanotechnology, Kasetsart University, Bangkok 10900, Thailand,

\*E-mail: fscisph@ku.ac.th, Fax: +66 25 62 55 55 ext. 2140

**Abstract:** To evaluate the role of the amino acids surrounding the binding pocket of K103N HIV-1 Reverse Transcriptase bound with novel NNRTIs, 68nv, T4 and T5, quantum chemical calculations were performed. The model systems were obtained from, GOLD docking (model A) and AMBER force fields (model B). Particular interaction energies between an inhibitor and an individual residue within 4 Å, consisted of twenty residues, were calculated at B3LYP/6-31G(d,p) level of theory. Then, the basis set superposition error with counterpoise scheme was applied to correct the estimated energy. The obtained interaction energies of model B are reasonable than model A, which implied that relaxation of the enzyme complex by molecular dynamic simulations is important in the starting geometry. Based on model B, Lys101 showed the higher energy contribution by forming hydrogen bonding interactions. However, the key interaction is the mutation residue (Asn103) where attractive energies of -0.52 and -3.16 kcal/mol found from 68nv and T4 inhibitors, respectively. On the other hand, repulsive energy of 0.27 kcal/mol found from T5 inhibitor. The calculated results agree well with the experimental activities of each inhibitor. The results showed that quantum chemical calculations can be used to investigate the key residue interactions.

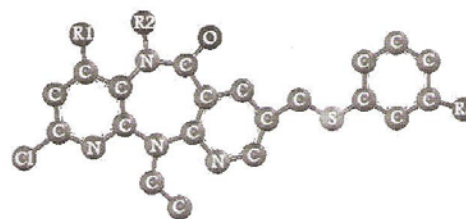
### Introduction

Acquired immunodeficiency syndrome (AIDs) is a disease caused by the human immunodeficiency virus (HIV). The human immunodeficiency virus type 1 (HIV-1) is a major worldwide infection.[1] The important enzyme of HIV-1 is reverse transcriptase (RT), which is a special enzyme converting the single-stranded RNA viral genome into a double-stranded proviral DNA before integrating into the host chromosome.[2] Moreover, HIV-1 RT is an asymmetric heterodimer consisting of a p66 and p51 subunits that is responsible for the replication of single-stranded viral RNA into double-stranded DNA prior to integration into the genome of the human host.[3] Therefore, HIV-1 RT is widely studied because it is an important role in treatment of AIDs.

Nevirapine is the first generation of non-nucleoside inhibitors of HIV-1 RT. The efficiency of nevirapine is satisfied for wild type but it lose efficiency for mutant type.[4] In particular, the K103N and Y181C mutant types are mostly reported in the resistance of nevirapine inhibitors.[5-7] In an attempt to improve the activity of

nevirapine against mutant RT enzyme, the 2-chloro-8-arylthiomethyl dipyrrodozepinone derivatives, which containing unsubstituted lactam nitrogen and 2-chloro-8-arylthiomethyl moiety (T4 and T5), had been designed recently.[8] A comparison of the experimental test between 68nv, T4 and T5 against the K103N HIV-1 RT are shown in Table 1. [9]

Table 1: Structure and inhibitory activity of dipyrrodozepinone derivatives (68nv, T4 and T5) against K103N HIV-1 RT.



Cpds	R1	R2	R3	IC <sub>50</sub> (μM)
				K103N
68nv	H	CH <sub>3</sub>	H	0.390
T4	CH <sub>3</sub>	H	H	0.224
T5	CH <sub>3</sub>	H	OCH <sub>3</sub>	0.428

Recently, quantum chemical calculations were used to study the effect of mutation related to inhibitor resistant. It was found that the calculations are important for guiding the cause of resistant.[10-15] The aim of this work is to evaluate the role of the amino acids surrounding the binding pocket K103N HIV-1 RT with 68nv, T4 and T5, using the quantum chemical calculations. Consequently, the results can be used to compare with their experimental activities and observed the main contributed interaction of residues in the binding site.

Amphawan Maitarad<sup>1,2</sup>, Wittha Treesuwan<sup>1,2</sup>, Phomphimon Maitarad<sup>1,2</sup>, Patchreenart Sarpapakorn<sup>1,2</sup>,  
Supanna Techasakul<sup>1</sup>, and Supa Hannongbua<sup>1,2\*</sup>

## Methodologies

Nevirapine is the first generation of non-nucleoside inhibitors of HIV-1 RT. The efficiency of nevirapine is satisfied for wild type but it loses efficiency for mutant type. In particular, the K103N and Y181C mutant types are mostly reported in the resistance of nevirapine [1]. Therefore, it is necessary to improve the efficiency of nevirapine against mutant RT enzyme. The 2-chloro-8-azetidinylmethyl-2-phenyl-6-thio-1,2,3,4-tetrahydropyrimidin-4-one, which contains substituted lactam nitrogen and 2-chloro-8-azetidinylmethyl moiety (T4 and T5), had been designed recently. A comparison of the experimental test between 88nv, T4 and T5 against the K103N-HM-1 RT are shown in Table 1. Recently, quantum chemical calculations were used to study the effect of mutation related to inhibitor resistance. It was found that the calculations are important for outlining the cause of resistance [2].

**Table 1:** Structure and inhibitory activity of dipyridodiazepinone derivatives (68nv, T4 and T5) against K103N HIV-1 RT.

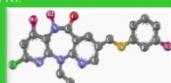


**Table 2:** Interaction energies between inhibitors (68nv, T4 and T5) and individual residues (in kcal/mol), calculate at the B3LYP/6-31G(d,p) level of theory for K103N HIV-1 RT.

Residue	Interaction energies (kcal/mol)					
	6Bw*	6Bw*	T4*	T4*	T5*	T5*
Pro99S	0.49	0.44	0.54	0.61	0.22	0.01
Ser100	3.29	3.17	1.80	2.69	2.43	2.41
Lys101	-1.61	-3.12	-3.02	-3.75	-2.00	-4.40
Asn102	0.91	-2.49	1.24	-0.72	2.19	1.90
Lys103	6.30	-0.82	9.66	-3.16	13.28	0.27
Lys104	0.40	-0.02	0.20	0.10	1.64	0.24
Ser105	0.45	-0.14	0.34	-0.24	0.57	-0.01
Val106	12.22	3.87	13.56	4.70	5.17	5.13
Val179	0.02	0.27	0.43	0.56	1.03	0.65
Pro182	7.15	5.14	6.73	5.90	9.46	7.22
Thr188	7.44	5.10	6.73	2.60	1.71	2.23
Val189	0.08	-0.02	0.36	-0.14	0.52	-0.01
Gly190	1.11	1.52	1.12	2.29	0.61	1.60
Pro227	5.31	1.63	5.31	1.50	1.50	1.50
Thr229	-0.85	-1.25	0.31	-0.35	1.75	-0.40
Leu234	5.96	1.78	1.33	0.77	1.08	1.62
His235	3.40	-0.92	0.46	-0.75	0.58	-1.03
Pro236	2.25	1.62	1.40	0.92	9.94	2.04
Pro237	5.31	1.63	5.31	1.50	1.50	1.50

<sup>a</sup> Model A and <sup>b</sup>Model B.

This work was focused on the particular interaction energy between an inhibitor, which is dipyrroldiazepione derivatives (85bN, T4 and T5), and an amino acid residue in active site of K103N HIV-1 RT. The results can be inferred that minimization by AMBER force fields are essential in the starting geometry of enzyme complex. From the investigation of the particular interaction energies by using B3LYP-311G(d,p) level of calculations with BSSE corrections show in Figure 2, the results from this work can be indicated that the quantum chemical calculations are in good agreement with the experimental results. It was found that T4 showed the lowest interaction energy to mutation residue (Asn103). These results from calculations agree to their experimental activities. In addition, Lys101 is the main interaction by forming hydrogen bonding with all compounds in molecular detail as display in Figure 2. Therefore, the results from this work can be indicated that the quantum chemical calculations are in good agreement with the experimental results. T4 and T5 are the best inhibitors. Additionally, T4 can be used as a guideline inhibitor for K103N HIV-1 RT.

The geometry of target enzyme structure of HIV-1 RT in wild-type was retrieved from the Protein Data Bank (PDB entry code:1KLM). Then, K103N HIV-1 RT was prepared by mutating the residue using biopolymer module in sybyl 7.0 program.

Inhibitors (68nv, T4 and T5) were constructed and optimized by GAUSSIAN 03 program and the complex structures were obtained from molecular docking by GOLD docking program (model A). Then, whole enzyme complexes were optimized by AMBER force fields (model B).

The system was set up by selecting amino acid surrounding inhibitors within the interatomic distance of 4 Å and the particular interaction energy was focused on the couple of inhibitor and each amino acid.

Hydrogen atoms were added into the cutting regions using SYBYL 7.0 program and was investigated using B3LYP/6-31G(d,p) level of calculations by GAUSSIAN 03 program.

### Quantum Chemical Calculations

The particular interaction energy can be defined as shown in equation (1).

Moreover, the basis set superposition error (BSSE) based on counterpoise scheme of Boys-Bernardi were also computed to correct the particular interaction energy as shown in equation (2):

where  $E_{(\text{complex})}$  is the energy of inhibitor-residue,  $E_{(\text{inhibitor})}$  is the energy of inhibitor and  $E_{(\text{residue})}$  is the energy of individual residue. AB is molecular orbital of inhibitor-residue.

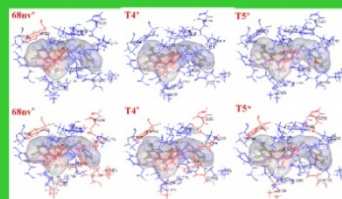


**Figure 1.** Graphical representation of the attractive interactions (red) and repulsive interactions (blue) between inhibitors from model A (68nv\*, T4\* and T5\*), model B (68nv\*, T4\* and T5\*) and amino acid residues.



**Figure 2.** Distance of hydrogen bonding interactions between inhibitors (68nv, T4 and T5) and Lys101 from model B.

## References

1. N. Khunnawutmanotham, N. Chierici, A. Thitsayanont, S. Hannongbua, and S. Techasakul, [submitted]
2. Mei, Y.; He, X.; Xiang, Y.; Zhang, D.W.; Zhang, J.Z.H. *J. PROTEINS: structure, Function, and Bioinformatics* **2006**, 59, 480-490.
3. Nuriy, P.; Kuno, M.; Saen-con, S.; Hannongbua, S. *Chemical Physics Letters* **2006**, 405, 198-202.

### Acknowledgements

**Acknowledgements**  
This work was supported by the Thailand Research Fund (TRF), Commission on Higher Education (CHE), The Graduate Education and Research Program in Petroleum and Petrochemical Technology and Advance Material, and Center of Nanotechnology, Kasetsart University, Research and Development Institute (KURDI).

## 2. National/International Conferences

Amphawan Maitarad, Phornphimon Maitarad, Patchreenart Saparpakorn, Supanna Techasakul, and Supa Hannongbua. Quantum Chemical Calculations on Particular Interaction Energy of HIV-1 reverse transcriptase Inhibitors (68NV, T4 and T5) Bound in Various Types of HIV-1 RT Enzymes. 34<sup>th</sup> Congress on Science and Technology of Thailand, 2008, Queen Sirikit National Convention Center, Bangkok, Thailand.

Amphawan Maitarad, Withcha Treesuwan, Phornphimon Maitarad, Paul Matthew Gleeson, Patchreenart Saparpakorn, Supanna Techasakul, and Supa Hannongbua. Influence of AMBER Force Fields on Particular Interaction Energy of HIV-1 Reverse Transcriptase Inhibitors (68NV, T4 and T5) Bound in Various Types of HIV-1 RTs. The 13<sup>th</sup> Asian Chemical Congress. 2009, Shanghai, China.



large volume and ability of surface modification, several research groups have developed carbon nanotubes as the targeted delivery vehicles for anticancer drugs. In this study, we focus on an anticancer drug, *doxorubicin*, encapsulated in the single-walled carbon nanotube (SWNT). Structural properties of zigzag nanotubes are studied by comparing the pristine and functionalized SWNT using quantum chemical calculations. The interactions between model SWNT, doxorubicin and water molecules are investigated using molecular dynamics simulations. The hydroxyl and carboxyl functional groups at the open-end of the tubes are investigated. This study is performed in order to find the most stable conformation and investigate the behaviors of the complex SWNT and doxorubicin drug by using the most optimistic level of accuracy.

#### C4\_C0248 QUANTUM CHEMICAL CALCULATIONS ON PARTICULAR INTERACTION ENERGY OF HIV-1 REVERSE TRANSCRIPTASE INHIBITORS (68NV, T4 AND T5) BOUND IN VARIOUS TYPE OF HIV-1 RT ENZYMES

Amphawan Maitarad<sup>1,2</sup>, Phornphimon Maitarad<sup>1,2</sup>, Patchreenart Saparpakorn<sup>1,2</sup>, Supanna Techasakul<sup>1</sup>, and Supa Hannongbua<sup>1,2\*</sup>

<sup>1</sup>Department of Chemistry, Faculty of Science, Kasetsart University, Bangkok 10900, Thailand,

<sup>2</sup>Center of Nanotechnology, Kasetsart University, Bangkok 10900, Thailand,

\*Correspondence: Supa Hannongbua, Dept. of Chemistry, Kasetsart University, Bangkok 10900, Thailand.  
Email: fscisph@ku.ac.th

**Abstract:** The objective of this work is to evaluate the role of the amino acids surrounding the binding pocket of three types of HIV-1 Reverse transcriptase (wild type, K103N and Y181C), bound with 68NV, T4 and T5. The modeled systems, obtained from GOLD docking, contained each inhibitor and twenty residues in the binding site, interacting with inhibitor within 4 Å. The calculated interaction energies between inhibitor and individual residues were performed at B3LYP and MP2 methods with the 6-31G(d,p) basis set, and then the basis set superposition error with counterpoise scheme was applied to correct the energy. The interaction energies obtained from both methods are consistent except interaction between 68NV with TRP229, where H- $\pi$  interaction occurred. MP2 calculations show attractive interaction of about -2.5 kcal/mol, whereas B3LYP results reveal repulsive interaction of about 0.5 kcal/mol. In addition, the H-bond interactions between three inhibitors with LYS101 show attractive interaction about -1.7 and -1.1 kcal/mol from MP2 and B3LYP methods, respectively, in wild type and both mutant types.

#### C4\_C0250 THEORETICAL STUDIES OF POLY(PHENYLENE-VINYLENE) COPOLYMER BY SUBSTITUTIONS TO FUNCTIONAL GROUP

Suphawarat Phalinyot<sup>1,2</sup>, Songwut Suramit<sup>1,2\*</sup> and Supa Hannongbua<sup>1,2</sup>

<sup>1</sup>Department of Chemistry, Faculty of Science, Kasetsart University, Bangkok 10900, Thailand,

<sup>2</sup>Center of Nanotechnology, Kasetsart University, Bangkok 10900, Thailand,

\*E-mail: fsciswsm@ku.ac.th, Tel. +66 25 62 55 55 ext. 2227

**Abstract:** Structure and energetic properties of poly(phenylene-vinylene) (PPV) copolymer with its derivatives have been studied, by quantum chemical calculations. Some functional groups (thiophene, pyrrole, carbazole and fluorene) were substituted on PPV to investigate the optical properties. All structures were optimized at the B3LYP/6-31G/\*\* level of calculations. Calculated energy gaps of (PPV)<sub>n</sub>, (PPV-Thiophene)<sub>n</sub>, (PPV-Pyrrole)<sub>n</sub>, (PPV-Carbazole)<sub>n</sub> and (PPV-Fluorene)<sub>n</sub>,  $n=\infty$  are 2.08, 1.84, 2.03, 2.70 and 2.78 eV, respectively. The energy gaps can be ordered as following: (PPV-Thiophene)<sub>n</sub> > (PPV-Pyrrole)<sub>n</sub> > (PPV)<sub>n</sub> > (PPV-Carbazole)<sub>n</sub> > (PPV-Fluorene)<sub>n</sub>. It was found that (PPV-Thiophene)<sub>n</sub> revealed the lowest energy gap. Therefore, the (PPV-Thiophene)<sub>n</sub> was supposed to a promising semiconductor material and will be further synthesized.

#### C4\_C0254 EFFECTS OF TUBE DIAMETER AND BORON DOPING ON ELECTRONIC BAND STRUCTURE OF SINGLE-WALLED CARBON NANOTUBES.

Arthit Vongachariya and Vudhichai Parasuk

Department of Chemistry, Faculty of Science, Chulalongkorn University, Bangkok 10330, Thailand

**Abstract:** Electronic structures of zigzag (n,0) and armchair (m,m) single-walled carbon nanotubes (SWCNT), where n being 5-10 and m being 4-8 were investigated using density functional theoretical calculations. The generalized gradient approximation (GGA) based on Perdew, Burke and Ernzerhof (PBE) functional and double numerical double zeta (DND) basis set were employed. SWCNT calculations revealed that zigzag SWCNTs are semiconductor when  $n/3 \neq \text{integer}$  and they are metal otherwise, in agreement with Saito et al.[1]. Band structures of SWCNTs were also found to be depended on type (zigzag or armchair), tube diameter (chiral vector) and Boron doping. With increasing tube diameter, band gaps of SWCNT were



**PT-PP44: Influence of AMBER Force Fields on Particular Interaction  
Energy of HIV-1 Reverse Transcriptase Inhibitors  
(68nv, T4 and T5) Bound in Various Types of HIV-1 RTs**

**MAITARAD, Amphawan<sup>a,b</sup>; TREESUWAN, Witcha<sup>a,b</sup>; MAITARAD, Phornpimon<sup>a,b</sup>;  
GLEESON, PaulMatthew<sup>a,b</sup>; SAPARPAKORN, Patchreenart<sup>a,b</sup>; TECHASAKUL, Supannand<sup>a</sup>;  
HANNONGBUA, Supa<sup>a,b\*</sup>**

a: Department of Chemistry, Faculty of Science, Kasetsart University, Bangkok 10900, Thailand,

b: Center of Nanotechnology, Kasetsart University, Bangkok 10900, Thailand

Mutations of the HIV-1 Reverse Transcriptase protein (HIV-1 RT) is an increasing problem in the treatment of HIV and considerable effort has been expended in both industry and academia to tackle this problem. At Kasetsart University efforts to minimize the loss in potency of Nevirapine derivatives to HIV-1 RT mutants, have led to the synthesis of 2-chloro-8-arylthiomethyl dipyridodiazepinone derivatives which show very interesting biological activities at known mutants. The aim of this computationally based study is to investigate the role of the key active site amino acid residues in the HIV-1 RT allosteric binding pocket and help understand their role in inhibitor binding. Theoretical protein-ligand complexes for HIV-1 RT proteins (wild-type (WT), K103N and Y181C) and three NNRTIs were generated using: GOLD docking (model A) and GOLD docking with AMBER minimization (model B). The pairwise interaction energies between the inhibitors and individual residues within 4 Å were calculated at MP2/6-31G(d,p) level of theory (BSSE corrected). We use principal components analysis (PCA) to study the relationship between the theoretical parameters obtained for the 3 different inhibitors at 3 distinct protein variants, because of the large number of variables generated, and the significant cross correlation in the dataset. From an analysis of the loading and scores plots derived PCA model we discuss (a) the impact the different starting models have on the individual residue interaction energies and H-bond distances, (b) the origin of the activity increases for certain mutant-inhibitor combinations but not others and (c) how the subtly different binding modes of the different Nevirapine derivatives are dependent on multiple different active site residues to differing degrees and the implications this has for their mutant activities generally.

**Keywords:** HIV-1 RT, NNRTIs, AMBER force fields, GOLD docking, Interaction Energy, Quantum Chemical Calculations, PCA

**References**

- Kuno, M., Hongkengkai, R. and Hannongbua, S., ONIOM-BSSE scheme for H...[pi] system and applications on HIV-1 reverse transcriptase, *Chemical Physics Letters*, **2006**, 424, 172-177.
- Rodriguez-Barrios, F. and Gago, F., Understanding the Basis of Resistance in the Irksome Lys103Asn HIV-1 Reverse Transcriptase Mutant through Targeted Molecular Dynamics Simulations, *Journal of the American Chemical Society*, **2004**, 126, 15386-15387.
- Tantanak, D., Limtrakul, J. and Gleeson, M. P., Probing the Structural and Electronic Factors Affecting the Adsorption and Reactivity of Alkenes in Acidic Zeolites Using DFT Calculations and Multivariate Statistical Methods, *Journal of Chemical Information and Modeling*, **2005**, 45, 1303-1312.
- Corresponding author's Email, \*fscisph@ku.ac.th Tel. +66-2-5625555 ext. 2140 Fax. +66-2-5793955
- Project supported by Thailand Research Fund (RTA5080005), Commission on Higher Education (CHE), Postgraduate Education and Research Programs in Petroleum and Petrochemicals, and Advanced Materials (NCE-PPAM) and Kasetsart University Research and Development Institute (KURDI).



## Quantum Chemical Calculations on Particular Interaction Energy of HIV-1 reverse transcriptase Inhibitors (68nv, T4 and T5) Bound in Various Type of HIV-1 RT Enzymes

Amphawan Maitrad<sup>1,2</sup>, Phornphimon Maitrad<sup>1,2</sup>, Patchreenart Saparpakorn<sup>1,2</sup>, Supanna Techasakul<sup>1</sup>, and Supa Hannongbua<sup>1,2\*</sup>

<sup>1</sup>Department of Chemistry, Faculty of Science, Kasetsart University, Bangkok 10500, Thailand.

<sup>2</sup>Center of Nanotechnology, Kasetsart University, Bangkok 10500, Thailand.

\*Correspondence: Supa Hannongbua, Dept. of Chemistry, Kasetsart University, Bangkok 10500, Thailand. Fax: +66 25 62 55 55 ext. 2140 Email: fscisph@ku.ac.th

### Introduction

The human immunodeficiency virus type1 reverse transcriptase (HIV-1 RT) is an essential enzyme in the life cycle of the virus and it is an attractive target for the development of new drugs. 68nv, T4 and T5 (Figure 1) are dipyrrodoazepinone nevirapine derivatives of non-nucleoside RT inhibitors (NNRTI) which have high activities against HIV-1 RT. However, the efficacy of highly potent NNRTIs is limited by drug-resistant. The Y181C and K103N mutations are the most common HIV-1 RT mutations associated with resistance to NNRTIs. In order to evaluate the role of the amino acids surrounding the binding pocket of three types of HIV-1 RTs (wild-type, K103N and Y181C) bound with 68nv, T4 and T5, the quantum chemical calculations were applied to study the particular interactions between inhibitors and binding site of the HIV-1 RT.

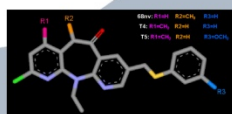


Figure 1. Structure of dipyrrodoazepinone nevirapine derivatives.

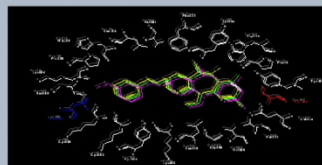


Figure 2. The adopted model system of 68nv (green), T4 (green) and T5 (pink) bound to HIV-1 RT binding site (wild type (white), K103N (blue) and Y181C (red)) consisting of 20 amino acid residues.

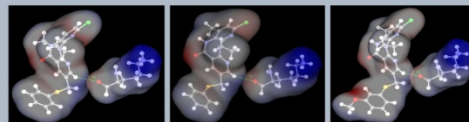


Figure 3. The H-bond between inhibitors ( 68nv(A), T4(B) and T5(C) ) and Lys101

### Methodology

All ligand-enzyme complexed structures were constructed from molecular docking using the GOLD program, based on wild-type HIV-1 RT structure with PDB code 1KLM. The model system was set up by selecting amino acids surrounding inhibitors within the interatomic distance of 4 Å. The obtained twenty residues in this study were Glu138, Gly190, His235, Leu100, Leu234, Lys101, Lys102, Lys/Asn103, Lys104, Phe227, Pro236, Pro95, Ser105, Trp229, Tyr/Cys181, Tyr188, Tyr318, Val106, Val179, and Val189. The particular interaction energy was focused on the couple of inhibitor and each amino acid. Then, H atoms were added into the cutting regions using SYBYL 7.0 program. The B3LYP/6-31G(d,p) and MP2/6-31G(d,p) level of calculations implemented in the GAUSSIAN 03 program were performed to calculate the energy. Moreover, the basis set superposition error (BSSE) based on counterpoise scheme of Boys-Bernardi were also computed in the interaction energy as see in below equation;

$$E_{\text{int}} = E_{\text{complex}} - E_{\text{inhibitor}} - E_{\text{residue}}$$

Where : AB = Combined basis set of inhibitor and amino acid  
A = Number basis set of inhibitor  
B = Number basis set of residue

### Results

Table1. Interaction energies of 68nv, T4 and T5 with individual residues calculated by B3LYP/6-31G(d,p) and MP2/6-31G(d,p) methods (kcal/mol)

Residue	Interaction Energy (kcal/mol)																	
	Wild type						K103N						Y181C					
	B3LYP/6-31G(d,p)	T4	T5	68nv	T4	T5	B3LYP/6-31G(d,p)	T4	T5	68nv	T4	T5	B3LYP/6-31G(d,p)	T4	T5	68nv	T4	T5
Glu138	5.12	8.08	10.58	4.47	7.57	9.98	5.00	7.92	10.58	4.35	7.40	9.98	5.12	8.08	10.58	4.47	7.57	9.98
Gly190	3.50	3.24	2.09	3.35	1.28	0.97	2.38	2.39	2.09	1.96	1.49	0.97	3.50	2.24	2.09	3.35	1.28	0.97
His235	4.91	1.57	1.79	4.54	0.66	0.72	4.89	1.56	1.79	4.51	0.65	0.72	4.91	1.57	1.79	4.54	0.65	0.72
Leu100	5.33	3.62	4.40	1.27	-0.23	-0.03	5.24	3.52	4.40	1.19	-0.33	-0.03	5.33	3.62	4.40	1.27	-0.23	-0.03
Leu234	8.11	2.38	2.20	4.43	-0.56	-0.51	8.23	2.50	2.20	4.55	-0.56	-0.51	8.11	2.38	2.20	4.43	-0.56	-0.51
Lys101	-1.08	-1.46	-0.99	-1.74	-2.13	-1.71	-1.06	-1.44	-0.99	-1.72	-2.11	-1.71	-1.08	-1.46	-0.99	-1.74	-2.13	-1.71
Lys102	1.33	1.63	3.07	-0.23	0.13	0.92	1.32	1.63	3.07	-0.24	0.13	0.92	1.33	1.63	3.07	-0.23	0.13	0.92
Lys103(Asn103)	8.87	10.56	9.90	6.39	7.86	6.23	10.34	14.20	18.32	7.97	12.03	15.86	8.87	10.56	9.90	6.39	7.86	6.23
Lys104	1.59	2.26	3.84	0.49	1.16	2.78	1.59	2.25	3.84	0.48	1.16	2.78	1.59	2.26	3.84	0.49	1.16	2.78
Phe227	7.85	7.26	3.23	5.28	5.14	1.49	8.14	8.14	3.23	5.59	5.25	1.49	7.85	7.26	3.23	5.28	5.14	1.49
Pro236	3.95	2.93	12.85	2.03	1.08	10.04	3.95	2.93	12.85	2.03	1.08	10.04	3.95	2.93	12.85	2.03	1.08	10.04
Pro95	0.99	1.03	0.65	0.27	0.32	-0.19	0.99	1.03	0.65	0.27	0.32	-0.19	0.99	1.03	0.65	0.27	0.32	-0.19
Ser105	1.30	1.58	1.25	0.27	0.39	0.11	1.03	1.13	1.25	0.03	-0.02	0.11	1.30	1.58	1.25	0.27	0.39	0.11
Trp229	0.28	7.79	3.03	-2.70	4.69	0.33	0.46	7.90	3.03	-2.52	4.80	0.33	0.28	7.79	3.03	-2.70	4.69	0.33
Tyr181(Cys181)	9.48	12.31	11.21	5.69	7.44	6.88	9.07	11.85	11.21	5.31	7.00	6.88	11.5	11.5	9.62	11.5	10.75	8.97
Tyr188	10.5	9.95	5.11	6.04	5.78	1.33	10.5	10.19	5.11	6.27	5.99	1.33	10.2	9.95	5.11	6.04	5.78	1.33
Tyr318	9.95	4.16	7.30	6.99	1.86	4.29	9.66	4.16	7.30	6.97	1.84	4.29	9.66	4.16	7.30	6.99	1.86	4.29
Val106	15.6	17.43	8.69	10.0	11.47	3.74	15.6	17.43	8.69	10.0	11.47	3.74	15.6	17.43	8.69	10.0	11.47	3.74
Val179	0.62	1.36	2.09	-0.14	0.27	0.88	0.57	1.30	2.09	-0.17	0.22	0.88	0.62	1.36	2.09	-0.14	0.27	0.88
Val189	0.89	1.20	1.06	-0.49	0.09	0.02	0.51	0.88	1.06	-0.49	-0.22	0.02	0.89	1.20	1.06	-0.47	0.09	0.02





# Influence of AMBER Force Fields on Particular Interaction Energy of HIV-1 Reverse Transcriptase Inhibitors (68nv, T4 and T5) Bound in Various Types of HIV-1 RTs

MAITARAD Amphawan<sup>a,b</sup>, TREESUWAN Witcha<sup>a,b</sup>, MAITARAD Phornphimon<sup>a,b</sup>, GLEESON Paul Matthew<sup>a,b</sup>, SAPARPAKORN Patchreenart<sup>a,b</sup>, TECHASAKUL Supann<sup>a</sup> and HANNONGBUA Supa<sup>a,b,\*</sup>

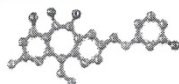
<sup>a</sup> Department of Chemistry Faculty of Science, Kasetsart University, Bangkok 10900, Thailand, <sup>b</sup> Center of Nanotechnology, Kasetsart University, Bangkok 10900, Thailand  
\*E-mail: fscieph@ku.ac.th, Fax: +66 25 62 55 55 ext 2140



## Introduction

Nevirapine is a first generation non-nucleoside inhibitor of HIV-1 RT. Nevirapine is highly effective against the wild type protein but loses its efficiency for common mutant. In particular, the K103N and Y181C mutants are reported to be resistant to nevirapine inhibitors and its analogs. This has led to the synthesis of 2-chloro-6-arylimethyl dipyrrolozadepinone derivatives which show very interesting biological activities at known mutants (Table 1). To understand the cause of this effect, we have applied quantum chemical calculations to study the effect of mutation on inhibition. We use principal components analysis (PCA) to study the relationship between the theoretical parameters obtained for the 3 different inhibitors at 3 distinct protein variants, because of the large number of variables generated, and the significant cross correlation in the dataset. From this work it is clear that theoretical calculations can prove useful in gaining understanding of the underlying causes of drug resistance at HIV-1 RT.

Table 1: Structure and inhibitory activity of dipyrrolozadepinone derivatives (68nv, T4 and T5) against various type of HIV-1 RT.



Cpds	R1	R2	R3	IC <sub>50</sub> (μM)		
				WT	K103N	Y181C
68nv	H	CH <sub>3</sub>	H	0.086	0.390	0.005
T4	CH <sub>3</sub>	H	H	0.019	0.224	0.269
T5	CH <sub>3</sub>	H	OCH <sub>3</sub>	0.023	0.428	0.059

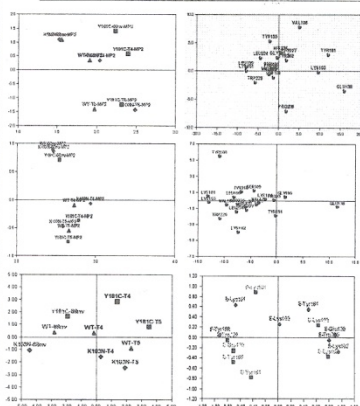


Figure 1. PCA scores (left) and loading (right) plots: plot of component one (x axis) against component two (y axis) of model A (top), model B (middle) and structural and energetic parameters of model B (down)

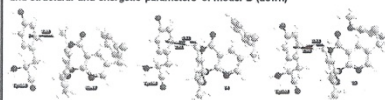


Figure 4. Interaction between inhibitors (68nv, T4 and T5) with the Tyr188 residue

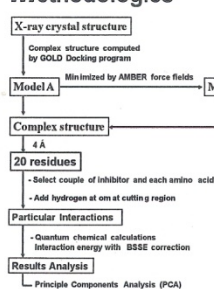
## References

1. Kuno, M., Hongkengai, R. and Hannongbua, S. *Chemical Physics Letters*, 2006, 424, 172-177.
2. Rodriguez-Barrios, F. and Gago, F. *Journal of the American Chemical Society*, 2004, 126, 15386-15387.
3. Tantanak, D., Lintrakul, J. and Gleeson, M. P. *Journal of Chemical Information and Modeling*, 2006, 45, 1303-1312.

## Acknowledgements

This work was supported by the Thailand Research Fund (RTA5080005), Commission on Higher Education (CHE), NANOTEC Center of Excellence, National Nanotechnology Center Kasetsart University, The Graduate Education and Research Program in Petroleum and Petrochemical Technology and Advance Material, and Center of Nanotechnology Kasetsart University Research and Development Institute (KURDI).

## Methodologies



## Definition of Interaction Energy

$$E_{int} = E_{complex}^{AB} - E_{inhibitor}^{AB} - E_{residue}^{AB} \quad \dots (1)$$

Where,  $E_{complex}^{AB}$  is the energy of inhibitor-residue  
 $E_{inhibitor}^{AB}$  is the energy of inhibitor  
 $E_{residue}^{AB}$  is the energy of individual residue  
AB is molecular orbital of inhibitor-residue

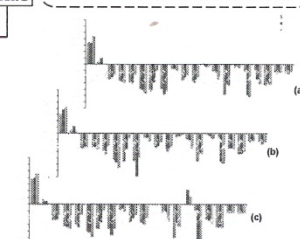


Figure 2. Relationship of interaction energy of three inhibitors (68nv, T4 and T5) in WT(a), K103N(b) and Y181C(c)

## Results and Discussion

The AMBER force field minimizations of model B can SIGNIFICANTLY decreases the interaction energy of Tyr181, Lys103, Val106 and Pro236, when compared with GOLD docking o derived model A. Moreover, it remained same interaction that seen with residues; Leu100, Lys101, Trp229 and Glu138 as shown in Figure 1 (top and middle).

We therefore used the model B derived energies to analyze the differences between the inhibitor/protein interactions in more detail. In addition to the interaction energies, distances associated with each of the key residues were extracted and these were used to build the PCA model. The residues chosen for the analysis are: Lys101, Lys103, Tyr188, Tyr181, Trp229 and Glu138 because they have effected on interaction energy, as shown in Figure 1 (down).

In WT, Tyr188, Lys102, Trp229 and Glu138 have effect on this enzyme. The difference of interactions of three inhibitors are clearly seen in Lys102 (Figure 3) and Tyr188 (Figure 4), indicating that T4 has high potent than T5 and 68nv, respectively, as displayed in Figure 2(a).

In Y181C, HIV-1 RT found that Lys101, Lys103 and Tyr181 have effect on this enzyme. The difference of interactions of three inhibitors are clearly seen in Cys181 (Figure 5), indicating that 68nv has high potent than T5 and T4, respectively, as displayed in Figure 2(b).

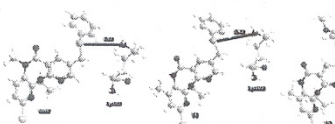


Figure 3. Interaction between inhibitors (68nv, T4 and T5) with the Lys102 residue in WT

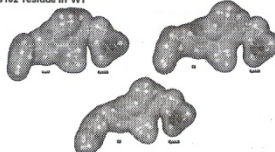


Figure 5. Overlapping factor between chloride atom in three inhibitors and hydrogen atom in side chain of Cys 181

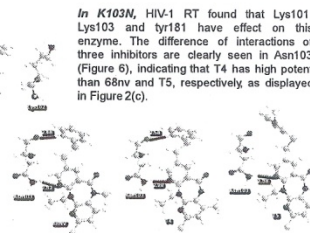


Figure 6. Interaction between inhibitors (68nv, T4 and T5) with the Asn103 residue

## Conclusions

The AMBER force field minimizations (model B) can decrease more repulsive interaction energy of in binding site of GOLD docking (model A) and in can remained important attractive interaction in binding site. The results can be inferred that AMBER force field minimizations are essential in the starting geometry of enzyme complex.

Moreover, the calculated results from quantum chemical calculations are consistent with their experimental activities in WT, K103N and Y181C HIV-1 RTs.



## CURRICULUM VITAE

NAME : Miss Amphawan Maitarad

BIRTH DATE : April 21, 1985

BIRTH PLACE : Phichit, THAILAND

NATIONALITY : Thai

EDUCATION :      YEAR      INSTITUTION      DEGREE/DIPLOMA  
                                          2007      Naresuan University      B.Sc.(Chemistry)

SCHOLASHIP : Thailand Research Fund (RTA5080005)

Commission on Higher Education (CHE)

The Kasetsart University Research and Development Institute (KURDI), and National Nanotechnology Center (NANOTEC)

The National Center of Excellence for Petroleum, Petrochemicals, and Advanced Materials (NCE-PPAM)

Kasetsart University Research and Development Institute (KURDI)

Faculty of Science Kasetsart University

## **PUBLICATIONS**

1. Amphawan Maitarad, Patchreenart Saparpakorn , Withcha Treesuwan, Phornphimon Maitarad, Paul Matthew Gleeson, Supanna Techasakul, and Supa Hannongbua. A theoretical study of HIV-1 RT inhibition using MM, QM and multivariate methods: A comparison of Docking and MM optimized starting complexes and an assessment of residues contributions in the wild-type and two Major Mutants, 2009, to be submitted.